8-2018

Determining the Effect of Locally Delivered Bioactive Modulators on Macrophage Activation at the Implantation Site of Different Biomaterials in Rats

Kamel Alkhatib
University of Arkansas, Fayetteville

Determining the Effect of Locally Delivered Bioactive Modulators on Macrophage Activation at the Implantation Site of Different Biomaterials in Rats

A dissertation submitted in partial fulfillment
of the requirements for the degree of
Doctor of Philosophy in Cell and Molecular Biology

by

Kamel Alkhatib
University of Aleppo
Bachelor of Pharmacy and Pharmaceutical Chemistry, 2013

August 2018
University of Arkansas

This dissertation is approved for recommendation to the Graduate Council.

_____
Julie A. Stenken, PhD
Dissertation Director

_____
Jeannine M Durdik, PhD
Committee Member

_____
David Paul, PhD
Committee Member

_____
Timothy J. Muldoon, PhD
Committee Member

_____
Yuchun Du, PhD
Committee Member

Abstract

Altering the foreign body reaction by targeting macrophages has been of interest in the biomaterials field to improve the integration of longevity of implanted biomedical devices. The objective of this dissertation was to study the effect of locally delivered bioactive modulators on macrophage activation at the implantation site of different biomaterials in rats. Iloprost, a prostacyclin analog, was tested for its ability to direct macrophages to their pro-wound healing phenotype after the implantation of microdialysis probe in the subcutaneous space of male Sprague Dawley rats. This study showed that iloprost can shift macrophage activation states *in vivo* to the pro-wound healing phenotype and decrease the levels of the pro-inflammatory chemokine (CCL2) at two days post implantation. It also demonstrated the need of more experiments to confirm iloprost effect in shifting macrophage activation to their $CD163^{+}CD68^{+}$ pro-wound healing phenotype at a longer time point than two days post implantation.

To achieve this goal, iloprost was studied for its ability to modulate macrophages to their pro-wound healing, pro-tissue remodeling phenotype at 7 days post implantation time point, after the implantation of the PVA sponges and compared to dexamethasone effect on macrophage activation. This project focused on assessing macrophage activation caused by implanted polyvinyl alcohol non-biodegradable vs. collagen biodegradable sponges in the subcutaneous space of male Sprague Dawley rats. Like dexamethasone, iloprost was able to shift the macrophage to their $CD163^{+}CD68^{+}$ pro-wound healing phenotype and decreased the levels of CCL2 found in the collected wound fluid from the explanted sponges. Additionally, iloprost administration significantly decreased the number of infiltrating cells around PVA sponge.

Once the ability of iloprost to modulate the macrophages phenotype was confirmed, a material-based study was designed to compare macrophage activation caused by implanted polyvinyl alcohol non-biodegradable vs. collagen biodegradable sponges in the subcutaneous space of male Sprague Dawley rats. Collagen scaffolds, isolated from the same rat strain, were

synthesized and implanted subcutaneously to perform this study. The administration of iloprost and dexamethasone lead to a decrease in the levels of pro-inflammatory CCL2, and an increase in the population of $CD163^{+}CD68^{+}$ in both sponge models compared to their correspondent control sponges. Although, the levels of CCL2 in the wound fluid collected from the collagen control sponges were significantly less those collected from the PVA sponges, both materials initiated an inflammatory response cascade that was similar in terms of collagen distribution, and $CD163^{+}CD68^{+}$ macrophages around the implant.

Acknowledgments

The completion of this dissertation would not have been possible without the support of several people. I would like to express my special appreciation to the people who have supported me throughout my graduate career. I would first like to sincerely thank my advisor Dr. Julie A. Stenken, her advice on research and career opportunities have been invaluable. She provided support throughout my years in graduate school, and I would like to thank her for encouraging me to grow as a research scientist. Thank you for providing the unpredicted opportunities to attend conferences and meet individuals to further my education and career. While Dr. Stenken gave me the freedom explore new research areas, she continued to contribute feedback and appreciated advice. I am grateful to her as it was a privilege and an honor for me to benefit from her incomparable scientific knowledge. Dr. Stenken allowed me to take this work to completion through her straightforward criticism and support and has set an example of excellence as a mentor, instructor, and role model.

I am thankful for the members of my committee, Dr. David W. Paul, Dr. Jeannine M. Durdik, Dr. Timothy J. Muldoon, and Dr. Yuchun Du for investing their time and providing constructive feedback throughout the stages of my dissertation. I am grateful to Dr. Jeannine M. Durdik for providing me with academic support and the immunology supervision that were essential to completing this dissertation. A special thanks goes to Dr. Wayne J. Kuenzel and Dr. Elizabeth M. Martin for my initial training on using the cryostat and the confocal microscope as well as allowing me to use these instruments throughout my graduate career.

I am thankful for NIH EB 014404 and the Provost Collaborative Research Grant at The University of Arkansas for funding the years of my graduate work. The completion of this dissertation would have been impossible without the backing of these funds.

This journey would not have been possible were it not for the support and friendship from the current and past members in my lab: Geoff, Tina, Geetika, Randy, Sarah, Thad, Alda, Patrick, Taylor, and Victoria. Each member contributed unique characteristics to the lab and provided an environment that helped shape me as a researcher. We have all been there for one another for advice and assistance during the difficulties of graduate school. I would like to thank Asya Ozkizilcik for bringing significant expertise in biomaterials creation to this project. I would like to acknowledge the time and effort she put into our collaborative project.

Finally, my deep and sincere gratitude to my family for their continuous love and support. I dedicate this dissertation to the memory of my father who unfortunately could not see this dissertation completed but offered the support to make it possible and whose memory will never be erased. To the strongest woman in my life, my mother, who selflessly encouraged me to achieve my goals throughout the years. To my brothers and my family for their patience and immeasurable love during my journey.

Contents

List of Figures and Tables

Chapter 1.

Chapter 2.

Chapter 3.

List of Published Papers

Chapter 3: published

K. Alkhatib, T.M. Poseno, A. Diaz Perez, J.M. Durdik, J.A. Stenken, Iloprost Affects Macrophage Activation and CCL2 Concentrations in a Microdialysis Model in Rats, Pharm. Res. 35(1) (2018) 1-10.

List of Abbreviation

ANOVA	Analysis of variance
BSA	Bovine Serum Albumin
cAMP	Cyclic adenosine monophosphate
CCL2	C-C motif chemokine ligand 2
CD	Cluster of Differentiation
C_{dial}	Iloprost concentration in the dialysates
cDNA	Complimentary Deoxyribonucleic Acid
C_i	Iloprost concentration in the perfusion fluid
DHA	Docosahexaenoic acid
EE	Extraction Efficiency
ECM	Extracellular Matrix
ELISA	Enzyme-Linked Immunosorbent Assay
EPA	Eicosapentaenoic acid
FBR	Foreign Body Response
H&E	Hematoxylin and Eosin
HPLC	High Performance Liquid Chromatography
HPLC-ESI-MS/MS	High-performance liquid chromatography-electrospray ionization-tandem mass spectrometry
IACUC	Institutional Animal Care and Usage Committee
IFN-γ	Interferon Gamma
IgG	Immunoglobulin G
iNOS	Inducible Nitric Oxide
kDa	Kilodalton
IL	Interleukin

LC-MS/MS	Liquid chromatography-tandem mass spectrometry
LOD	Limit of detection
LOQ	Limit of quantification
LPS	Lipopolysaccharide
MAPK	Mitogen-Activated Protein Kinase
M-CSF	Macrophage Colony Stimulating Factor
MCP-1	Monocyte chemoattractant protein-1
MDa	Megadalton
MHC II	Major Histocompatibility Complex II
MPS	Mononuclear phagocytic system
MWCO	Molecular Weight Cut-off
NF-κB	Nuclear Factor Kappa-Light-Chain-Enhancer of activated B cells
NIH	National Institutes of Health
OCT	Optimal Cutting Solution
PAMP	Pathogen-associated Molecular Pattern
PBS	Phosphate Buffered Saline
PDGF	Platelet derived growth factor
PES	Polyethersulfone
PGI_2	Prostacyclin
PMNs	Polymorphonuclear leukocytes
PRR	Pattern Recognition Receptor
PVA	Polyvinyl alcohol
qRT-PCR	Quantitative Real Time Polymerase Chain Reaction
REST	Relative Expression Software Tool
RNA	Ribonucleic Acid

SD	Standard Deviation
TGF-β	Transforming Growth Factor Beta
Th1	T helper cell type 1
Th2	T helper cell type 2
TLR	Toll Like Receptor
TNF-α	Tumor Necrosis Factor alpha
VEGF	Vascular endothelial growth factor

Chapter 1

General Introduction

1.1. Foreign body response and wound healing

Over the past decades, there has been an extensive interest in bioengineered implantable devices such as artificial joints [1], sensors [2-5], heart valves [6], catheters [7], and both reconstructive and cosmetic implants [8, 9]. The term “biomaterial” is defined as a substance that has been engineered to perform supportive therapeutic or diagnostic procedure through directly interacting with the living organism [10]. The biomaterial/ blood interface interactions and the normal homeostatic response to the implantation of these devices result in limited *in vivo* functionality and longevity for the implanted devices [11, 12]. The excessive growth of collagen around these implants as a mechanism to protect the host against foreign materials has been a major obstacle referred to as foreign body response (FBR) [13-16]. This response is characterized by persistent inflammation, macrophage infiltration, foreign body giant cells, and fibrotic cell formation [17]. Materials bigger than 10 μm in size cannot be phagocytosed, hence these materials are identified as foreign objects and get encapsulated in a collagenous bag as an ultimate result to the foreign body response [13]. Biomaterial malfunction, infections, and soft-tissue contractures can be some of the consequences of the biomaterial encapsulation [18].

The foreign body response is initiated by the surgical implantation of biomaterials, which causes a mechanical disruption to tissue homeostasis that eventually leads to fibrin-dominated thrombus activation, platelet activation and the activation of the complement system [13]. A, group of different proteins including fibronectin, fibrinogen, IgG and other proteins, adsorb to the surface of biomaterials immediately after implantation forming a biodegradable matrix called the provisional matrix [13, 15]. The provisional matrix releases mediators that initiate the resolution and repair processes that include inflammatory cells and fibroblast recruitment (Figure 1.1). The fibrin network also activates the platelets to release the platelet derived growth factor (PDGF), transforming growth factor β (TGF-β), and other chemokines, which later contribute to fibroblast and neutrophil recruitment to the implantation site [19, 20]. The events of spontaneous adsorption

of nonspecific proteins on the implant surface that eventually lead to phagocyte and fibroblast recruitment are defined by the term device biofouling.

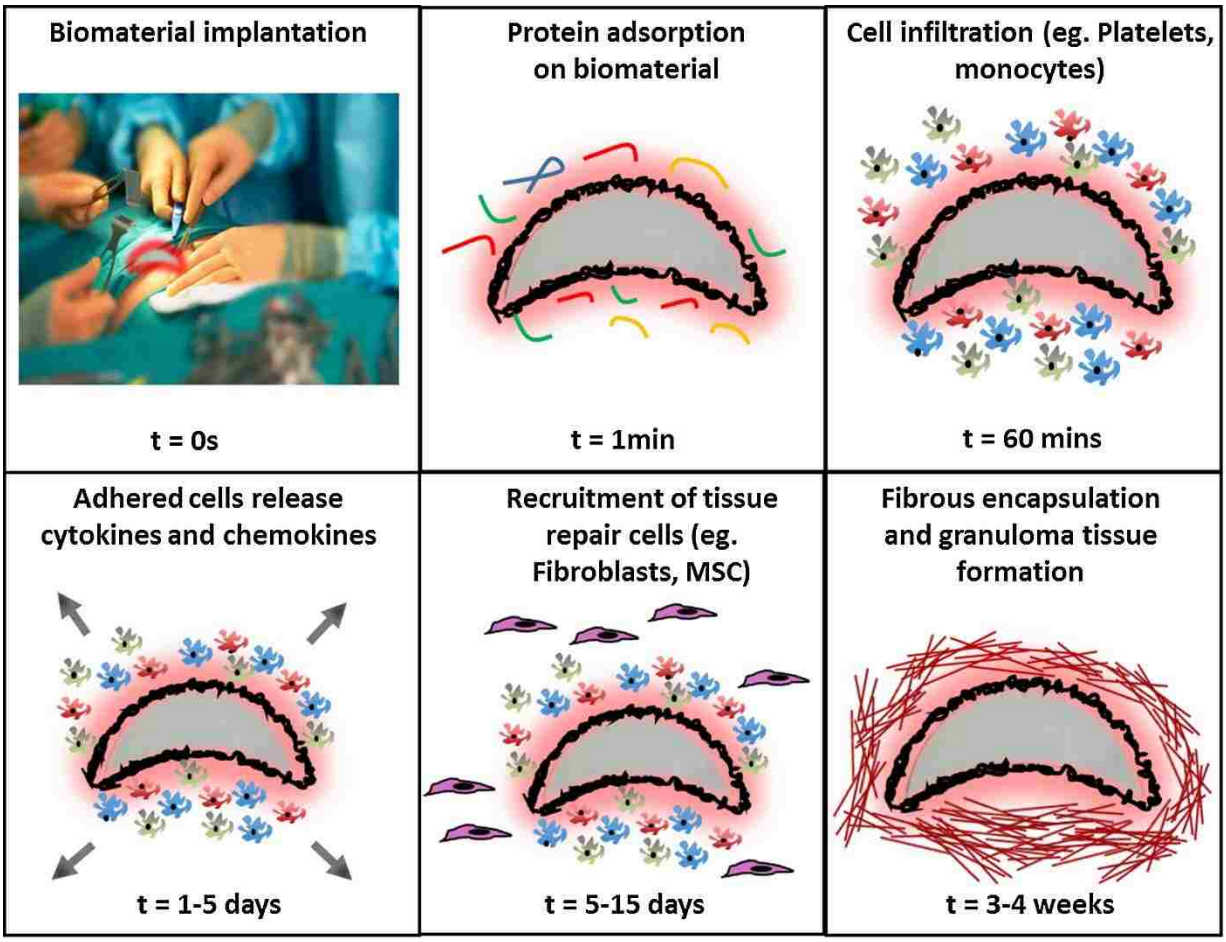

Figure 1.1. Steps of the foreign body response following the implantation of biomaterial. Reprinted from Materials Today.,18, Sridharan, R., Cameron, A. R., Kelly, D. J., Kearney, C. J., O'Brien, F. J. Biomaterial based modulation of macrophage polarization: a review and suggested design principles, 2015, 313-325, with permission from Elsevier Under a Creative Commons license.

Following the adsorption of proteins to the implant surface, the inflammatory cells arrive at the implantation site. This cellular cascade is usually characterized by an acute inflammatory state which can last minutes to several days depending on the extent of the injury caused by the biomaterial implantation. Neutrophils have a short a life time (24 – 48 hours) and are the predominant cells at the wound site that characterize acute inflammation. Neutrophils arrive at the wound site in response to the chemokine gradient within a few hours of the injury and play an essential role in the removal of debris and dead cells around the wound [21].

Chemokines, cytokines with chemoattractant properties, are subdivided into four major families: C, CC, CXC, and CX_3C. The chemokine family is responsible for the recruitment of specific cell types to a wound site. The chemokine (C-C motif) ligand 2 (CCL2), monocyte chemoattractant protein-1 (MCP-1), is a 13 kDa chemokine that is known to recruit monocytes to an inflammation site caused by either injury or infection [22]. Chemokines also play a key role in angiogenesis, tumor metastasis, and lymphocyte differentiation [23, 24]. CXCL8 (IL-8) is the main chemokine responsible for neutrophil recruitment to the implant site [25].

Within three to five days post implantation, monocytes/macrophages start to migrate to the wound site, becoming the predominant cell type, and playing a significant role in regulating various aspects of inflammation throughout the wound healing process [26]. As those events progress in the inflammation cellular cascade, monocytes/macrophages are driven to the implant site in response to chemokines and other chemoattractants, such as CCL2, platelet- derived growth factor (PDGF), CXCL4, Interleukin 1 (IL-1) and TGF-β [27-30]. CCL2 (macrophage chemoattractant protein, MCP-1), CCL3 (macrophage inflammatory protein, MIP-α), CCL-4 (macrophage inflammatory protein, MIP-1β), and CCL7 (MCP-3) are chemokines that have been shown to recruit monocytes/ macrophages to the wound site [24, 31].

The recruited macrophages adhere to the provisional matrix proteins using their surface receptors and the receptor-ligand interactions. This adhesion is mainly orchestrated by the integrin family, surface receptors that facilitate the adhesion, binding and signal transduction between cells and their surrounding microenvironment [32]. Some studies showed that macrophage adhesion is partially mediated by the interaction between the phagocyte integrin, the leukocytes integrin Mac-1 (CD11b/CD18), and other protein ligands such as fibrinogen, fibronectin, immunoglobulin G (IgG) and complement factor fragment C3bi [33-36]. Mainly, the proteins involved with cellular adhesion are rich with RGD tri-peptide sequence (Arg-Gly-Asp tri-peptide sequence) which binds to several integrins ($\alpha_v\beta_3$, $\alpha_v\beta_5$, and $\alpha_5\beta_1$) [37].

The most common classes of integrins expressed by macrophages are β_1, β_2, and β_3. In addition to their role in macrophage adhesion, β_1 integrins have been shown to play a role in the formation of foreign body giant cells (FBGCs) resulting from Interleukin-4 (IL-4) induced macrophages fusion [38]. β_2 integrins are important for macrophage initial adhesion to the provisional matrix adhesion and play a crucial role in podosomes formation [39-41]. Podosomes, actin-rich structures present on the plasma membrane of macrophages and dendritic cells, provide the macrophages with the ability to spread over the surface of biomaterials which later allow the macrophages to fuse together, forming foreign body giants cells (FBGCs) [42, 43].

While some biomaterials are too big (particle sizes > 10 μm in diameter) to be phagocytosed, macrophages and foreign body giant cells persist at the implant site secreting mediators into the microenvironment existing between the cellular membrane and the biomaterial surface with the aim of destructing the biomaterial surface [44-46]. During the frustrated phagocytosis process, as labeled by Henson, macrophages and foreign body giant cells release a wide spectrum of chemical degradative mediators and cytotoxic substances, such as reactive oxygen intermediates (ROIs), oxygen free radicals, degradative enzymes and phagosomes to the

biomaterial thus enhancing the potential oxidation and biodegradation biomaterial surface and eventually leading to potential biomaterial failure [47, 48].

Once adherent macrophages on the biomaterial surface are activated in an attempt to phagocytose the biomaterial, they secrete different inflammatory mediators, such as cytokines, chemokines, growth factors and other bioactive agents that direct the progress of inflammatory state and the wound healing response to the biomaterial implantation [49, 50]. Table 1 summarizes the chemical mediators secreted by macrophages during the foreign body response.

Table 1.1. Molecules secreted by macrophages during the foreign body response.

Group of secreted molecules	Secreted molecules
Growth factors	TGF-α, TGF-β1, M-CSF, VEGF/VPF [51, 52].
Bioactive lipid mediators	Prostaglandins, prostacyclin (PGI2), thromboxane leukotrienes [53, 54].
Chemokines and Cytokines	CCL2, IL-1 β, IL-6, IL-8, IL-10, IL-12, IL-18, INF-γ MIPs, TNF-α [31, 55].
Reactive nitrogen intermediates	Nitric oxide, nitrites, nitrates [56, 57].
Reactive oxygen intermediates	Hydrogen peroxide, hydroxyl radical, superoxide [58, 59].
Tissue reorganization enzymes	collagenase, elastase, hyaluronidase [60].

Due to the excessive collagen production and low degradation rate, an acellular fibrotic capsule starts to form around the implanted biomaterial that isolates the microenvironment around the implant from the whole body which potentially hinders the functionality of biomaterials that entail communication with the body enzymes such as biosensors [61, 62].

Modulating the foreign body reaction to biomaterial implants to provide an appropriate microenvironment that leads to improved tissue integration and implant outcomes has been of historical interest for biomaterials scientists [63-66]. While research has been focused relationship between the chemistry of the biomaterial and its influence on the foreign body reaction progression in terms of protein adsorption and complement activation, other research focused on the physio-chemical properties of the biomaterial surface which play a major role in the composition of the early provisional matrix. [67-69]. Numerous studies highlighted the importance of well controlled inflammatory response that is mediated by the macrophages role in tissue repair and regeneration, as well as presented strategies to promote tissue regeneration including, controlled delivery of anti-inflammatory drugs [70, 71], cytokines delivery [72, 73], and the delivery of nanoparticles that promote that phagocytic behavior of macrophages [74].

1.2. Macrophages

Macrophages are myeloid cells that are known to play a key role in orchestrating the inflammatory state progression after biomaterial implantation, in addition to their role in clearing and degrading cellular debris [75]. Both macrophages and their fused morphologic multinucleated giant cells (FGBCs) represent the dominant early active responders to different biomaterial implants of various materials [46], including polymers [76, 77], metals [78, 79], protein based materials such as collagen [80, 81], and ceramics [82].

The main function of macrophages is to facilitate the host immune and inflammatory responses against foreign bodies. Thus, a clear understanding of the complex interaction between

macrophages and biomaterials is crucial for the improved integration of the implanted biomaterial and the surrounding tissues.

1.2.1. Origin of macrophages and macrophages heterogeneity.

Monocytes, macrophages, and dendritic cells constitute the main cells in the mononuclear phagocytic system [83] . Mononuclear phagocytes originate from myeloid progenitor cells in the bone marrow that are regulated by macrophage colony stimulating factor (MCSF-1) and granulocyte colony stimulating factor (GM-CSF) [84]. Monocytes, amoeboid shaped leukocytes, are known to be recruited to a wound site where they are differentiated to macrophages [85]. Within 24 hours, monocytes leave the bone marrow to the peripheral blood stream where they circulate for a few days before being transferred to multiple tissues to replenish different resident macrophages [86, 87]. Once monocytes get transferred to the tissues, they don't return to blood circulation but rather reside in the tissue as mature differentiated macrophages [85].

The migrated monocytes differentiate into highly distinct cell populations, such as macrophages, osteoclasts and dendritic cells [88, 89]. First discovered by Ilya Mechnikov in 1882, macrophages are known to have multiple morphologies, from round pancake shaped, to elongated with large nuclei [90]. Macrophages are distributed throughout different regions of the body where they display a wide range of functional and morphological diversity despite having the same origin.

Macrophages are heterogeneous cells with respect to their phenotype and function. in addition to their morphological and functional diversity, macrophages express various cell surface receptors and release different signaling molecules. Alveolar macrophages in the lungs, Kupffer cells in the liver, microglia in the brain, osteoclasts in the bones, and Langerhans cells in the epidermis are common examples of cell types that are differentiated from migrated monocytes [89]. Macrophages exhibit a recognizable plasticity that has been extensively studied as a means to improve the outcome of different inflammation-associated disease states in which

macrophages engage such as cancer [91-94], fibrosis [95-98], obesity [99, 100], wound healing and tissue remodeling [101, 102].The differentiation pathways for these cells have been of major interest to the scientific community [103-105].

It has also been shown that the surrounding microenvironment plays a role in the functional regulation of the differentiated macrophages [106]. Remarkably, a specific macrophage differentiation profile is generated at the site of biomaterial implantation based on the tissue physiology and the physiochemical properties of the biomaterial [88, 104, 107]. Human peripheral blood monocytes have been shown to express cell surface receptors, such as cluster of differentiation 14 (CD14), CD16 and CD64, in addition to chemokine receptor expression CCR2 and CX3CR1. Macrophages, in the initial differentiation stages, express different markers including the β_2 integrin CD11b, mannose receptor (MR), and macrophage colony stimulating factor 1 receptor precursor (MCSF-1) [108].

1.2.2. Macrophage functions

Macrophages clear cellular debris of neutrophils and erythrocytes on a daily basis. They also clear dead cells from the spleen, thymus and other tissues. Homeostasis is another critical process that involves the intervention of macrophages to maintain the hematopoietic stem cell (HSC) niches [109].

Macrophages play an essential role in both innate and adaptive immunity. Both macrophages and dendritic cells are called antigen presenting cells (APC), where they facilitate the initial recognition and capturing of antigens and later help in the activation of both T and B lymphocyte effector mechanisms [110]. Pattern recognition receptors, a repertoire of plasma membrane receptors expressed by antigen presenting cells, are capable of initially recognizing all classes of macromolecules known as pathogen-associated molecular patterns (PAMPs). These include bacterially-derived carbohydrates (lipopolysaccharide (LPS)) that constitute the cell wall in gram negative bacteria, peptidoglycans found on the gram positive bacteria cell wall,

nucleic acids such as bacterial or viral DNA or RNA, glucans from fungi, and lipoproteins [110]. This demonstrates the macrophages crucial role in tissue homeostasis organization, clearing the extracellular microenvironment from potential undesirable objects that project any threat on the host [111].

Toll like receptors, transmembrane proteins associated with differential recognition of foreign pathogens, are usually expressed on the surface of antigen presenting cells [112]. Toll-like receptors (TLR) mainly recognize ligands of exogenous origin such as bacteria, fungi and viruses. However, there have been studies where Toll-like receptors (TLR) were involved in recognizing ligands of endogenous origin, such as apoptotic cells, heat shock proteins and fibrinogen [110, 111]. Biomaterials activate macrophage responses via Toll-like receptor 4 (TLR4), which is similar to macrophage activation by lipopolysaccharide (LPS), though, the response magnitude following gram-negative bacterial invasion and biomaterial implantation is different. Gram-negative bacterial invasion leads to infections, which are primarily cleared by adaptive immune responses through antibody-producing cell activation such as B cells and T cells. On other hand, biomaterial implantation leads to inflammation and foreign body responses without the intervention of B and T lymphocyte activation [113].

Antigen presenting cells (APC) also express scavenger receptors (SR) which play an important role in the uptake and clearance of end products, such as modified host molecules and apoptotic cells [114]. Scavenger receptors are involved in the recognition of modified low-density lipoproteins, binding, phagocytosis and clearance of microbial pathogens and modified endogenous molecules from the host. Other pattern recognition receptors involved in the innate and adaptive immune responses are the mannose receptors (MR), phagocytic receptors from the C-type lectin superfamily. Mannose receptors bind to carbohydrate moieties on several pathogens, such as bacteria, fungi, parasites and viruses. Recent studies have shown that mannose receptors are also involved in the silent clearance of inflammatory molecules [115-117]. A list of macrophage pattern recognition receptors and ligands is shown in Table 2.

Macrophages play a dynamic role in tissue repair and wound healing. The wound healing process is divided into four phases, hemostasis, inflammation, proliferation and resolution. This process starts by vasoconstriction and clot formation (hemostasis), followed by the inflammatory stage [28]. During the inflammatory stage, monocytes, attracted by a variety of chemokines, migrate from blood to the wound site to differentiate into macrophages. Infiltrated macrophages amplify the inflammatory response by secreting various inflammatory mediators to attract more macrophages to the wound site. Those mediators include various cytokines, chemical mediators (NO and prostaglandins) and growth factors such as PDGF (platelet derived growth factor), TGF (transforming growth factor) and FGF (fibroblast growth factor) which stimulate angiogenesis, extracellular matrix deposition, fibroproliferation and migration of cells such as fibroblasts at the wound site which indirectly influences the extracellular matrix (ECM) deposition [28, 30, 118]. They also secrete pro-angiogenic factors such as VEGF (vascular endothelial growth factor) which promote vascularization at the wound site to improve wound healing [20]. Additionally, macrophage presence at the wound site is essential to remove neutrophils, a process known as efferocytosis which has been proven to be a critical part of wound healing [119, 120]. Macrophage-derived growth factors such as TGF-β and platelet-derived growth factor (PDGF) have been shown to directly stimulate collagen synthesis and fibroblast proliferation [121]. Macrophages also secrete a wide array of chemokines, inflammatory and anti-inflammatory cytokines, such as IL-1β, IL-4, IL-6, IL-10 and TNF-α during various stages of FBR/wound healing progression. Macrophage inflammatory protein 1α (MIP-1α) and MCP-1 are chemokines that are known for their distinguished expression patterns during the wound repair process and their crucial role in macrophage recruitment to the wound site [122, 123] .

Table 1.2. Macrophage pattern recognition receptors and their ligands

Pattern recognition receptors	Ligand
Mannose receptor (MR)	Lipoarabinomannan, L-selectin [115, 124]
Scavenger receptors (SR)	Apoptotic cells [114, 125]
Toll-like receptors (TLR) **TLR-2** **TLR-3** **TLR-4** **TLR-5** **TLR-6** **TLR-7** **TLR-8** **TLR-9**	 Lipoproteins and glycolipids [112] Virus [126] Lipopolysaccharide (LPS) [112, 127] Flagellin [128] Lipoproteins [129] single-stranded RNA [130] single-stranded RNA [130] Bacterial (CpG) DNA [112, 131]
Type 3 complement receptor (CR3)	β-glucan, fibrinogen [132]

1.2.3. Macrophage activation

Macrophages are highly versatile immune cells that play a significant role in regulating various aspects of inflammation. Macrophages direct outcomes during the foreign body response using different cytokines [26, 133, 134]. Macrophages exist in a continuum of activation states with sufficient plasticity to be altered between an inflammatory and a wound healing/tissue remodeling phenotype [135, 136]. Macrophages are activated through multiple engaged specific cell surface receptors with different stimulants found within the local microenvironment of the macrophage [137].

Macrophage activation exists along a continuum of phenotypes [138]. Macrophages get activated by producing mediators that change their phenotype through autocrine signaling. Those mediators are secreted in response to different stimulants, such as bacterial related products (LPS and peptidoglycans), lipids, and cytokines. Macrophages have been classified into two activation states, M1, or classically activated macrophages and M2, or alternatively activated states [136]. Lately, Murray et al. endorsed new nomenclature guidelines that recommended referring to the term “macrophage polarization” as “macrophage activation” and referencing the macrophage activation states based on their stimuli rather than using the broad M1/M2 paradigm [139]. The work presented in this dissertation will follow the new nomenclature recommendation, however, the M1/M2 paradigm will still be discussed to relate the new findings to what has been presented in the literature by the scientific community in the past.

Classically activated macrophages, pro-inflammatory macrophages, are produced during a cell-mediated immune response [140, 141]. This macrophage phenotype is produced by the presence of interferon-γ (INF-γ) and tumor necrosis factor (TNF-α), or lipopolysaccharide (LPS) and is known to secrete pro-inflammatory cytokines [142, 143]. INF-γ is a pro-inflammatory cytokine that is primarily produced by natural killer cells in response to infections to activate macrophages, causing them to secrete their own pro-inflammatory cytokines. This leads to a

phenotype of macrophages with microbicidal and tumoricidal functions. T-helper (Th1) cells also produce INF-γ where the activated macrophage phenotype becomes more susceptible to LPS presence in the host [144, 145]. TNF-α is a pro-inflammatory cytokine produced primarily by macrophages when a ligand of the toll-like receptor (TLR-4) gets activated [146]. Activation of TNF-α receptors leads to the activation of transcription factors (NF-κB) and activation protein 1 (AP-1) which eventually leads to apoptosis [147].

Classically activated macrophages are generally recognized through the secretion of pro-inflammatory cytokines (IL-1β, IL-6, and TNF-α, IL-12, IL-23), and inducible nitric oxide synthase [88, 148]. These cells also showed an increased expression of CCR7, CD64, CD80, CD86 and MCH II. Cluster of differentiation 64 (CD64), a transmembrane glycoprotein (72-kDa), has been presented as a therapeutic agent in antibody-mediated immune diseases and chronic inflammatory diseases [149]. Both CD80 and CD86 are known to be co-stimulators for T-cell activation by interacting with cytotoxic T lymphocyte antigen-4 (CTLA-4 or CD152) [150]. Major histocompatibility complex class II (MCH II) plays a role in presenting the processed exogenous antigens to T-helper cells and activating the intracellular pathway [151]. M1 macrophages are known to secrete a variety of chemokines such as CCL15, CCL20, CXCL9, CXCL10, and CXCL13 which play a role in attracting more macrophages to the wound site [152].

Alternatively activated macrophages, M2 macrophages, are also activated through innate and adaptive signaling mechanisms, however, they are more involved in wound repair than orchestrating defense mechanisms [88]. Apoptotic cells and implanted biomaterials that fail to be phagocytosed because of their large surface area have been shown to activate this group of macrophages [153]. Other cytokines such as IL-4 and IL-13 have been identified to induce the M2 macrophage phenotype. IL-4 is secreted by mast cells and basophils promoting the formation of macrophages that promote wound healing during the early phases of tissue injury. The adaptive immune response can also produce IL-4 and is proposed by some to be the predominant pathway

for the development of wound healing macrophages. IL-4 and IL-13 are also secreted by Th2 cells to induce the formation of wound healing macrophages. Unlike M1 macrophages, M2 macrophages are not considered antigen presenting cells and are not as efficient as M1 macrophages at producing oxygen free radicals [154]. Additionally, the M2 macrophage activation profile is characterized by the expression of low levels of IL-12 and IL-23, and high levels of IL-10, an anti-inflammatory cytokine [155]. IL-10 secretion from M2 macrophages leads to dampening the immune response and limiting the inflammatory progression [156]. M2 macrophages reroute the metabolism of arginine by producing ornithine and polyamine, thus fostering cell growth and leading to tissue repair [157]. Cluster of differentiation 206 (CD206) has been shown to be highly expressed on M2 cell surface receptors and has been widely accepted as a non-specific M2 marker [158].

M2 macrophages are sub-divided into three different groups, M2a, M2b, and M2c [141]. M2a macrophages are activated in response to IL-4/IL-13 secretion [159], and have been shown to play a role in encapsulation, killing parasites and helminths, and allergic responses. Besides suppressing the production of the pro-inflammatory cytokines (IL-1β, IL-6, IL-12, and TNF-α), M2a macrophages secrete anti-inflammatory cytokines (IL-1ra, IL-4, and IL-10) [141].

M2b macrophages are activated in response to bacterial liposaccharides (LPS), immune complexes (Fc or complement), IL-1R, and the clearance of apoptotic neutrophils [160]. These cells are recognized by producing pro-inflammatory cytokines (IL-1β, IL-6, TNF-α and CCL1) in addition to their ability to produce nitric oxide (NO) which is different from other M2 macrophages [141, 161]. Nevertheless, these cells resemble the rest of the M2 subpopulation in producing large amounts of IL-10. These cells express MCH II on their surface and uniquely express both LIGHT and SPHK1 genes [160, 162]. M2b macrophages have been exploited in regulating Leishmania major infection and reducing early reperfusion injury after myocardial ischemia in mice [163, 164].

M2c macrophages are activated in response to glucocorticoids, IL-10 and TGF-β. Like M2a, these cells are considered anti-inflammatory by inhibiting the production of pro-inflammatory cytokines (IL-1β, IL-6, IL-12, and TNF-α) and rerouting the metabolism of arginine by producing ornithine and polyamine which leads to a decrease in iNOS levels [141, 165]. M2c macrophages are further characterized by releasing the anti-inflammatory cytokines IL-1RII, IL-10 and TGF-β.

Alternatively activated macrophages are typed by their production of the surface marker CD206. Macrophages with CD206 and with high expression of CD163 are considered by many to be valuable during wound healing and integration [102, 138].These cells are recognized by their high expression of CD163 on their cell surface which is essential for the clearance of hemoglobin in deformed red blood cells. CD163, a130 kDa type 1 transmembrane protein that is heavily glycosylated, is a member of scavenger receptor cysteine-rich group B family [166]. Those receptors have been found responsible for the endocytosis of hemoglobin-haptoglobin (Hb-Hp) complexes and converting it into anti-inflammatory metabolites [167]. CD163 has been recognized as a marker for M2c macrophages since it is expressed on the surface of wound healing macrophages. M2c macrophages are poor antigen presenting cells because of their low expression of MHC II [166, 168, 169].

M2c macrophages have been recognized as being anti-inflammatory, pro-wound healing, and pro-tissue remodeling cells which make them of high interest in the field of biomaterials [102]. These characteristics were exploited in shifting the macrophage activation state to be predominantly M2c at the implantation site in the aim of providing improved host/implant integration and functional outcomes. The focus of the biomaterials community to reach this aim has been either material-based or chemical modulators-based macrophage activation [52, 64, 66, 101, 170, 171].

Table 1.3. Macrophage activation states characteristics

Macrophage phenotype	Inducers	Cytokines secreted	Expressed markers	Roles
M1	INF-γ, LPS, TNF-α	IL-1β, IL-6, IL-12, IL-15, IL-18, IL-23, TNF-α, CCL15, CCL20, CXCL9, CXCL10, CXCL11, CXCL13	CD68, ↑CD80, CD86, ↑ MHC II, ↓ MRC1	Pro-inflammatory, killing of intracellular Pathogens, and phagocytosis initiation [152, 172].
M2a	IL-4, IL-13	IL-10, IL-1ra, IL-4	CD68, CD204, CD206, MHC II	Anti-inflammatory, killing of parasites and helminths, allergic responses [141, 152, 173].
M2b	LPS, ICs, IL-1β	IL-10, IL-1β, IL-6, TNF- α, CCL1, CCL20, CXCL1, CXCL2, CXCL3	CD68, CD86, ↑ IL-10, ↓ IL-12, MHC II, CD86	Immuno-regulation, interaction with B cells, both pro-inflammatory and anti-inflammatory function (ambiguous) [141, 160, 174].
M2c	IL-10, TGF- β, GCs	IL-10, IL-1ra, IL-18, TGF-β	CD68, ↑ CD163, CD204, CD206, ↓IL-6, ↓TNF- α,	Matrix deposition, clearance of apoptotic cells, tissue remodeling and pro-wound healing [138, 154, 156, 173].

1.3. The use of modulators in macrophage activation studies

Macrophage activation (macrophage polarization) has recently emerged as a new means of promoting wound healing by modulating the outcome of foreign body response to implanted biomaterials using stimulants or modulators (cytokines or glucocorticoids such as dexamethasone)[64, 101, 138, 175, 176]. Many studies have concluded that the local delivery of glucocorticoids such as dexamethasone reduced the collagen capsule formation around the biomaterial implants and shifted macrophages to their M2c state, which are known to be anti-inflammatory and pro-wound healing macrophages [177-179]. On the other hand, some studies proved that the delivery of certain cytokines can modulate the foreign body response to implanted biomaterials such as the delivery of interleukin-4 (IL-4) [73, 180-182] and interleukin 10 (IL-10) [183-186]. Other studies evaluated the effect of lipoxin A4 (LxA4) and resolvin D1 (RvD1), two different pro-resolution lipid mediators, on the modulation of the inflammatory response to biomaterials [187-189]. Other strategies involved the delivery of nitric oxide which inhibits the collagen deposition at the implanted biomaterial [190, 191].

Dexamethasone, a synthetic glucocorticoid, has been widely used as an immunosuppressant and anti-inflammatory drug [179]. Dexamethasone's mechanism of action is represented by binding to the glucocorticoid receptors that further translocate it to the nucleus. Trans-repression and transactivation are the main mechanisms where dexamethasone utilizes its anti-inflammatory effect [192]. Trans-repression is the down regulation of pro-inflammatory genes through the direct binding of the glucocorticoid receptor to negative glucocorticoid receptor elements and by interfering with activator protein-1 and nuclear factor kappa-light-chain-enhancer of activated B cells (NF-κB) [193]. Transactivation is the increase in the expressions of certain anti-inflammatory genes including lipocortin-1 and the type II IL-1 receptor [194]. Macrophage glucocorticoid receptors have also been shown to regulate Toll-like receptor-4-mediated inflammatory responses by selective inhibition of p38 MAP kinase [195]. Due to these processes

dexamethasone has been shown to down-regulate pro-inflammatory cytokines such as CCL2, IL-6, and TNF-α at the transcriptional level [29] as well as reducing CCL2, IL-6, and TNF-α protein concentrations in different studies [171, 178, 196, 197]. Recent studies have concluded that the local delivery of dexamethasone reduced the collagen capsule formation around the biomaterial implants and shifted macrophage to their M2c state which is known to be anti-inflammatory and pro-wound healing macrophages[170, 177, 178]. Thus, dexamethasone is the “gold standard” for biomaterials studies and is a commonly-used anti-inflammatory compound which enables comparing new macrophage modulators to [175, 179, 198-200].

Iloprost was studied as an *in vivo* macrophage modulator. Iloprost is a synthetic prostacyclin (PGI2) stable analog reported to have anti-inflammatory effects [201-204]. Prostacyclin is the common name for the prostaglandin, PGI2. It is a metabolite of arachidonic acid with a half-life of seconds which has been reported to have anti-inflammatory effects via the I prostanoid receptor, E prostanoid receptor, and the cyclic adenosine monophosphate (cAMP) pathway [205]. PGI2 and iloprost have been recently described as efficacious treatments for reducing fibrosis [205-207]. PGI2 analogs have also been reported to suppress LPS induced monocyte chemoattractant protein-1 (MCP-1 or CCL2) in human monocytes and dendritic cells [201, 203].

IL-10 is an 18 kDa cytokine that is secreted by monocytes, macrophages and T helper type II cells and T regulatory cells. IL-10 has been reported to inhibit the production of pro-inflammatory cytokines, (IL-1β, TNF-α and INF-γ), down regulate MHCII antigens, and block the NF-κB activity [208]. IL-10 suppressive effect on inflammatory cytokines IL-1β, IL-6 and TNF-α happens via the STAT3 signaling pathway [209]. IL-10 has also been employed in tissue remodeling and wound healing studies and was presented as anti-fibrotic agent [210, 211].

Resolvin is an endogenous lipid mediator that is derived from eicosapentaenoic acid (EPA), termed resolvin E, or docosahexaenoic acid (DHA), termed resolvin D. Recently, studies

have shown that lipid mediators such as lipoxins, resolvins and protectins are active modulators in the resolution of inflammation [187]. The resolution of inflammation is comprised of three phases: downregulation of pro-inflammatory signaling molecules, apoptosis of polymorphonuclear leukocytes (PMNs), and activating macrophages to mediate phagocytosis of the apoptotic PMNs which is followed by the migration to the lymph nodes [188]. This is initially represented by a suppression of pro-inflammatory signaling molecules and then by a release of anti-inflammatory molecules which is known to help in the apoptosis of inflammatory PMNs. It has also been shown that these pro-resolving molecules can block PMN trafficking, attract monocytes, reverse vascular permeability, induce apoptosis of residual activated PMNs and facilitate the removal of exudate and fibrin. Recent studies have shown that RvE1 at nanomolar concentrations can suppress PMN migration and pro-inflammatory cytokines signaling of IL-6, TNF-α and lL-1. Moreover, it can attract macrophage and promote the clearance of PMN at the tissue site. Like E-series, D-series and protectins have been shown to suppress PMNs, pro-inflammatory cytokines, and promote monocytes infiltration and phagocytosis [212].

1.4. Wound healing- material chemistry of implant relationship

Biomaterial surface properties have been found to have a crucial impact on the foreign body reaction during the first two weeks after implantation [213]. The events during the foreign body reaction may impact the functionality of implanted devices and affect both short- and long-term integration at the host/biomaterial interface, which explains the need of the foreign body reaction mechanism to different biomaterials. The relationship between physiochemical properties of implanted biomaterials, adsorbed proteins, adherent cells, and the released cytokines is not yet fully characterized since the interaction among these factors is complex and dynamic. Macrophages are known to regulate the host inflammatory responses against the invasion of foreign bodies. Thus, a clear understanding of the complex interaction between macrophages and biomaterials is crucial for the improvement of materials employed in the

construction of biomedical devices to elicit a favorable immune response while simultaneously performing their intended applications [107, 214].

Different materials-based approaches to elicit M2 macrophages microenvironment around an implant have been elucidated. Bioactive hydrogels, such as those based on alginate, chitosan, collagen, elastin, hyaluronic acid, and (poly)ethylene glycol (PEG) precursors have been used [80, 215] and have been recognized not to induce significant inflammatory responses and to embrace their physicochemical properties to improve tissue regeneration and wound healing processes [170, 216, 217]. Being the prime structural protein in connective tissues, collage based-scaffolds have been incorporated in the structures of many biomaterial implants for tissue regeneration [218-220]. Chitin and chitosan are other polymers that have been used in biomaterial structures, since they have adhesive, antibacterial and fungicidal properties [221-223]. PEG- and alginate-based biomaterials have been used as controlled release vehicles since those materials are easily functionalized using chemical conjugation methods [224-226].

The surface interaction between biomaterials and tissues have impact on tissue remodeling and wound repair based on the area of physical contact, tissue ingrowth, and chemical bonding [227-230]. Additionally, changes in cell phenotype, including the cell morphology, development, or biochemical properties have been recognized by changing biomaterial surfaces [78, 231]. The pore size of scaffolds has been denoted as a critical property for modulating macrophages to their pro-wound healing state [78, 232, 233]. The pore size of a scaffold can be exploited to regulate the migration speed of cells: the smaller the average pore size, the lower the fibroblast migration speed in collagen-GAG scaffolds. This can be employed to control the tissue regeneration rate [78, 214, 232]. Furthermore, controlling the crosslinking degree of collagen and preserving the native polymer structure can delay the biomaterial degradation [234, 235]. However, a study reported that cross-linked implants elicited a majority of M1 macrophages, whereas non-cross-linked scaffolds elicited a predominantly M2c macrophages response [236].

Another study pointed out the effect of cellular scaffolds vs. acellular scaffolds on macrophage activation states. Interestingly, cellular scaffolds elicited M1 macrophages state; however, acellularized scaffolds elicited a predominantly M2c macrophages state [237, 238].

Polyvinyl alcohol (PVA) based scaffolds have been also used in wound healing and tissue repair studies [239-241]. PVA sponges, unlike other materials, are made of an inert non-biodegradable material, can be easily sectioned for histological and immunohistochemical analysis, and their implantation and excision have been well described in the literature [242, 243]. PVA sponges have been very useful tool to study the biomaterial/tissue integration, collagen deposition, wound fluid composition, and the effects of chemical modulators on the wound healing process [242, 244]. Due its low protein adsorption characteristics, high water solubility, and its chemical resistance PVA has been commonly used in medical devices [245]. Such biomaterials have been used in several applications including connective tissue replacement, drug delivery, fibrovascular tissue ingrowth studies, ophthalmic materials [246-250]. Collecting wound fluid from implanted PVA sponges allows for both qualitative and quantitative analyses that can evaluate the macrophage activation and cytokines profile around the implant.

Collagen is a natural raw material that has been widely used and accepted as a scaffold that is impregnated with either different cells (e.g., stem cells) and/or different drugs or bioactive proteins [251, 252]. Collagen popularity in biomaterial structures comes from the fact that collagen-based scaffold conserves the biochemical composition and the structural properties of the extracellular matrix (ECM) [253-255]. Maintaining the three dimensional microstructural properties of the extracellular matrix has been deemed important for directing the cellular phenotype through the geometric cues and growth factors which have multiple roles in cells adhesion and differentiation [256].

Table 1.4. Selected biomaterial features with their effect on the foreign body response

Biomaterial Feature	Effect on FBR
↑ **Porosity**	↓ Fibrosis [257, 258]
Uniform 30–40 μm pores	↓ Encapsulation, ↑ M2 macrophages [259]
↑ **roughness of the surface**	↓ Fibrosis, ↑ protein adsorption [260-262]
↑ **Sharp edges**	↑ Inflammation [263]
RGD-, chitosan-adsorbed surfaces	↑ Macrophage fusion [255]
Hydrophilic surfaces	↓ Protein adsorption, ↓ macrophage fusion [264]
Hydrophobic surfaces	↑ Protein adsorption, ↑ macrophage fusion [265]
surface charge	↓ protein adsorption [266]

1.5. Microdialysis sampling

Microdialysis is a well-established minimally-invasive diffusion-based sampling technique that has been widely used for monitoring bioactive molecules in the pharmaceutical and neuroscience fields [267-275]. A microdialysis probe consists of a semi-permeable membrane with a defined molecular weight cut-off (MWCO), an inlet tubing, inner canula, and an outlet tubing (Figure 1.2). Being a device that can be implanted in multiple tissue regions, microdialysis sampling probes can be exploited in many studies as drug delivery device while simultaneously collecting dialysates from surrounding extracellular fluid in a real-time manner to later be analyzed using different quantification methods [178, 276, 277]. With 100 kDa or greater MWCO membranes, microdialysis has been used to collect large macromolecules such as the cytokines [278]. Large pore microdialysis with 1000 kDa MWCO has been also used to determine the tissue distribution and the pharmacokinetic (PK) properties of larger molecules, such as R7072 therapeutic monoclonal antibodies [279].

The *in-vivo* sampling process starts when a perfusion fluid, closely matching the ionic strength and composition of the extracellular fluid, passes through the inlet tubing using a syringe pump, that tunes the infusion rate, and comes out of outlet tubing, which is referred to as the dialysate. Microdialysis is a diffusion-based method, where the analytes can diffuse into the semi-permeable membrane due to the molecular concentration gradient existing between both sides of the molecular weight cutoff semi-permeable membrane. In other words, the molecules delivered through the microdialysis probe are at a higher concentration inside than their concentration at the extracellular space where the probe is implanted. This concentration gradient allows these molecules to pass through the semi-permeable membrane out to the extracellular space. Following the same manner, the molecules dissolved in the extracellular space form a concentration gradient at both sides of the semi-permeable membrane. This results in molecules smaller than the molecular weight cutoff to cross the membrane and being collected in the

dialysates, which can be quantified using different analysis methods. Microdialysis sampling has been exploited in biomaterial/host interaction and provides a tool for the collection of small proteins such as cytokines. Cytokines are typically present in low picomolar to femtomolar concentrations in the extracellular space and have low diffusivity which results in poor recovery of cytokines. However, microdialysis sampling has been advantageous since it allows continuous real time sampling in awake-and-freely moving animals and acquisition of analytically-clean samples that does not require any further processing. Noteworthy, the ability to implant more than one probe per animal allows each animal to serve as its own control which reduces the number of animals required for study completion [280-283].

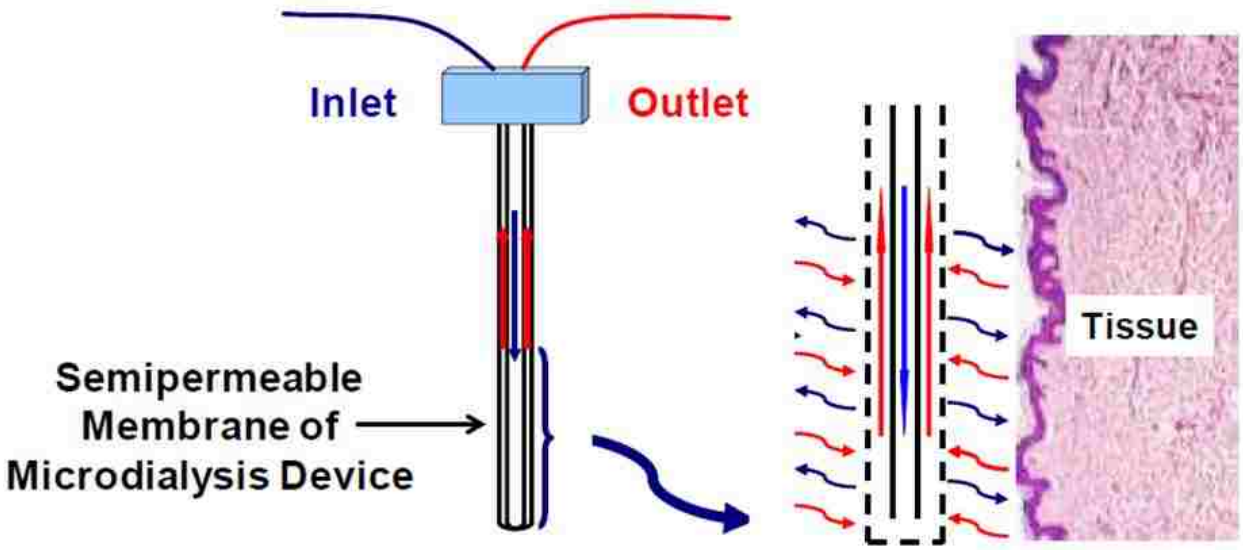

Figure 1.2. A schematic of a microdialysis probe. Reprinted form European Journal of Pharmaceutical Sciences, 57, Geoffrey D. Keeler, Jeannine M. Durdik, Julie A. Stenken, Comparison of microdialysis sampling perfusion fluid components on the foreign body reaction in rat subcutaneous tissue, 2013, 60-67, with permission from Elsevier.

1.6. Dissertation aims

The focus of this dissertation is to study the effect of locally delivered modulators on macrophage activation at the implantation site of different biomaterials in rats. Chapter 3 presents the use of iloprost as a macrophage modulator *in vivo* to shift macrophages to their pro-wound healing phenotype after the implantation of microdialysis probe in the subcutaneous space of male Sprague Dawley rats at two days post implantation. As previously mentioned, the microdialysis sampling probes is advantageous as they serve as both the implanted biomaterial as well as simultaneously delivering the modulator and collecting the dailysates from the extracellular fluid. These initial studies showed that iloprost can shift macrophage activation states *in vivo* to the pro-wound healing phenotype at two days post implantation time point and presented the necessity to design more studies to confirm the effect of locally delivered iloprost at a longer time periods post implantation.

Chapter 4 focuses on studying effect of iloprost on macrophage activation at 7 days post implantation of non-biodegradable PVA sponges. This was achieved by comparing the effect of iloprost to the effect of dexamethasone, a gold standard in macrophage activation studies. The implanted PVA sponges present a robust tool to study the macrophage activation profile at 7 days post implantation time point and to deliver drug modulators to the surrounding tissues in the aim of shifting the macrophages to their pro-wound healing phenotype.

The last part of the dissertation, presented in chapter 5, focuses on assessing macrophage activation after implanting collagen biodegradable sponges in the subcutaneous space of male Sprague Dawley rats and comparing the findings to those in chapter 4 after implanting polyvinyl alcohol non-biodegradable sponges. Collagen scaffolds, isolated from the same rat strain, were synthesized and implanted subcutaneously the subcutaneous space of male Sprague Dawley rats to determine if a difference in the level or extent of macrophage activations exists between using these two different implants.

1.7. References

[1] A. Prokop, Bioartificial organs in the twenty-first century: nanobiological devices, Ann N Y Acad Sci 944 (2001) 472-90.

[2] G.S. Wilson, Y. Zhang, G. Reach, D. Moatti-Sirat, V. Poitout, D.R. Thevenot, F. Lemonnier, J.C. Klein, Progress toward the development of an implantable sensor for glucose, Clin. Chem. (Winston-Salem, N. C.) 38(9) (1992) 1613-17.

[3] D.C. Klonoff, Technological advances in the treatment of diabetes mellitus: better bioengineering begets benefits in glucose measurement, the artificial pancreas, and insulin delivery, Pediatr Endocrinol Rev 1(2) (2003) 94-100.

[4] H.E. Koschwanez, W.M. Reichert, In vitro, in vivo and post explantation testing of glucose-detecting biosensors: Current methods and recommendations, Biomaterials 28(25) (2007) 3687-3703.

[5] B. Buckingham, K. Caswell, D.M. Wilson, Real-time continuous glucose monitoring, Curr. Opin. Endocrinol., Diabetes Obes. 14(4) (2007) 288-295.

[6] M.M. Black, P.J. Drury, Mechanical and other problems of artificial valves, Curr Top Pathol 86 (1994) 127-59.

[7] M.F. Flessner, X. Li, R. Potter, Z. He, Foreign-body response to sterile catheters is variable over 20 weeks, Adv Perit Dial 26 (2010) 101-4.

[8] A.J. Salgado, O.P. Coutinho, R.L. Reis, Bone tissue engineering: State of the art and future trends, Macromol. Biosci. 4(8) (2004) 743-765.

[9] T. Matsumoto, M. Okazaki, A. Nakahira, J. Sasaki, H. Egusa, T. Sohmura, Modification of apatite materials for bone tissue engineering and drug delivery carriers, Curr. Med. Chem. 14(25) (2007) 2726-2733.

[10] D.F. Williams, The Williams Dictionary of Biomaterials, Liverpool University Press1999.

[11] R. Arshady, Polymeric biomaterials: chemistry, concepts, criteria, PBM Ser. 1(Introduction to Polymeric Biomaterials) (2003) 1-64.

[12] T.A. Horbett, B.D. Ratner, J.M. Schakenraad, F.J. Schoen, Some background concepts, Academic, 1996, pp. 133-164.

[13] J.M. Anderson, A. Rodriguez, D.T. Chang, Foreign body reaction to biomaterials, Semin. Immunol. 20(2) (2008) 86-100.

[14] M. Kastellorizios, N. Tipnis, D.J. Burgess, Foreign Body Reaction to Subcutaneous Implants, Advances In Experimental Medicine And Biology 865 (2015) 93-108.

[15] J.M. Anderson, Biological responses to materials, Annu. Rev. Mater. Res. 31 (2001) 81-110.

[16] D.T. Luttikhuizen, M.C. Harmsen, M.J.A. Van Luyn, Cellular and Molecular Dynamics in the Foreign Body Reaction, Tissue Eng. 12(7) (2006) 1955-1970.

[17] J.D. Bryers, C.M. Giachelli, B.D. Ratner, Engineering biomaterials to integrate and heal: The biocompatibility paradigm shifts, Biotechnol. Bioeng. 109(8) (2012) 1898-1911.

[18] W.-J. Hu, J.W. Eaton, L. Tang, Molecular basis of biomaterial-mediated foreign body reactions, Blood 98(4) (2001) 1231-1238.

[19] R. Gillitzer, M. Goebeler, Chemokines in cutaneous wound healing, J Leukoc Biol 69(4) (2001) 513-21.

[20] K.J. Sonnemann, W.M. Bement, Wound repair: toward understanding and integration of single-cell and multicellular wound responses, Annu Rev Cell Dev Biol 27 (2011) 237-63.

[21] D.C. Dale, L. Boxer, W.C. Liles, The phagocytes: neutrophils and monocytes, Blood 112(4) (2008) 935-45.

[22] N. Ashida, H. Arai, M. Yamasaki, T. Kita, Distinct signaling pathways for MCP-1-dependent integrin activation and chemotaxis, J. Biol. Chem. 276(19) (2001) 16555-16560.

[23] D. D'Ambrosio, P. Panina-Bordignon, F. Sinigaglia, Chemokine receptors in inflammation: an overview, J Immunol Methods 273(1-2) (2003) 3-13.

[24] C. Esche, C. Stellato, L.A. Beck, Chemokines: key players in innate and adaptive immunity, J Invest Dermatol 125(4) (2005) 615-28.

[25] M. Baggiolini, A. Walz, S.L. Kunkel, Neutrophil-activating peptide-1/interleukin 8, a novel cytokine that activates neutrophils, J Clin Invest 84(4) (1989) 1045-9.

[26] J. Kzhyshkowska, A. Gudima, V. Riabov, C. Dollinger, P. Lavalle, N.E. Vrana, Macrophage responses to implants: prospects for personalized medicine, J Leukoc Biol (2015).

[27] E.J. Leonard, T. Yoshimura, Human monocyte chemoattractant protein-1 (MCP-1), Immunol Today 11(3) (1990) 97-101.

[28] G. Broughton, 2nd, J.E. Janis, C.E. Attinger, The basic science of wound healing, Plast Reconstr Surg 117(7 Suppl) (2006) 12s-34s.

[29] T. Velnar, T. Bailey, V. Smrkolj, The wound healing process: an overview of the cellular and molecular mechanisms, J Int Med Res 37(5) (2009) 1528-42.

[30] G. Broughton, 2nd, J.E. Janis, C.E. Attinger, Wound healing: an overview, Plast Reconstr Surg 117(7 Suppl) (2006) 1e-S-32e-S.

[31] J.W. Griffith, C.L. Sokol, A.D. Luster, Chemokines and chemokine receptors: positioning cells for host defense and immunity, Annu Rev Immunol 32 (2014) 659-702.

[32] E.J. Brown, Integrins of macrophages and macrophage-like cells, Handb. Exp. Pharmacol. 158(Macrophage as Therapeutic Target) (2003) 111-130.

[33] T.D. Zaveri, J.S. Lewis, N.V. Dolgova, M.J. Clare-Salzler, B.G. Keselowsky, Integrin-directed modulation of macrophage responses to biomaterials, Biomaterials 35(11) (2014) 3504-3515.

[34] T.D. Zaveri, N.V. Dolgova, J.S. Lewis, K. Hamaker, M.J. Clare-Salzler, B.G. Keselowsky, Macrophage integrins modulate response to ultra-high molecular weight polyethylene particles and direct particle-induced osteolysis, Biomaterials 115 (2017) 128-140.

[35] S.M. Kanse, R.L. Matz, K.T. Preissner, K. Peter, Promotion of leukocyte adhesion by a novel interaction between vitronectin and the beta2 integrin Mac-1 (alphaMbeta2, CD11b/CD18), Arterioscler Thromb Vasc Biol 24(12) (2004) 2251-6.

[36] V.K. Lishko, N.P. Podolnikova, V.P. Yakubenko, S. Yakovlev, L. Medved, S.P. Yadav, T.P. Ugarova, Multiple binding sites in fibrinogen for integrin alphaMbeta2 (Mac-1), J Biol Chem 279(43) (2004) 44897-906.

[37] E. Ruoslahti, RGD and other recognition sequences for integrins, Annu Rev Cell Dev Biol 12 (1996) 697-715.

[38] A.K. McNally, J.M. Anderson, β1 And β2 integrins mediate adhesion during macrophage fusion and multinucleated foreign body giant cell formation, Am. J. Pathol. 160(2) (2002) 621-630.

[39] S. Lukacsi, Z. Nagy-Balo, A. Erdei, N. Sandor, Z. Bajtay, The role of CR3 (CD11b/CD18) and CR4 (CD11c/CD18) in complement-mediated phagocytosis and podosome formation by human phagocytes, Immunol. Lett. 189 (2017) 64-72.

[40] C. Gawden-Bone, M.A. West, V.L. Morrison, A.J. Edgar, S.J. McMillan, B.D. Dill, M. Trost, A. Prescott, S.C. Fagerholm, C. Watts, A crucial role for β2 integrins in podosome formation, dynamics and Toll-like-receptor-signaled disassembly in dendritic cells, J. Cell Sci. 127(19) (2014) 4213-4224.

[41] S. Pacini, R. Fazzi, M. Montali, V. Carnicelli, E. Lazzarini, M. Petrini, Specific Integrin Expression Is Associated with Podosome-Like Structures on Mesodermal Progenitor Cells, Stem Cells Dev. 22(12) (2013) 1830-1838.

[42] M. Gimona, R. Buccione, S.A. Courtneidge, S. Linder, Assembly and biological role of podosomes and invadopodia, Current Opinion in Cell Biology 20(2) (2008) 235-241.

[43] D.A. Murphy, S.A. Courtneidge, The 'ins' and 'outs' of podosomes and invadopodia: characteristics, formation and function, Nature reviews. Molecular cell biology 12(7) (2011) 413-426.

[44] A.K. McNally, J.M. Anderson, Macrophage fusion and multinucleated giant cells of inflammation, Adv. Exp. Med. Biol. 713(Cell Fusion in Health and Disease, Part I) (2011) 97-111.

[45] Z. Xia, J.T. Triffitt, A review on macrophage responses to biomaterials, Biomed. Mater. (Bristol, U. K.) 1(1) (2006) R1-R9.

[46] Z. Sheikh, P.J. Brooks, O. Barzilay, N. Fine, M. Glogauer, Macrophages, Foreign Body Giant Cells and Their Response to Implantable Biomaterials, Materials (Basel) 8(9) (2015) 5671-5701.

[47] P.M. Henson, Immunologic release of constituents from neutrophil leukocytes. I. Role of antibody and complement on nonphagocytosable surfaces or phagocytosable particles, J. Immunol. 107(6) (1971) 1535-46.

[48] P.M. Henson, Immunologic release of constituents from neutrophil leukocytes. II. Mechanisms of release during phagocytosis, and adherence to nonphagocytosable surfaces, J. Immunol. 107(6) (1971) 1547-57.

[49] D.J. Holt, D.W. Grainger, Host response to biomaterials, CRC Press, 2012, pp. 91-118.

[50] M.L. Godek, D.W. Grainger, The macrophage in wound healing surrounding implanted devices, Chem. Anal. (Hoboken, NJ, U. S.) 174(In Vivo Glucose Sensing) (2010) 29-58.

[51] F.H. Barnett, M. Rosenfeld, M. Wood, W.B. Kiosses, Y. Usui, V. Marchetti, E. Aguilar, M. Friedlander, Macrophages form functional vascular mimicry channels in vivo, Sci. Rep. 6 (2016) 36659.

[52] C.W. Hsu, R.A. Poche, J.E. Saik, S. Ali, S. Wang, N. Yosef, G.A. Calderon, L. Scott, Jr., T.J. Vadakkan, I.V. Larina, J.L. West, M.E. Dickinson, Improved Angiogenesis in Response to Localized Delivery of Macrophage-Recruiting Molecules, PLoS One 10(7) (2015) e0131643.

[53] J. Morley, Role of prostaglandins secreted by macrophages in the inflammatory process, Lymphokines (N. Y.) 4 (1981) 377-94.

[54] D. Gemsa, W. Deimann, E. Baerlin, M. Seitz, H.G. Leser, Role of prostaglandins released by macrophages in regulation and suppression of the immune response, Allergologie 5(4) (1982) 142-50.

[55] R.D. Stout, J. Suttles, Functional plasticity of macrophages: reversible adaptation to changing microenvironments, Journal of leukocyte biology 76(3) (2004) 509-513.

[56] L. Bosca, M. Zeini, P.G. Traves, S. Hortelano, Nitric oxide and cell viability in inflammatory cells: a role for NO in macrophage function and fate, Toxicology 208(2) (2005) 249-58.

[57] J.W. Coleman, Nitric oxide in immunity and inflammation, Int Immunopharmacol 1(8) (2001) 1397-406.

[58] G. Weiss, U.E. Schaible, Macrophage defense mechanisms against intracellular bacteria, Immunol. Rev. 264(1) (2015) 182-203.

[59] E. Bignell, Reactive oxygen intermediates, pH, and calcium, American Society for Microbiology, 2009, pp. 217-228.

[60] C.M. Minutti, J.A. Knipper, J.E. Allen, D.M.W. Zaiss, Tissue-specific contribution of macrophages to wound healing, Semin. Cell Dev. Biol. 61 (2017) 3-11.

[61] M.R. Major, V.W. Wong, E.R. Nelson, M.T. Longaker, G.C. Gurtner, The Foreign Body Response: At the Interface of Surgery and Bioengineering, Plast. Reconstr. Surg. 135(5) (2015) 1489-1498.

[62] S.N. Christo, K.R. Diener, A. Bachhuka, K. Vasilev, J.D. Hayball, Innate immunity and biomaterials at the nexus: friends or foes, BioMed Res. Int. (2015) 342304/1-342304/23.

[63] S. Browne, A. Pandit, Biomaterial-mediated modification of the local inflammatory environment, Front Bioeng Biotechnol 3 (2015) 67.

[64] R. Garash, A. Bajpai, B.M. Marcinkiewicz, K.L. Spiller, Drug delivery strategies to control macrophages for tissue repair and regeneration, Exp. Biol. Med. (London, U. K.) 241(10) (2016) 1054-1063.

[65] P.M. Kou, J.E. Babensee, Macrophage and dendritic cell phenotypic diversity in the context of biomaterials, J. Biomed. Mater. Res., Part A 96A(1) (2011) 239-260.

[66] K. Spiller, Novel strategies to modulate the inflammatory response to biomaterial, American Chemical Society, 2016, pp. COLL-449.

[67] A. YazdanYar, U. Aschauer, P. Bowen, Interaction of biologically relevant ions and organic molecules with titanium oxide (rutile) surfaces: A review on molecular dynamics studies, Colloids Surf., B 161 (2018) 563-577.

[68] C.B. Borkner, S. Wohlrab, E. Moeller, G. Lang, T. Scheibel, Surface Modification of Polymeric Biomaterials Using Recombinant Spider Silk Proteins, ACS Biomater. Sci. Eng. 3(5) (2017) 767-775.

[69] S. Pacelli, V. Manoharan, A. Desalvo, N. Lomis, K.S. Jodha, S. Prakash, A. Paul, Tailoring biomaterial surface properties to modulate host-implant interactions: implication in cardiovascular and bone therapy, J. Mater. Chem. B 4(9) (2016) 1586-1599.

[70] J. Long, S. Lewis, T. Kuklo, Y. Zhu, K.D. Riew, The effect of cyclooxygenase-2 inhibitors on spinal fusion, J Bone Joint Surg Am 84-A(10) (2002) 1763-8.

[71] K.R. Stevens, N.J. Einerson, J.A. Burmania, W.J. Kao, In vivo biocompatibility of gelatin-based hydrogels and interpenetrating networks, J. Biomater. Sci., Polym. Ed. 13(12) (2002) 1353-1366.

[72] N. Mokarram, A. Merchant, V. Mukhatyar, G. Patel, R.V. Bellamkonda, Effect of modulating macrophage phenotype on peripheral nerve repair, Biomaterials 33(34) (2012) 8793-8801.

[73] K.L. Spiller, S. Nassiri, C.E. Witherel, R.R. Anfang, J. Ng, K.R. Nakazawa, T. Yu, G. Vunjak-Novakovic, Sequential delivery of immunomodulatory cytokines to facilitate the M1-to-M2

transition of macrophages and enhance vascularization of bone scaffolds, Biomaterials 37 (2015) 194-207.

[74] T. Harel-Adar, T. Ben Mordechai, Y. Amsalem, M.S. Feinberg, J. Leor, S. Cohen, Modulation of cardiac macrophages by phosphatidylserine-presenting liposomes improves infarct repair, Proc Natl Acad Sci U S A 108(5) (2011) 1827-32.

[75] S. Mukhopadhyay, A. Pluddemann, S. Gordon, Macrophage pattern recognition receptors in immunity, homeostasis and self tolerance, Adv Exp Med Biol 653 (2009) 1-14.

[76] R.S. Labow, D. Sa, L.A. Matheson, D.L. Dinnes, J.P. Santerre, The human macrophage response during differentiation and biodegradation on polycarbonate-based polyurethanes: dependence on hard segment chemistry, Biomaterials 26(35) (2005) 7357-66.

[77] R.S. Labow, D. Sa, L.A. Matheson, J.P. Santerre, Polycarbonate-urethane hard segment type influences esterase substrate specificity for human-macrophage-mediated biodegradation, J Biomater Sci Polym Ed 16(9) (2005) 1167-77.

[78] A. Boddupalli, L. Zhu, K.M. Bratlie, Methods for Implant Acceptance and Wound Healing: Material Selection and Implant Location Modulate Macrophage and Fibroblast Phenotypes, Adv Healthc Mater 5(20) (2016) 2575-2594.

[79] D.H. Kim, M.T. Novak, J. Wilkins, M. Kim, A. Sawyer, W.M. Reichert, Response of monocytes exposed to phagocytosable particles and discs of comparable surface roughness, Biomaterials 28(29) (2007) 4231-9.

[80] F. Piraino, S. Selimovic, A Current View of Functional Biomaterials for Wound Care, Molecular and Cellular Therapies, Biomed Res Int 2015 (2015) 403801.

[81] X. Shi, L. Chen, S. Li, X. Sun, F.Z. Cui, H. Ma, The observed difference of RAW264.7 macrophage phenotype on mineralized collagen and hydroxyapatite, Biomed Mater (2018).

[82] H.H. Xu, P. Wang, L. Wang, C. Bao, Q. Chen, M.D. Weir, L.C. Chow, L. Zhao, X. Zhou, M.A. Reynolds, Calcium phosphate cements for bone engineering and their biological properties, Bone Res 5 (2017) 17056.

[83] A. Lasser, The mononuclear phagocytic system: a review, Hum Pathol 14(2) (1983) 108-26.

[84] D.A. Hume, The mononuclear phagocyte system, Curr Opin Immunol 18(1) (2006) 49-53.

[85] J. Diebold, Mononuclear phagocyte system. Morphology and function of the principal constituting cells, Ann Pathol 6(1) (1986) 3-12.

[86] A. Volkman, J.L. Gowans, THE ORIGIN OF MACROPHAGES FROM BONE MARROW IN THE RAT, Br J Exp Pathol 46 (1965) 62-70.

[87] R. van Furth, Z.A. Cohn, The origin and kinetics of mononuclear phagocytes, J Exp Med 128(3) (1968) 415-35.

[88] A. Das, M. Sinha, S. Datta, M. Abas, S. Chaffee, C.K. Sen, S. Roy, Monocyte and Macrophage Plasticity in Tissue Repair and Regeneration, Am. J. Pathol. 185(10) (2015) 2596-2606.

[89] S. Gordon, P.R. Taylor, Monocyte and macrophage heterogeneity, Nat Rev Immunol 5(12) (2005) 953-64.

[90] N.N. Klemparskaya, 100 years of the phagocytosis doctrine (Ilya Ilyich Mechnikov), J Hyg Epidemiol Microbiol Immunol 27(3) (1983) 249-52.

[91] I. Rhee, Diverse macrophages polarization in tumor microenvironment, Arch. Pharmacal Res. 39(11) (2016) 1588-1596.

[92] J.W. Pollard, Macrophages define the invasive microenvironment in breast cancer, J Leukoc Biol 84(3) (2008) 623-30.

[93] M. Tariq, J. Zhang, G. Liang, L. Ding, Q. He, B. Yang, Macrophage Polarization: Anti-Cancer Strategies to Target Tumor-Associated Macrophage in Breast Cancer, J. Cell. Biochem. 118(9) (2017) 2484-2501.

[94] M.W. Teng, J.B. Swann, C.M. Koebel, R.D. Schreiber, M.J. Smyth, Immune-mediated dormancy: an equilibrium with cancer, J Leukoc Biol 84(4) (2008) 988-93.

[95] F. Tacke, H.W. Zimmermann, Macrophage heterogeneity in liver injury and fibrosis, J. Hepatol. 60(5) (2014) 1090-1096.

[96] D. Zhou, K. Yang, L. Chen, Y. Wang, W. Zhang, Z. Xu, J. Zuo, H. Jiang, J. Luan, Macrophage polarization and function: new prospects for fibrotic disease, Immunol Cell Biol 95(10) (2017) 864-869.

[97] A. Sica, P. Invernizzi, A. Mantovani, Macrophage plasticity and polarization in liver homeostasis and pathology, Hepatology 59(5) (2014) 2034-42.

[98] R.J. Homer, J.A. Elias, C.G. Lee, E. Herzog, Modern concepts on the role of inflammation in pulmonary fibrosis, Arch Pathol Lab Med 135(6) (2011) 780-8.

[99] C.N. Lumeng, J.L. Bodzin, A.R. Saltiel, Obesity induces a phenotypic switch in adipose tissue macrophage polarization, J Clin Invest 117(1) (2007) 175-84.

[100] F.M. Wensveen, S. Valentic, M. Sestan, T. Turk Wensveen, B. Polic, The "Big Bang" in obese fat: Events initiating obesity-induced adipose tissue inflammation, Eur J Immunol 45(9) (2015) 2446-56.

[101] K.L. Spiller, T.J. Koh, Macrophage-based therapeutic strategies in regenerative medicine, Adv. Drug Delivery Rev. (2017) Ahead of Print.

[102] A. Mantovani, S.K. Biswas, M.R. Galdiero, A. Sica, M. Locati, Macrophage plasticity and polarization in tissue repair and remodelling, J. Pathol. 229(2) (2013) 176-185.

[103] D. Strauss-Ayali, S.M. Conrad, D.M. Mosser, Monocyte subpopulations and their differentiation patterns during infection, J Leukoc Biol 82(2) (2007) 244-52.

[104] C.V. Jakubzick, G.J. Randolph, P.M. Henson, Monocyte differentiation and antigen-presenting functions, Nat Rev Immunol 17(6) (2017) 349-362.

[105] M. Collin, V. Bigley, Monocyte, Macrophage, and Dendritic Cell Development: the Human Perspective, Microbiol Spectr 4(5) (2016).

[106] F. Verdeguer, M. Aouadi, Macrophage heterogeneity and energy metabolism, Exp Cell Res (2017).

[107] J.E. Rayahin, R.A. Gemeinhart, Activation of Macrophages in Response to Biomaterials, Results Probl Cell Differ 62 (2017) 317-351.

[108] J.L. Shepard, L.I. Zon, Developmental derivation of embryonic and adult macrophages, Curr Opin Hematol 7(1) (2000) 3-8.

[109] I.G. Winkler, N.A. Sims, A.R. Pettit, V. Barbier, B. Nowlan, F. Helwani, I.J. Poulton, N. van Rooijen, K.A. Alexander, L.J. Raggatt, J.P. Levesque, Bone marrow macrophages maintain

hematopoietic stem cell (HSC) niches and their depletion mobilizes HSCs, Blood 116(23) (2010) 4815-28.

[110] S. Gordon, Pattern recognition receptors: doubling up for the innate immune response, Cell 111(7) (2002) 927-30.

[111] S. Gordon, Pathogen recognition or homeostasis? APC receptor functions in innate immunity, C R Biol 327(6) (2004) 603-7.

[112] S. Akira, K. Takeda, T. Kaisho, Toll-like receptors: critical proteins linking innate and acquired immunity, Nat Immunol 2(8) (2001) 675-80.

[113] S.S. Mano, K. Kanehira, A. Taniguchi, Comparison of Cellular Uptake and Inflammatory Response via Toll-Like Receptor 4 to Lipopolysaccharide and Titanium Dioxide Nanoparticles, International Journal of Molecular Sciences 14(7) (2013) 13154-13170.

[114] L. Peiser, S. Mukhopadhyay, S. Gordon, Scavenger receptors in innate immunity, Curr Opin Immunol 14(1) (2002) 123-8.

[115] S. Zamze, L. Martinez-Pomares, H. Jones, P.R. Taylor, R.J. Stillion, S. Gordon, S.Y. Wong, Recognition of bacterial capsular polysaccharides and lipopolysaccharides by the macrophage mannose receptor, J Biol Chem 277(44) (2002) 41613-23.

[116] Z. Szondy, Z. Sarang, B. Kiss, É. Garabuczi, K. Köröskényi, Anti-inflammatory Mechanisms Triggered by Apoptotic Cells during Their Clearance, Frontiers in Immunology 8 (2017) 909.

[117] P. Allavena, M. Chieppa, P. Monti, L. Piemonti, From pattern recognition receptor to regulator of homeostasis: the double-faced macrophage mannose receptor, Crit Rev Immunol 24(3) (2004) 179-92.

[118] S. Guo, L.A. Di Pietro, Factors affecting wound healing, J. Dent. Res. 89(3) (2010) 219-229.

[119] J.E. Allen, D. Ruckerl, The Silent Undertakers: Macrophages Programmed for Efferocytosis, Immunity 47(5) (2017) 810-812.

[120] J. Dalli, C. Serhan, Macrophage proresolving mediators-the when and where, Microbiol. Spectrum 4(3) (2016) 1-2.

[121] A. Blocki, S. Beyer, J.-Y. Dewavrin, A. Goralczyk, Y. Wang, P. Peh, M. Ng, S.S. Moonshi, S. Vuddagiri, M. Raghunath, E.C. Martinez, K. Bhakoo, Microcapsules engineered to support

mesenchymal stem cell (MSC) survival and proliferation enable long-term retention of MSCs in infarcted myocardium, Biomaterials 53 (2015) 12-24.

[122] C.D. Paavola, S. Hemmerich, D. Grunberger, I. Polsky, A. Bloom, R. Freedman, M. Mulkins, S. Bhakta, D. McCarley, L. Wiesent, B. Wong, K. Jarnagin, T.M. Handel, Monomeric monocyte chemoattractant protein-1 (MCP-1) binds and activates the MCP-1 receptor CCR2B, J. Biol. Chem. FIELD Full Journal Title:Journal of Biological Chemistry 273(50) (1998) 33157-33165.

[123] L.A. DiPietro, M. Burdick, Q.E. Low, S.L. Kunkel, R.M. Strieter, MIP-1alpha as a critical macrophage chemoattractant in murine wound repair, J Clin Invest 101(8) (1998) 1693-8.

[124] A.K. Azad, M.V.S. Rajaram, L.S. Schlesinger, Exploitation of the Macrophage Mannose Receptor (CD206) in Infectious Disease Diagnostics and Therapeutics, Journal of cytology & molecular biology 1(1) (2014) 1000003.

[125] S. Mukhopadhyay, S. Gordon, The role of scavenger receptors in pathogen recognition and innate immunity, Immunobiology 209(1-2) (2004) 39-49.

[126] M. Kulka, L. Alexopoulou, R.A. Flavell, D.D. Metcalfe, Activation of mast cells by double-stranded RNA: evidence for activation through Toll-like receptor 3, Journal of Allergy and Clinical Immunology 114(1) 174-182.

[127] B.S. Park, J.-O. Lee, Recognition of lipopolysaccharide pattern by TLR4 complexes, Experimental &Amp; Molecular Medicine 45 (2013) e66.

[128] F. Hayashi, K.D. Smith, A. Ozinsky, T.R. Hawn, E.C. Yi, D.R. Goodlett, J.K. Eng, S. Akira, D.M. Underhill, A. Aderem, The innate immune response to bacterial flagellin is mediated by Toll-like receptor 5, Nature 410 (2001) 1099.

[129] O. Takeuchi, T. Kawai, P.F. Mühlradt, M. Morr, J.D. Radolf, A. Zychlinsky, K. Takeda, S. Akira, Discrimination of bacterial lipoproteins by Toll-like receptor 6, International Immunology 13(7) (2001) 933-940.

[130] F. Heil, H. Hemmi, H. Hochrein, F. Ampenberger, C. Kirschning, S. Akira, G. Lipford, H. Wagner, S. Bauer, Species-Specific Recognition of Single-Stranded RNA via Toll-like Receptor 7 and 8, Science 303(5663) (2004) 1526.

[131] T. Kawai, S. Akira, The role of pattern-recognition receptors in innate immunity: update on Toll-like receptors, Nat Immunol 11(5) (2010) 373-84.

[132] G.D. Ross, Regulation of the adhesion versus cytotoxic functions of the Mac-1/CR3/alphaMbeta2-integrin glycoprotein, Crit Rev Immunol 20(3) (2000) 197-222.

[133] F. Porcheray, S. Viaud, A.C. Rimaniol, C. Leone, B. Samah, N. Dereuddre-Bosquet, D. Dormont, G. Gras, Macrophage activation switching: An asset for the resolution of inflammation, Clin. Exp. Immunol. 142(3) (2005) 481-489.

[134] R. Sridharan, A.R. Cameron, D.J. Kelly, C.J. Kearney, F.J. O'Brien, Biomaterial based modulation of macrophage polarization: a review and suggested design principles, Mater. Today (Oxford, U. K.) 18(6) (2015) 313-325.

[135] R.D. Stout, C. Jiang, B. Matta, I. Tietzel, S.K. Watkins, J. Suttles, Macrophages Sequentially Change Their Functional Phenotype in Response to Changes in Microenvironmental Influences, J. Immunol. 175(1) (2005) 342-349.

[136] C.D. Mills, K. Kincaid, J.M. Alt, M.J. Heilman, A.M. Hill, M-1/M-2 macrophages and the Th1/Th2 paradigm, J. Immunol. 164(12) (2000) 6166-6173.

[137] C. Shi, E.G. Pamer, Monocyte recruitment during infection and inflammation, Nat. Rev. Immunol. 11(11) (2011) 762-774.

[138] D.M. Mosser, J.P. Edwards, Exploring the full spectrum of macrophage activation, Nat. Rev. Immunol. 8(12) (2008) 958-969.

[139] P.J. Murray, J.E. Allen, S.K. Biswas, E.A. Fisher, D.W. Gilroy, S. Goerdt, S. Gordon, J.A. Hamilton, L.B. Ivashkiv, T. Lawrence, Macrophage activation and polarization: nomenclature and experimental guidelines, Immunity 41(1) (2014) 14-20.

[140] C.D. Mills, K. Ley, K. Buchmann, J. Canton, Sequential Immune Responses: The Weapons of Immunity, J Innate Immun 7(5) (2015) 443-9.

[141] F.O. Martinez, A. Sica, A. Mantovani, M. Locati, Macrophage activation and polarization, Frontiers in bioscience : a journal and virtual library 13 (2008) 453-461.

[142] G.B. Mackaness, Cellular immunity and the parasite, Adv Exp Med Biol 93 (1977) 65-73.

[143] J.J. O'Shea, P.J. Murray, Cytokine signaling modules in inflammatory responses, Immunity 28(4) (2008) 477-87.

[144] K. Schroder, P.J. Hertzog, T. Ravasi, D.A. Hume, Interferon-gamma: an overview of signals, mechanisms and functions, J Leukoc Biol 75(2) (2004) 163-89.

[145] H. Yamada, M.A. Odonnell, T. Matsumoto, Y. Luo, Interferon-gamma up-regulates toll-like receptor 4 and cooperates with lipopolysaccharide to produce macrophage-derived chemokine and interferon-gamma inducible protein-10 in human bladder cancer cell line RT4, J Urol 174(3) (2005) 1119-23.

[146] M. Yamamoto, S. Sato, H. Hemmi, K. Hoshino, T. Kaisho, H. Sanjo, O. Takeuchi, M. Sugiyama, M. Okabe, K. Takeda, S. Akira, Role of adaptor TRIF in the MyD88-independent toll-like receptor signaling pathway, Science 301(5633) (2003) 640-3.

[147] N. Parameswaran, S. Patial, Tumor necrosis factor-alpha signaling in macrophages, Crit Rev Eukaryot Gene Expr 20(2) (2010) 87-103.

[148] C.L. Langrish, Y. Chen, W.M. Blumenschein, J. Mattson, B. Basham, J.D. Sedgwick, T. McClanahan, R.A. Kastelein, D.J. Cua, IL-23 drives a pathogenic T cell population that induces autoimmune inflammation, J Exp Med 201(2) (2005) 233-40.

[149] O.A. Akinrinmade, S. Chetty, A.K. Daramola, M.U. Islam, T. Thepen, S. Barth, CD64: An Attractive Immunotherapeutic Target for M1-type Macrophage Mediated Chronic Inflammatory Diseases, Biomedicines 5(3) (2017).

[150] C. Vasu, A. Wang, S.R. Gorla, S. Kaithamana, B.S. Prabhakar, M.J. Holterman, CD80 and CD86 C domains play an important role in receptor binding and co-stimulatory properties, Int Immunol 15(2) (2003) 167-75.

[151] T.M. Holling, E. Schooten, P.J. van Den Elsen, Function and regulation of MHC class II molecules in T-lymphocytes: of mice and men, Hum Immunol 65(4) (2004) 282-90.

[152] A. Mantovani, A. Sica, S. Sozzani, P. Allavena, A. Vecchi, M. Locati, The chemokine system in diverse forms of macrophage activation and polarization, Trends in immunology 25(12) (2004) 677-686.

[153] B.N. Brown, B.D. Ratner, S.B. Goodman, S. Amar, S.F. Badylak, Macrophage polarization: An opportunity for improved outcomes in biomaterials and regenerative medicine, Biomaterials 33(15) (2012) 3792-3802.

[154] J.P. Edwards, X. Zhang, K.A. Frauwirth, D.M. Mosser, Biochemical and functional characterization of three activated macrophage populations, J Leukoc Biol 80(6) (2006) 1298-307.

[155] M.L. Novak, T.J. Koh, Phenotypic Transitions of Macrophages Orchestrate Tissue Repair, Am. J. Pathol. 183(5) (2013) 1352-1363.

[156] D.M. Mosser, The many faces of macrophage activation, J Leukoc Biol 73(2) (2003) 209-12.

[157] S. Galván-Peña, L.A.J. O'Neill, Metabolic Reprograming in Macrophage Polarization, Frontiers in Immunology 5 (2014) 420.

[158] T. Roszer, Understanding the Mysterious M2 Macrophage through Activation Markers and Effector Mechanisms, Mediators Inflamm 2015 (2015) 816460.

[159] N. Wang, H. Liang, K. Zen, Molecular mechanisms that influence the macrophage m1-m2 polarization balance, Front Immunol 5 (2014) 614.

[160] A.A. Filardy, D.R. Pires, M.P. Nunes, C.M. Takiya, C.G. Freire-de-Lima, F.L. Ribeiro-Gomes, G.A. DosReis, Proinflammatory clearance of apoptotic neutrophils induces an IL-12(low)IL-10(high) regulatory phenotype in macrophages, J Immunol 185(4) (2010) 2044-50.

[161] A. Asai, K. Nakamura, M. Kobayashi, D.N. Herndon, F. Suzuki, CCL1 released from M2b macrophages is essentially required for the maintenance of their properties, J Leukoc Biol 92(4) (2012) 859-67.

[162] K.F. MacKenzie, K. Clark, S. Naqvi, V.A. McGuire, G. Nöehren, Y. Kristariyanto, M. van den Bosch, M. Mudaliar, P.C. McCarthy, M.J. Pattison, P.G.A. Pedrioli, G.J. Barton, R. Toth, A. Prescott, J.S.C. Arthur, PGE(2) Induces Macrophage IL-10 Production and a Regulatory-like Phenotype via a Protein Kinase A–SIK–CRTC3 Pathway, The Journal of Immunology Author Choice 190(2) (2013) 565-577.

[163] F.L. Ribeiro-Gomes, A.C. Otero, N.A. Gomes, M.C. Moniz-De-Souza, L. Cysne-Finkelstein, A.C. Arnholdt, V.L. Calich, S.G. Coutinho, M.F. Lopes, G.A. DosReis, Macrophage interactions with neutrophils regulate Leishmania major infection, J Immunol 172(7) (2004) 4454-62.

[164] Y. Yue, X. Yang, K. Feng, L. Wang, J. Hou, B. Mei, H. Qin, M. Liang, G. Chen, Z. Wu, M2b macrophages reduce early reperfusion injury after myocardial ischemia in mice: A predominant role of inhibiting apoptosis via A20, Int J Cardiol 245 (2017) 228-235.

[165] F.O. Martinez, S. Gordon, The M1 and M2 paradigm of macrophage activation: time for reassessment, F1000Prime Rep 6 (2014) 13.

[166] J.H. Graversen, M. Madsen, S.K. Moestrup, CD163: a signal receptor scavenging haptoglobin-hemoglobin complexes from plasma, Int J Biochem Cell Biol 34(4) (2002) 309-14.

[167] J.H. Thomsen, A. Etzerodt, P. Svendsen, S.K. Moestrup, The haptoglobin-CD163-heme oxygenase-1 pathway for hemoglobin scavenging, Oxid Med Cell Longev 2013 (2013) 523652.

[168] A. Etzerodt, S.K. Moestrup, CD163 and inflammation: biological, diagnostic, and therapeutic aspects, Antioxid Redox Signal 18(17) (2013) 2352-63.

[169] K. Kowal, R. Silver, E. Slawinska, M. Bielecki, L. Chyczewski, O. Kowal-Bielecka, CD163 and its role in inflammation, Folia Histochem Cytobiol 49(3) (2011) 365-74.

[170] Y. Qiu, K. Park, Environment-sensitive hydrogels for drug delivery, Adv Drug Deliv Rev 53(3) (2001) 321-39.

[171] G.D. Keeler, J.M. Durdik, J.A. Stenken, Effects of delayed delivery of dexamethasone-21-phosphate via subcutaneous microdialysis implants on macrophage activation in rats, Acta Biomaterialia 23 (2015) 27-37.

[172] A. Mantovani, S.K. Biswas, M.R. Galdiero, A. Sica, M. Locati, Macrophage plasticity and polarization in tissue repair and remodelling, The Journal of pathology 229(2) (2013) 176-185.

[173] F.O. Martinez, L. Helming, S. Gordon, Alternative activation of macrophages: an immunologic functional perspective, Annu. Rev. Immunol. 27 (2009) 451-483.

[174] M. Sironi, F.O. Martinez, D. D'Ambrosio, M. Gattorno, N. Polentarutti, M. Locati, A. Gregorio, A. Iellem, M.A. Cassatella, J. Van Damme, S. Sozzani, A. Martini, F. Sinigaglia, A. Vecchi, A. Mantovani, Differential regulation of chemokine production by Fcgamma receptor engagement in human monocytes: association of CCL1 with a distinct form of M2 monocyte activation (M2b, Type 2), J Leukoc Biol 80(2) (2006) 342-9.

[175] J.M. Morais, F. Papadimitrakopoulos, D.J. Burgess, Biomaterials/tissue interactions: possible solutions to overcome foreign body response, AAPS J. 12(2) (2010) 188-196.

[176] B.N. Brown, B.M. Sicari, S.F. Badylak, Rethinking regenerative medicine: a macrophage-centered approach, Front. Immunol. 5 (2014) 1-11.

[177] G.D. Keeler, J.M. Durdik, J.A. Stenken, Effects of delayed delivery of dexamethasone-21-phosphate via subcutaneous microdialysis implants on macrophage activation in rats, Acta Biomater 23 (2015) 27-37.

[178] G.D. Keeler, J.M. Durdik, J.A. Stenken, Localized delivery of dexamethasone-21-phosphate via microdialysis implants in rat induces M(GC) macrophage polarization and alters CCL2 concentrations, Acta Biomater 12 (2015) 11-20.

[179] N.M. Vacanti, H. Cheng, P.S. Hill, J.D.T. Guerreiro, T.T. Dang, M. Ma, S. Watson, N.S. Hwang, R. Langer, D.G. Anderson, Localized Delivery of Dexamethasone from Electrospun Fibers Reduces the Foreign Body Response, Biomacromolecules 13(10) (2012) 3031-3038.

[180] D. Akilbekova, R. Philiph, A. Graham, K.M. Bratlie, Macrophage reprogramming: influence of latex beads with various functional groups on macrophage phenotype and phagocytic uptake in vitro, Journal Of Biomedical Materials Research. Part A 103(1) (2015) 262-268.

[181] A.R.D. Reeves, K.L. Spiller, D.O. Freytes, G. Vunjak-Novakovic, D.L. Kaplan, Controlled release of cytokines using silk-biomaterials for macrophage polarization, Biomaterials 73 (2015) 272-283.

[182] W.J. Kao, A.K. McNally, A. Hiltner, J.M. Anderson, Role for interleukin-4 foreign-body giant cell formation on a poly(etherurethane urea) in vivo, J. Biomed. Mater. Res. 29(10) (1995) 1267-75.

[183] R.M. Boehler, R. Kuo, S. Shin, A.G. Goodman, M.A. Pilecki, J.N. Leonard, L.D. Shea, Lentivirus delivery of IL-10 to promote and sustain macrophage polarization towards an anti-inflammatory phenotype [Erratum to document cited in CA160:689265], Biotechnol. Bioeng. 111(7) (2014) 1469.

[184] M.M. Alvarez, J.C. Liu, G. Trujillo-de Santiago, B.-H. Cha, A. Vishwakarma, A.M. Ghaemmaghami, A. Khademhosseini, Delivery strategies to control inflammatory response: Modulating M1-M2 polarization in tissue engineering applications, J. Controlled Release 240 (2016) 349-363.

[185] C.M. Dumont, J. Park, L.D. Shea, Controlled release strategies for modulating immune responses to promote tissue regeneration, J. Controlled Release 219 (2015) 155-166.

[186] J.R. Potas, F. Haque, F.L. Maclean, D.R. Nisbet, Interleukin-10 conjugated electrospun polycaprolactone (PCL) nanofibre scaffolds for promoting alternatively activated (M2) macrophages around the peripheral nerve in vivo, J. Immunol. Methods 420 (2015) 38-49.

[187] D.P. Vasconcelos, M. Costa, I.F. Amaral, M.A. Barbosa, A.P. Águas, J.N. Barbosa, Development of an immunomodulatory biomaterial: using resolvin D1 to modulate inflammation, Biomaterials 53 (2015) 566-73.

[188] Q. Qu, W. Xuan, G.-H. Fan, Roles of resolvins in the resolution of acute inflammation, Cell Biol. Int. 39(1) (2015) 3-22.

[189] D.P. Vasconcelos, M. Costa, I.F. Amaral, M.A. Barbosa, A.P. Aguas, J.N. Barbosa, Modulation of the inflammatory response to chitosan through M2 macrophage polarization using pro-resolution mediators, Biomaterials 37 (2015) 116-123.

[190] E.M. Hetrick, H.L. Prichard, B. Klitzman, M.H. Schoenfisch, Reduced foreign body response at nitric oxide-releasing subcutaneous implants, Biomaterials 28(31) (2007) 4571-4580.

[191] S.P. Nichols, A. Koh, N.L. Brown, M.B. Rose, B. Sun, D.L. Slomberg, D.A. Riccio, B. Klitzman, M.H. Schoenfisch, The effect of nitric oxide surface flux on the foreign body response to subcutaneous implants, Biomaterials 33(27) (2012) 6305-6312.

[192] R. Newton, N.S. Holden, Separating transrepression and transactivation: a distressing divorce for the glucocorticoid receptor?, Mol. Pharmacol. 72(4) (2007) 799-809.

[193] M.A. Hoeppner, J.C. Mordacq, D.I.H. Linzer, Role of the composite glucocorticoid response element in proliferin gene expression, Gene Expression 5(2) (1995) 133-41.

[194] F. Re, M. Muzio, M. De Rossi, N. Polentarutti, J.G. Giri, A. Mantovani, F. Colotta, The type II "receptor" as a decoy target for interleukin 1 in polymorphonuclear leukocytes: characterization of induction by dexamethasone and ligand binding properties of the released decoy receptor, J. Exp. Med. 179(2) (1994) 739-43.

[195] S. Bhattacharyya, D.E. Brown, J.A. Brewer, S.K. Vogt, L.J. Muglia, Macrophage glucocorticoid receptors regulate Toll-like receptor-4-mediated inflammatory responses by selective inhibition of p38 MAP kinase, Blood 109(10) (2007) 4313-4319.

[196] J.-i. Tanabe, M. Watanabe, S. Mue, K. Ohuchi, Dexamethasone inhibits the production of macrophage inflammatory protein 2 in the leukocytes in rat allergic inflammation, Eur. J. Pharmacol. 284(3) (1995) 257-63.

[197] Y. Nakamura, T. Murai, Y. Ogawa, Effect of in vitro and in vivo administration of dexamethasone on rat macrophage functions: comparison between alveolar and peritoneal macrophages, Eur Respir J 9(2) (1996) 301-6.

[198] U. Klueh, M. Kaur, D.C. Montrose, D.L. Kreutzer, Inflammation and glucose sensors: use of dexamethasone to extend glucose sensor function and life span in vivo, J Diabetes Sci Technol 1(4) (2007) 496-504.

[199] L.W. Norton, J. Park, J.E. Babensee, Biomaterial adjuvant effect is attenuated by anti-inflammatory drug delivery or material selection, J. Controlled Release 146(3) (2010) 341-348.

[200] U. auf dem Keller, C.L. Bellac, Y. Li, Y. Lou, P.F. Lange, R. Ting, C. Harwig, R. Kappelhoff, S. Dedhar, M.J. Adam, T.J. Ruth, F. Benard, D.M. Perrin, C.M. Overall, Novel Matrix Metalloproteinase Inhibitor [18F]Marimastat-Aryltrifluoroborate as a Probe for In vivo Positron Emission Tomography Imaging in Cancer, Cancer Res. FIELD Full Journal Title:Cancer Research 70(19) 7562-7569.

[201] W. Zhou, K. Hashimoto, K. Goleniewska, J.F. O'Neal, S. Ji, T.S. Blackwell, G.A. FitzGerald, K.M. Egan, M.W. Geraci, R.S. Peebles, Jr., Prostaglandin I2 analogs inhibit proinflammatory cytokine production and T cell stimulatory function of dendritic cells, J. Immunol. 178(2) (2007) 702-710.

[202] W. Zhou, T.S. Blackwell, K. Goleniewska, J.F. O'Neal, G.A. Fitzgerald, M. Lucitt, R.M. Breyer, R.S. Peebles, Jr., Prostaglandin I2 analogs inhibit Th1 and Th2 effector cytokine production by CD4 T cells, Journal of leukocyte biology 81(3) (2007) 809-817.

[203] M.K. Tsai, C.C. Hsieh, H.F. Kuo, M.S. Lee, M.Y. Huang, C.H. Kuo, C.H. Hung, Effect of prostaglandin I2 analogs on monocyte chemoattractant protein-1 in human monocyte and macrophage, Clin Exp Med 15(3) (2015) 245-53.

[204] S.L. Dorris, R.S. Peebles, Jr., PGI2 as a regulator of inflammatory diseases, Mediators Inflammation (2012) 926968, 9 pp.

[205] D.M. Aronoff, C.M. Peres, C.H. Serezani, M.N. Ballinger, J.K. Carstens, N. Coleman, B.B. Moore, R.S. Peebles, L.H. Faccioli, M. Peters-Golden, Synthetic prostacyclin analogs differentially regulate macrophage function via distinct analog-receptor binding specificities, J Immunol 178(3) (2007) 1628-34.

[206] R. Stratton, X. Shiwen, Role of prostaglandins in fibroblast activation and fibrosis, J Cell Commun Signal 4(2) (2010) 75-7.

[207] R.J. Gryglewski, Prostacyclin among prostanoids, Pharmacol. Rep. 60(1) (2008) 3-11.

[208] K.N. Couper, D.G. Blount, E.M. Riley, IL-10: the master regulator of immunity to infection, J Immunol 180(9) (2008) 5771-7.

[209] C. Berlato, M.A. Cassatella, I. Kinjyo, L. Gatto, A. Yoshimura, F. Bazzoni, Involvement of suppressor of cytokine signaling-3 as a mediator of the inhibitory effects of IL-10 on lipopolysaccharide-induced macrophage activation, J Immunol 168(12) (2002) 6404-11.

[210] A. Gordon, E.D. Kozin, S.G. Keswani, S.S. Vaikunth, A.B. Katz, P.W. Zoltick, M. Favata, A.P. Radu, L.J. Soslowsky, M. Herlyn, T.M. Crombleholme, Permissive environment in postnatal wounds induced by adenoviral-mediated overexpression of the anti-inflammatory cytokine interleukin-10 prevents scar formation, Wound Repair Regen 16(1) (2008) 70-9.

[211] W. Ouyang, S. Rutz, N.K. Crellin, P.A. Valdez, S.G. Hymowitz, Regulation and functions of the IL-10 family of cytokines in inflammation and disease, Annu. Rev. Immunol. 29 (2011) 71-109.

[212] H.-N. Lee, Y.-J. Surh, Therapeutic potential of resolvins in the prevention and treatment of inflammatory disorders, Biochem. Pharmacol. (Amsterdam, Neth.) 84(10) (2012) 1340-1350.

[213] R. Mobasseri, L. Tian, M. Soleimani, S. Ramakrishna, H. Naderi-Manesh, Bio-active molecules modified surfaces enhanced mesenchymal stem cell adhesion and proliferation, Biochem Biophys Res Commun 483(1) (2017) 312-317.

[214] G.S. Boersema, N. Grotenhuis, Y. Bayon, J.F. Lange, Y.M. Bastiaansen-Jenniskens, The Effect of Biomaterials Used for Tissue Regeneration Purposes on Polarization of Macrophages, Biores Open Access 5(1) (2016) 6-14.

[215] G. Stynes, G.K. Kiroff, W.A. Morrison, M.A. Kirkland, Tissue compatibility of biomaterials: benefits and problems of skin biointegration, ANZ J Surg 78(8) (2008) 654-9.

[216] I. Tokarev, S. Minko, Stimuli-responsive porous hydrogels at interfaces for molecular filtration, separation, controlled release, and gating in capsules and membranes, Adv Mater 22(31) (2010) 3446-62.

[217] J.T. Zhang, S. Petersen, M. Thunga, E. Leipold, R. Weidisch, X. Liu, A. Fahr, K.D. Jandt, Micro-structured smart hydrogels with enhanced protein loading and release efficiency, Acta Biomater 6(4) (2010) 1297-306.

[218] N. Davidenko, C.F. Schuster, D.V. Bax, N. Raynal, R.W. Farndale, S.M. Best, R.E. Cameron, Control of crosslinking for tailoring collagen-based scaffolds stability and mechanics, Acta Biomater 25 (2015) 131-42.

[219] M. Monaghan, S. Browne, K. Schenke-Layland, A. Pandit, A collagen-based scaffold delivering exogenous microrna-29B to modulate extracellular matrix remodeling, Mol Ther 22(4) (2014) 786-96.

[220] F. Wang, M. Wang, Z. She, K. Fan, C. Xu, B. Chu, C. Chen, S. Shi, R. Tan, Collagen/chitosan based two-compartment and bi-functional dermal scaffolds for skin regeneration, Mater Sci Eng C Mater Biol Appl 52 (2015) 155-62.

[221] R. Jayakumar, M. Prabaharan, P.T. Sudheesh Kumar, S.V. Nair, H. Tamura, Biomaterials based on chitin and chitosan in wound dressing applications, Biotechnol Adv 29(3) (2011) 322-37.

[222] F. Ding, H. Deng, Y. Du, X. Shi, Q. Wang, Emerging chitin and chitosan nanofibrous materials for biomedical applications, Nanoscale 6(16) (2014) 9477-93.

[223] E. Khor, L.Y. Lim, Implantable applications of chitin and chitosan, Biomaterials 24(13) (2003) 2339-49.

[224] D.J. Hines, D.L. Kaplan, Poly(lactic-co-glycolic) acid-controlled-release systems: experimental and modeling insights, Crit Rev Ther Drug Carrier Syst 30(3) (2013) 257-76.

[225] S. Fredenberg, M. Wahlgren, M. Reslow, A. Axelsson, The mechanisms of drug release in poly(lactic-co-glycolic acid)-based drug delivery systems--a review, Int J Pharm 415(1-2) (2011) 34-52.

[226] G. Kumar, N. Shafiq, S. Malhotra, Drug-loaded PLGA nanoparticles for oral administration: fundamental issues and challenges ahead, Crit Rev Ther Drug Carrier Syst 29(2) (2012) 149-82.

[227] Y.P. Jiao, F.Z. Cui, Surface modification of polyester biomaterials for tissue engineering, Biomed Mater 2(4) (2007) R24-37.

[228] A. Privalova, E. Markvicheva, C. Sevrin, M. Drozdova, C. Kottgen, B. Gilbert, M. Ortiz, C. Grandfils, Biodegradable polyester-based microcarriers with modified surface tailored for tissue engineering, J Biomed Mater Res A 103(3) (2015) 939-48.

[229] P. Kingshott, G. Andersson, S.L. McArthur, H.J. Griesser, Surface modification and chemical surface analysis of biomaterials, Curr Opin Chem Biol 15(5) (2011) 667-76.

[230] R. Vasita, I.K. Shanmugam, D.S. Katt, Improved biomaterials for tissue engineering applications: surface modification of polymers, Curr Top Med Chem 8(4) (2008) 341-53.

[231] A.L. Moore, C.D. Marshall, M.T. Longaker, Minimizing Skin Scarring through Biomaterial Design, J Funct Biomater 8(1) (2017).

[232] E.M. Sussman, L.R. Madden, B.D. Ratner, Pore size of implanted biomaterials modulates macrophage polarity, Trans. Annu. Meet. Soc. Biomater. 32(Annual Meeting of the Society for Biomaterials: Giving Life to a World of Materials, 2010, Volume 1) (2010) 247.

[233] M. Jafari, Z. Paknejad, M.R. Rad, S.R. Motamedian, M.J. Eghbal, N. Nadjmi, A. Khojasteh, Polymeric scaffolds in tissue engineering: a literature review, J Biomed Mater Res B Appl Biomater 105(2) (2017) 431-459.

[234] M.L. Jarman-Smith, T. Bodamyali, C. Stevens, J.A. Howell, M. Horrocks, J.B. Chaudhuri, Porcine collagen crosslinking, degradation and its capability for fibroblast adhesion and proliferation, J Mater Sci Mater Med 15(8) (2004) 925-32.

[235] S.F. Badylak, T.W. Gilbert, Immune response to biologic scaffold materials, Semin Immunol 20(2) (2008) 109-16.

[236] S.F. Badylak, J.E. Valentin, A.K. Ravindra, G.P. McCabe, A.M. Stewart-Akers, Macrophage phenotype as a determinant of biologic scaffold remodeling, Tissue Engineering Part A 14(11) (2008) 1835-1842.

[237] B.N. Brown, J.E. Valentin, A.M. Stewart-Akers, G.P. McCabe, S.F. Badylak, Macrophage phenotype and remodeling outcomes in response to biologic scaffolds with and without a cellular component, Biomaterials 30(8) (2009) 1482-91.

[238] B.N. Brown, R. Londono, S. Tottey, L. Zhang, K.A. Kukla, M.T. Wolf, K.A. Daly, J.E. Reing, S.F. Badylak, Macrophage phenotype as a predictor of constructive remodeling following the implantation of biologically derived surgical mesh materials, Acta Biomater 8(3) (2012) 978-87.

[239] M. Kastellorizios, F. Papadimitrakopoulos, D.J. Burgess, Multiple tissue response modifiers to promote angiogenesis and prevent the foreign body reaction around subcutaneous implants, J Control Release 214 (2015) 103-11.

[240] V. Maquet, D. Martin, B. Malgrange, R. Franzen, J. Schoenen, G. Moonen, R. Jerome, Peripheral nerve regeneration using bioresorbable macroporous polylactide scaffolds, J. Biomed. Mater. Res. 52(4) (2000) 639-651.

[241] T. Noguchi, T. Yamamuro, M. Oka, P. Kumar, Y. Kotoura, S. Hyon, Y. Ikada, Poly(vinyl alcohol) hydrogel as an artificial articular cartilage: evaluation of biocompatibility, J Appl Biomater 2(2) (1991) 101-7.

[242] F. Gottrup, M.S. Agren, T. Karlsmark, Models for use in wound healing research: a survey focusing on in vitro and in vivo adult soft tissue, Wound Repair Regen 8(2) (2000) 83-96.

[243] D.L. Deskins, S. Ardestani, P.P. Young, The polyvinyl alcohol sponge model implantation, J Vis Exp (62) (2012).

[244] D.T. Efron, A. Barbul, Subcutaneous sponge models, Methods Mol Med 78 (2003) 83-93.

[245] M.I. Baker, S.P. Walsh, Z. Schwartz, B.D. Boyan, A review of polyvinyl alcohol and its uses in cartilage and orthopedic applications, J. Biomed. Mater. Res., Part B 100B(5) (2012) 1451-1457.

[246] S.J. Bryant, K.A. Davis-Arehart, N. Luo, R.K. Shoemaker, J.A. Arthur, K.S. Anseth, Synthesis and Characterization of Photopolymerized Multifunctional Hydrogels: Water-Soluble Poly(Vinyl Alcohol) and Chondroitin Sulfate Macromers for Chondrocyte Encapsulation, Macromolecules 37(18) (2004) 6726-6733.

[247] M. Yamamoto, Y. Tabata, H. Kawasaki, Y. Ikada, Promotion of fibrovascular tissue ingrowth into porous sponges by basic fibroblast growth factor, J Mater Sci Mater Med 11(4) (2000) 213-8.

[248] C.S. Brazel, N.A. Peppas, Dimensionless analysis of swelling of hydrophilic glassy polymers with subsequent drug release from relaxing structures, Biomaterials 20(8) (1999) 721-32.

[249] J.K. Li, N. Wang, X.S. Wu, Poly(vinyl alcohol) nanoparticles prepared by freezing-thawing process for protein/peptide drug delivery, J Control Release 56(1-3) (1998) 117-26.

[250] M. Gobbels, M. Spitznas, Effects of artificial tears on corneal epithelial permeability in dry eyes, Graefes Arch Clin Exp Ophthalmol 229(4) (1991) 345-9.

[251] J. Glowacki, S. Mizuno, Collagen scaffolds for tissue engineering, Biopolymers 89(5) (2008) 338-344.

[252] F.J. O'Brien, Biomaterials & scaffolds for tissue engineering, Mater. Today (Oxford, U. K.) 14(3) (2011) 88-95.

[253] M. Hidaka, K. Takahashi, Fine Structure and Mechanical Properties of the Catch Apparatus of the Sea-Urchin Spine, a Collagenous Connective Tissue with Muscle-Like Holding Capacity, Journal of Experimental Biology 103(1) (1983) 1.

[254] J.P. Orgel, A. Miller, T.C. Irving, R.F. Fischetti, A.P. Hammersley, T.J. Wess, The in situ supermolecular structure of type I collagen, Structure 9(11) (2001) 1061-9.

[255] R.A. Hortensius, B.A. Harley, Naturally derived biomaterials for addressing inflammation in tissue regeneration, Exp Biol Med (Maywood) 241(10) (2016) 1015-24.

[256] A.F. Elsaesser, C. Bermueller, S. Schwarz, L. Koerber, R. Breiter, N. Rotter, In vitro cytotoxicity and in vivo effects of a decellularized xenogeneic collagen scaffold in nasal cartilage repair, Tissue Eng Part A 20(11-12) (2014) 1668-78.

[257] L.M. Szott, T.A. Horbett, Protein interactions with surfaces: cellular responses, complement activation, and newer methods, Curr Opin Chem Biol 15(5) (2011) 677-82.

[258] D.E. MacDonald, B. Markovic, M. Allen, P. Somasundaran, A.L. Boskey, Surface analysis of human plasma fibronectin adsorbed to commercially pure titanium materials, Journal of Biomedical Materials Research 41(1) (1998) 120-130.

[259] W.G. Brodbeck, M. MacEwan, E. Colton, H. Meyerson, J.M. Anderson, Lymphocytes and the foreign body response: Lymphocyte enhancement of macrophage adhesion and fusion, Journal of Biomedical Materials Research Part A 74A(2) (2005) 222-229.

[260] W.G. Brodbeck, M.S. Shive, E. Colton, Y. Nakayama, T. Matsuda, J.M. Anderson, Influence of biomaterial surface chemistry on the apoptosis of adherent cells, Journal of Biomedical Materials Research 55(4) (2001) 661-668.

[261] S. Kamath, D. Bhattacharyya, C. Padukudru, R.B. Timmons, L. Tang, Surface chemistry influences implant-mediated host tissue responses, Journal of Biomedical Materials Research Part A 86A(3) (2008) 617-626.

[262] P. Thevenot, W. Hu, L. Tang, Surface chemistry influences implant biocompatibility, Curr Top Med Chem 8(4) (2008) 270-80.

[263] J. Hilborn, L.M. Bjursten, A new and evolving paradigm for biocompatibitity, Journal of Tissue Engineering and Regenerative Medicine 1(2) (2007) 110-119.

[264] S.Y. Seong, P. Matzinger, Hydrophobicity: an ancient damage-associated molecular pattern that initiates innate immune responses, Nature Reviews Immunology 4(6) (2004) 469-478.

[265] J. Andersson, K.N. Ekdahl, R. Larsson, U.R. Nilsson, B. Nilsson, C3 adsorbed to a polymer surface can form an initiating alternative pathway convertase, Journal of Immunology 168(11) (2002) 5786-5791.

[266] E.A. dos Santos, M. Farina, G.A. Soares, K. Anselme, Surface energy of hydroxyapatite and ss-tricalcium phosphate ceramics driving serum protein adsorption and osteoblast adhesion, Journal of Materials Science-Materials in Medicine 19(6) (2008) 2307-2316.

[267] Y. Wang, J.A. Stenken, Affinity-based microdialysis sampling using heparin for in vitro collection of human cytokines, Analytica Chimica Acta 651(1) (2009) 105-111.

[268] T.H. Tsai, C.F. Chen, F.C. Cheng, K.W. Kuo, T.R. Tsai, Analysis and pharmacokinetics of apomorphine in rat brain by microdialysis coupled with microbore HPLC electrochemical detection, J. Liq. Chromatogr. Relat. Technol. FIELD Full Journal Title:Journal of Liquid Chromatography & Related Technologies 20(3) (1997) 481-490.

[269] Y. Zhao, Analysis of pharmaceutical compounds in physiological fluids by microdialysis sampling and capillary electrophoresis, 1997, p. 186 pp.

[270] S.L. Wong, Y. Wang, R.J. Sawchuk, Analysis of zidovudine distribution to specific regions in rabbit brain using microdialysis, Pharmaceutical Research 9(3) (1992) 332-8.

[271] H.-S. Lee, E.-K. Goh, S.-G. Wang, K.-M. Chon, H.-K. Kim, H.-J. Roh, Detection of amino acids in human nasal mucosa using microdialysis technique: increased glutamate in allergic rhinitis, Asian Pacific Journal of Allergy and Immunology 23(4) (2005) 213-219.

[272] M.N. Woodroofe, G.S. Sarna, M. Wadhwa, G.M. Hayes, A.J. Loughlin, A. Tinker, M.L. Cuzner, Detection of interleukin-1 and interleukin-6 in adult rat brain, following mechanical injury, by in vivo microdialysis: evidence of a role for microglia in cytokine production, Journal of Neuroimmunology 33(3) (1991) 227-36.

[273] K.L. Snyder, C.E. Nathan, A. Yee, J.A. Stenken, Diffusion and calibration properties of microdialysis sampling membranes in biological media, Analyst 126(8) (2001) 1261-1268.

[274] J.A. Stenken, D.M. Holunga, S.A. Decker, L. Sun, Experimental and theoretical microdialysis studies of in situ metabolism, Analytical Biochemistry 290(2) (2001) 314-323.

[275] J.A. Stenken, C.E. Lunte, M.Z. Southard, L. Staahle, Factors That Influence Microdialysis Recovery. Comparison of Experimental and Theoretical Microdialysis Recoveries in Rat Liver, Journal of Pharmaceutical Sciences 86(8) (1997) 958-966.

[276] X. Wang, M.R. Lennartz, D.J. Loegering, J.A. Stenken, Interleukin-6 collection through long-term implanted microdialysis sampling probes in rat subcutaneous space, Anal. Chem. 79(5) (2007) 1816-1824.

[277] K. Alkhatib, T.M. Poseno, A. Diaz Perez, J.M. Durdik, J.A. Stenken, Iloprost Affects Macrophage Activation and CCL2 Concentrations in a Microdialysis Model in Rats, Pharm. Res. 35(1) (2018) 1-10.

[278] G.F. Clough, Microdialysis of large molecules, AAPS J 7(3) (2005) E686-92.

[279] S.B. Jadhav, V. Khaowroongrueng, M. Fueth, M.B. Otteneder, W. Richter, H. Derendorf, Tissue Distribution of a Therapeutic Monoclonal Antibody Determined by Large Pore Microdialysis, J. Pharm. Sci. 106(9) (2017) 2853-2859.

[280] M.I. Davies, J.D. Cooper, S.S. Desmond, C.E. Lunte, S.M. Lunte, Analytical considerations for microdialysis sampling, Advanced Drug Delivery Reviews 45(2-3) (2000) 169-188.

[281] C.R. Sides, J.A. Stenken, Microdialysis sampling techniques applied to studies of the foreign body reaction, Eur J Pharm Sci 57 (2014) 74-86.

[282] E.C. von Grote, V. Venkatakrishnan, J. Duo, J.A. Stenken, Long-term subcutaneous microdialysis sampling and qRT-PCR of MCP-1, IL-6 and IL-10 in freely-moving rats, Mol Biosyst 7(1) (2011) 150-61.

[283] G. Bajpai, R.C. Simmen, J.A. Stenken, In vivo microdialysis sampling of adipokines CCL2, IL-6, and leptin in the mammary fat pad of adult female rats, Mol Biosyst 10(4) (2014) 806-12.

Chapter 2

Materials and Methods

Sections 2.1. and 2.2. are reprinted from Pharmaceutical Research, 35, Kamel Alkhatib, Tina M. Poseno, Alda Diaz-Perez, Jeannine M. Durdik, and Julie A. Stenken, Iloprost affects macrophage activation and CCL2 concentrations in a microdialysis model in rats, Pages 1-10, Copyright (2018), with permission from Elsevier

2.1. Chemicals

Microdialysis and Sponges reagents.

Dexamethasone-21-phosphate disodium salt (Sigma Aldrich, St Louis, MO); Ethylene oxide (Anderson Sterilizers, Inc., Haw River, NC); iloprost (Cayman Chemicals, Ann Arbor, MI); Ringer's solution for chapter 3 (147 mM NaCl, 4.6 mM KCl, 2.3 mM $CaCl_2$), pH 7.4 and was prepared in HPLC-grade water (Fisher Scientific, Waltham, MA); 0.9% sterile saline USP (Hospira, Inc., Lake Forest, IL). Sterile lactate Ringer's solution (USP) (Hospira, Inc., Lake Forest, IL) was used in studies presented in chapters 4 and 5.

Surgical reagents.

Isoflurane (Abbot Laboratories, North Chicago, IL); povidone-iodine (Professional Disposables International, Orangeburg, NY); Super glue gel control (Henkel, Westlake, OH); Vetbond™ (3 M, St. Paul, MN); 10% neutral buffered formalin (BDH, VWR, West Chester, PA).

Analysis reagents.

Aniline blue/WS (Macron Fine Chemicals, Center Valley, PA); anti-CD68 antibody (Santa Cruz Biotechnology, Inc., Dallas, TX); anti-CD163 antibody (Santa Cruz Biotechnology, Inc., Dallas, TX); Apex™ antibody labeling kits (Alexa Fluor 488, Life Technologies, Carlsbad, CA); Apex™ antibody labeling kits (Alexa Fluor 647, Life Technologies, Carlsbad, CA); BD OptEIA™ rat MCP-1 (CCL2) ELISA set (BD Biosciences, San Jose, CA); Biebrich Scarlet / Acid Fuchsine solution (ScyTek laboratories, Inc, Logan, UT); Bouin's fixative solution, picric acid- formalin- acetic acid mixture (Ricca chemical company, Arlington, TX); Bovine serum albumin (BSA; Rockland Immunochemicals, Gilbertsville, PA); Halt protease inhibitor (Pierce, Rockford, IL); Hoechst 34580 (Sigma-Aldrich, St Louis, MO); high performance liquid chromatography water (HPLC)-grade water (Fisher Scientific, Waltham, MA); OCT [optimal cutting temperature solution] (Sakura®Finetek, Torrance, CA). VECTASHIELD (Vector Laboratories, Burlingame, CA).

2.2. Iloprost affects macrophage activation and CCL2 concentrations in a microdialysis model in rats

2.2.1. Cell culture

These *in vitro* experiments represent the initial study that demonstrated the use of iloprost as a potential modulator of macrophage phenotype *in vivo* [1]. NR8383 cells from American Type Culture Collection (ATCC) (Manassas, VA) were used for testing iloprost. NR8383 cells were cultured using 15 (v/v%) fetal bovine serum (Sigma-Aldrich, St. Louis, MO), 1 (v/v) % of 100 U/mL penicillin (Sigma-Aldrich, St. Louis, MO), and 84 (v/v%) of F-12K which contained a 100 g/mL streptomycin, 0.25 g/mL amphotericin (ATCC) and 2 mM glutamine (Sigma-Aldrich, St. Louis, MO). NR8383 cells were incubated at 37 °C and 5% CO_2.

Cultures were prepared in 1-mL of media in 6-well plates. For ELISA measurements, a density of 1.8×10^5 cells/ mL per well was used. For qRT-PCR, 2.8×10^5 cells/ mL were used to obtain sufficient levels of sample. Cells were exposed to 50 ng/mL lipopolysaccharide (Salmunella typhimurium (LPS), Calbiochem, obtained from EMD Millipore, Billerica, Massachusetts) or a combination of 50 ng/mL LPS plus 10 or 100 nM iloprost (Cayman Chemical, Ann Arbor, MI). Cells were allowed to incubate for 24 hours prior to ELISA or qRT-PCR measurement. ELISA measurement of CCL2 (BD Bioscience, San Jose, CA) was performed using the cell culture supernatant as provided in the manufacturer instructions.

RNA was extracted from treated cells using the Trizol reagent (Life Technologies, Grand Island, NY) following the provided manufacturer procedure. A RNeasy Kit from Qiagen (Germantown, MD) was used as a column clean up step. Primers were sourced from Life Technologies (Grand Island, NY). Total RNA was quantified using a Nanodrop Spectrophotometer 2000c at 260/280 and 260/230 nm absorbance ratio. Then, using a formaldehyde denaturing gel, the quality of the RNA was determined before synthesizing cDNA by reverse transcription (RT) using a high capacity RNA-to-cDNA kit (Life Technologies, Grand

Island, NY) and loaded in a thermo-cycle PCR TC-3000. qRT-PCR was performed using primers from Life Technologies with GADPH as a housekeeping gene (NM_017008.3) with CD-163 (NM_001107887.1) and CD-206 (NM_001106123.1) as the targets and measured on a 7500 Real Time PCR System (Applied Biosystems, Foster City, CA). For qRT-PCR, 40 cycles were used (50°C to 95°C to 60°C).

2.2.2. Microdialysis

Microdialysis sampling was performed using CMA 20 microdialysis probes with 10 mm polyether sulfone membranes and 100 kDa MWCO (Harvard Apparatus, Holliston, MA). All microdialysis probes were sterilized before implantation using ethylene oxide gas (Anderson Sterilizers, Inc., Haw River, NC). Ringer's solution (147 mM NaCl, 4.6 mM KCl, 2.3 mM $CaCl_2$), pH 7.4 in HPLC-grade water (Fisher Scientific, Waltham, MA) with 2% bovine serum albumin (BSA, Rockland Immunochemical, Gilbertsville, PA) was prepared. A BAS Bee pump (Bioanalytical Systems Inc., West Lafayette, IN) with 1-mL glass syringes was used to pass perfusion fluid through the microdialysis probe. Ringer's with 2% BSA was used as a control perfusion fluid while 1 pg/mL of Iloprost + 2% BSA in Ringer's was used as a treatment perfusion fluid. All perfusion fluids were autoclaved prior to the addition of BSA and iloprost and passed through a 0.2 µm sterile filter prior to use. Animals were placed in a CMA 120 freely-moving collection system (CMA Microdialysis, Solna, Sweden) after the implantation of microdialysis probes.

2.2.3. Probe implantation, cytokine sampling, and tissue harvesting

Surgical procedures and protocols were approved by University of Arkansas Institutional Animal Care and Usage Committee (IACUC) and followed the NIH Guide for Care and Use of Laboratory Animals. Male Sprague-Dawley rats (Harlan Laboratories, Indianapolis, IN) in a weight range of 275-335 grams were used. Animals were acclimated and housed for 1 week before being selected for surgical operation in a temperature-controlled facility at 72°F with ad libitum access

to food and water. Aseptic technique was used for all surgical procedures. All surgical instruments were autoclaved and cooled prior to use. Surgical procedures used for microdialysis probe implantation and subsequent daily handling have been previously described [2-4].

Animals were induced with anesthetic using 5% isoflurane (Abbot Laboratories, North Chicago, IL) in 1 L min^{-1} oxygen by placing them in an induction chamber. Rats were maintained under anesthesia, 3% isoflurane in 1 L min^{-1} oxygen, using a nose cone. Body temperature was monitored and maintained during surgical operation and collection period at 37°C using a temperature-controlled heating pad. The dorsal side, surgical site, was shaved to have a final clipped area approximately 5 cm width by 7.5 cm long. The surgical site was scrubbed using chlorhexidine scrub moistened gauzes and 70% alcohol wipes. Four incisions were made (approximate ~0.75 cm per incision) perpendicular to the spine through the skin to reach the subcutaneous space. Two incisions were positioned on the anterior end, slightly in front of the shoulders blades, while the other two were placed on the posterior end with ~4 cm longitude separation from the anterior incisions. A horizontal spacing of a minimum of 1 cm was maintained between the incisions at each end. After making the incisions, a sterile plastic straw (ethylene oxide sterilized) was fed from the posterior incisions up a through the anterior incision. The microdialysis device was then inserted into the straw. The probe was implanted in the posterior incision by first inserting sterile split tubing along with an introducer needle into the subcutaneous space through the posterior incision. The introducer needle then was removed leaving the split tubing in the subcutaneous space. The probes were gently fed into the split tubing. Both the inlet and the outlet tubing were carefully passed through the straw until they were externalized from the anterior incisions. The split tubing and the straw were then removed. Each probe's functionality was initially tested by passing sterile Ringer's solution through the inlet at 3 µL/min and observing the fluid coming from the outlet tubing. The posterior incisions were sealed using Vetbond™. After microdialysis probe implantation, rats were moved to a CMA 120 freely moving

collection system which provides a continuous collection of the dialysates in awake and freely moving rats. At the end of the collection, the rats were aestheticized and maintained under anesthesia as previously described. The inlet and outlet tubing lines were clipped to about 4 inches length and connected to each other. Wounds were flushed with sterile saline and the tubing lines were inserted into a subcutaneous pocket (~1 cm^2) that was dissected from the anterior incision area toward the head. All the incisions were closed using Vetbond™. Sterile saline (3.0 mL) was administered subcutaneously to prevent dehydration of the skin. All animals were checked and weighed daily for the duration of the study. All rats were given a broad-spectrum antibiotic, Baytril (5 mg), each day post microdialysis probe implantation. On the days of collection, the animals were anesthetized and maintained as previously outlined. The pocket was wiped with chlorhexidine, and the tubing lines were externalized out of the pocket. The pocket area was flushed with sterile saline. After ensuring the probes allowed fluid flow, the animals were moved to the CMA 120 collection bowl and followed the previous steps at the end of the collection.

For this study, two microdialysis probes were implanted in the subcutaneous space of a male Sprague- Dawley rat. One probe served as a control and the other was used to deliver iloprost. The collection period started by flushing the probes and associated tubing lines for 20 minutes at 3 µL/minute with a rate reduction of 0.5 µL every 5 minutes until the desired flow rate of 1 µL/minute was reached. Line flushing is necessary to clear any air bubbles that might cause blockage in the collection lines and to remove the dead volume of the liquid remaining in the lines between the collection periods. Dialysates collected during the flush period were saved for chemical analysis. Dialysates were collected once an hour for 4 hours. After the 4 hours collection period was completed, a final flush with Ringer's solution was performed on both sides at a flow rate of 3 µL/ minute for 30 minutes. The tubing lines were connected using tubing connectors (Harvard Apparatus) and placed back into the pocket at the nape of the animal's neck. The

collection procedure was performed on the same day of probe implantation, one-day post implantation, and two days post implantation.

Animals were euthanized using CO_2 at the end of the third day of collection (two days post implantation). Tissue surrounding the probe was excised and immediately embedded in optimal cutting temperature solution (Sakura®Finetek, Torrance, CA) and rapidly frozen using liquid nitrogen prior to immunohistochemical and histological staining procedures.

2.2.4. Iloprost release characterization

To estimate the concentration of Iloprost released into the subcutaneous tissue, a measurement of the drug loss from the dialysis probe in vitro was performed. This experiment was implemented based on retro dialysis concepts, where reverse dialysis of the drug was performed. In this technique, iloprost was added to the perfusion fluid and its extraction efficiency (EE) was used as a measure for the loss [5]. Retrodialysis is a commonly used calibration method of in vivo microdialysis and has been widely used in studying the effect of localized drug delivery studies [6-9]. A calibrator is usually included in the perfusate during retrodialysis studies and the fraction of loss across the membrane to the surrounding tissue is measured. By using this technique, it is possible to estimate the concentration of the iloprost released into the extracellular fluid. The loss of the iloprost from the perfusion fluid was quantified with liquid chromatography coupled with tandem mass spectrometry.

The concentration recovery was obtained using the concentration of iloprost in the perfusion fluid (C_i) and the concentration in the dialysates (C_{dial}) (Equations 1 and 2).

$$EE = \frac{C_i - C_{dial}}{C_i} \times 100 \quad (1)$$

$$\%\, Lost = 100 - EE \quad (2)$$

In vitro microdialysis and sample preparation:

In vitro experiments used the same CMA 20 microdialysis probes with 10 mm polyethersulfone (PES) membranes and 100 kDa MWCO perfused at 1 µL/min with 1 mg/mL of iloprost in Ringer's solution (147 mM NaCl, 4.6 mM KCl, 2.3 mM $CaCl_2$) and 2% BSA. Dialysates were collected in 60 µL aliquots over 3 hours. To extract iloprost from the perfusion fluid and to remove the interference of the BSA and the other salts prior to subsequent mass spectrometry analysis, C18 spin columns (G-Biosciences, St. Louis, MA) were used. The standard protocol provided by the manufacturer (G-Bioscience) was adopted with some modifications. First, the spin column was conditioned by spinning down 100 µL acetonitrile with 0.1% formic acid three times to clean any organic matter trapped in the C18 material and was followed by conditioning the column to enable loading the sample by spinning down 100 µL 0.1% of formic acid solution three times. Then, the sample was loaded to the spin column, followed by a desalting step performed by spinning down 100 µL of 0.1% formic acid three times. To elute iloprost from the C18 spin column, three volumes of 100 µL of 0.1% formic acid in methanol was used. The eluate was dried using a stream of nitrogen or vacuum concentrator. The obtained dried sample was reconstituted in 50 µL ethanol prior to LC-MS/MS analysis.

High-performance liquid chromatography-electrospray ionization-tandem mass spectrometry (HPLC-ESI-MS/MS)

Iloprost concentration was quantified by HPLC-ESI-MS/MS using an HP 1100 series HPLC coupled to a Bruker Esquire 2000 quadrupole ion trap mass spectrometer. The iloprost was chromatographically separated using a (Discovery 568222-U) 5 µM C18 (15 cm x 4.6 mm) column. Injection volume of 3 µL, column flow rate of 0.7 µL/min, and linear gradient of 70% - 100% methanol in water with 0.1% of formic acid were set as the conditions for the 15-min analysis. Mass spectra were obtained in the negative-ion mode. The capillary of ESI was set to +3800 V; the nebulizer was set to 32 psi, and the dry gas was set to 12 $L.min^{-1}$ at 300°C. The

signal was monitored using selected reaction monitoring mode at m/z 359.3 (M-H). Fragmentation of the 359.3 negative ion produced ion fragments of 174.5, 230.7, 268.6, and 341.0 m/z. To quantify iloprost, a four-point calibration curve was prepared using concentrations between 1 and 1000 µg/mL.

2.2.5. CCL2 quantification in the collected dialysates using ELISA

Collected dialysates were stored at -80°C at the end of the collection day. CCL2 concentrations were quantified in the dialysates collected over the collection period of 4 hours for the same day of the probe implantation, one-day post implantation, and two days post implantation using a BD OptEIA™ rat MCP-1 ELISA set (BD Biosciences, San Jose, CA). ELISA was run on the day following the three days collection period and the quantification procedure was followed according to the manufacturer's instructions with modifying the sample and the standards volume to a 50 µL to match the dialysate volume. The flush and first-hour dialysates collected on the day of implantation were diluted at 1:4 ratio while the other dialysates were diluted at 1:10 ratio with the assay diluent provided with the ELISA kit. The concentration range of the ELISA kit was between 31.25 pg/mL and 2000 pg/mL.

2.2.6. Immunohistochemical staining

Excised frozen tissues embedded in optimal cutting temperature solution were stored at -80°C and were cut at 5 µm thickness with a Leica CM3050 S cryostat (Leica Microsystems, Wetzlar, Germany) and mounted on microscope slides. Staining was performed as previously described [3, 4]. After mounting, slides were fixed with methanol for 20 minutes at -20°C. Tissue sections were marked after that with a hydrophobic barrier pen then they were incubated with a blocking buffer which was composed of (PBS + 2% (v/v) horse serum + 0.05% (v/v) Tween 20 + 0.1% (w/v) BSA for 30 minutes in a humidity chamber. After that, 4 cycles of washes were applied for 5 minutes per wash. The primary antibodies that were used for staining were cluster of differentiation 68 (CD68) (Santa Cruz Biotechnology, Dallas, TX) and cluster of differentiation 163

(CD163) (Santa Cruz Biotechnology, Dallas, TX). Fluorophore conjugation to the antibodies was performed using APEX Antibody Labeling Kits (Life Technologies, Carlsbad, CA). CD68 was conjugated with Alexa Fluor 488 (Life Technologies, Carlsbad, CA), while CD163 was conjugated with Alexa Fluor 647 (Life Technologies, Carlsbad, CA). After the washing cycles, the tissue sections were incubated in the fluorophore-antibody conjugate solution at 4°C in the dark overnight. The antibodies-fluorophores conjugate solution had the following ratio (1:50 for CD163 and 1:125 for CD68). On the next day, the slides were washed three times for 15 minutes per wash in phosphate buffered saline with protection from light. The washing buffer residues were removed from the biological tissues using a KimWipe tissue. After that, the slides were counterstained with a nuclear stain (Hoechst 34580) and were incubated for 12 minutes at room temperature, protected from light with three wash cycles with phosphate buffered saline for 10 minutes per cycle. The washing buffer residues were removed from the tissues using KimWipes. Then, the tissue sections were covered with VECTASHIELD (Vector Laboratories, Burlingame, CA) and a cover slip was placed on top. A TCS SP5 II confocal microscope (Leica Microsystems, Wetzlar, Germany) was used to obtain images for the stained slides.

2.2.7. Histological Staining (H&E and Masson's Trichrome staining)

Tissue sections were prepared at 5 µm thickness using a Leica CM3050 S cryostat (Leica Microsystems, Wetzlar, Germany) and mounted on microscope slides. Tissues were first fixed with 10% neutral buffered formalin (BDH, VWR, West Chester, PA) for 90 minutes. Both H&E and Masson's Trichrome Staining were performed on the tissue sections following the standard protocol instructions. A Zeiss Axioskop II plus microscope (Carl Zeiss Inc., Thornwood, NY) with Cannon EOS Digital camera software was used to image the stained tissues.

2.2.8. Statistical analysis

Origin® 2015 software platform (OriginLab Corporation, Northampton, MA) was used for performing statistical analyses. For the cell culture samples analyzed by ELISA, ANOVA followed

by Tukey post-hoc test was used with significance set to $p \leq 0.05$. For qRT-PCR the relative expression software tool (Multiple condition solver) REST-MCS version 2 using pair wise fixed reallocation randomization test was used and significance was set to $p \leq 0.05$. For the dialysates, the normality of the collected data, and thus the possibility of using parametric statistics, was determined using a Shapiro-Wilk test. For CCL2 concentrations measured in the collected dialysates, the data was presented as box-and-whiskers plots. Two-way ANOVA with repeated measurements and Bonferroni post-hoc test were performed to determine if there was a significant difference between the samples within the collection periods. For comparing the $CD163^+$ $CD68^+$ cell percentages in the tissues around the microdialysis probe, a two-sample t–test was performed to determine if there is a significant difference in the percentage between the tissues around the control and treatment probes. Significance was defined as $p \leq 0.01$.

2.3. Optimizing the Use of Sponge Implants as a Model to Study Macrophage Activation

2.3.1. Sponge Implantation procedure.

Surgical procedures and protocols were approved by University of Arkansas Institutional Animal Care and Usage Committee (IACUC) and followed the NIH Guide for Care and Use of Laboratory Animals. Male Sprague-Dawley rats (Harlan Laboratories, Indianapolis, IN) in a weight range of 250 – 300 grams were used. Animals were acclimated and housed for 1 week before being selected for surgical operation in a temperature-controlled facility at 72°F with ad libitum access to food and water. Aseptic technique was used for all surgical procedures. All surgical instruments were autoclaved and cooled prior to use.

The PVA sponges (PVA Unlimited Inc, Warsaw, IN) measured 12 mm × 3 mm in size. Sponges were soaked in 0.9% sterile saline USP (Hospira, Inc., Lake Forest, IL) overnight and then sterilized by autoclaving at 121ºC for 30 minutes prior to use. On the day of surgical procedures, animals were transported from the housing room to an appropriate procedure room in the animal care facility. Animals were induced with anesthetic using 5% isoflurane (Abbot Laboratories, North Chicago, IL) in 1 $L.min^{-1}$ oxygen by placing them in an induction chamber. Rats were maintained under anesthesia 3% isoflurane in 1 $L.min^{-1}$ oxygen using a nose cone. Body temperature was monitored and maintained during surgical operation at 37°C using a temperature-controlled heating pad. The dorsal side, surgical site, was shaved to have a final clipped area approximately 5 cm width by 7.5 cm long. The surgical site was scrubbed using chlorhexidine scrub moistened gauzes and 70% alcohol wipes. Two incisions were made (approximate ~1cm per incision) parallel to the spine through the skin to reach the subcutaneous space. One incision was positioned on the anterior end, slightly in front of the shoulders blades, while the other was placed on the opposite posterior end. A small (1 cm) subcutaneous pocket was created on the dorsal side where one PVA sponge was inserted into each pocket (Figure 2.1).

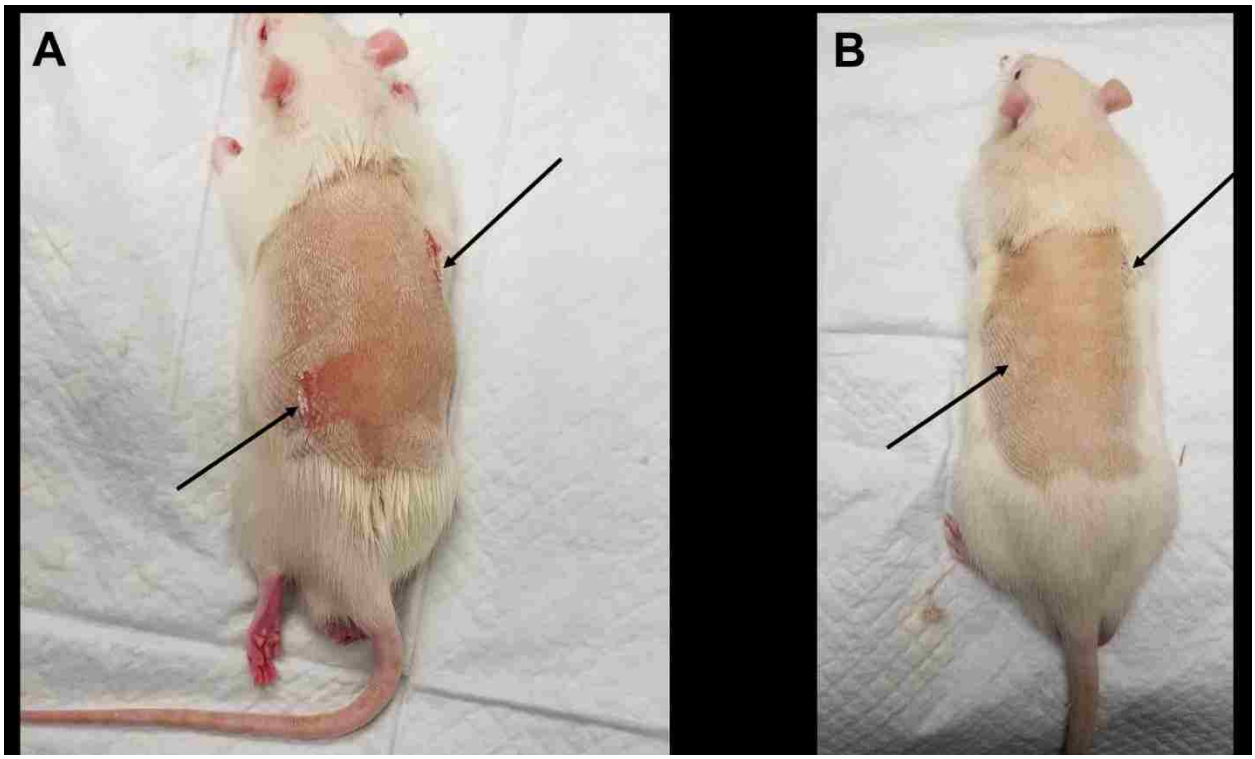

Figure 2.1. Image showing the placement positions of PVA sponges. **(A)** Image taken at the same day of implantation. **(B)** Image taken after 7 days of implantation. Arrows point the sites of incisions. Images were taken by the author.

Optimizing the direct dosing protocol using IR750:

Two sponges were implanted in the dorsal subcutaneous space of 3 male Sprague-Dawley rats. All sponges were soaked in sterile lactate Ringer's solution (USP) (Hospira, Austin, TX) 24 hours prior implantation. One day after implantation, subcutaneous injections of 100 µL IR750 (1 µM) were administered to one site of sponge implantation in each animal. One hour after the injections, the rats were euthanized, and fluorescence images were obtained using the IVIS Lumina XR system. To compare the distribution profiles of the fluorophore subcutaneous images, another set of 100 µL IR750 (1 µM) subcutaneous IR750 injections were administered to the other sponges in each animal right before obtaining images.

Bioactive modulators studies:

Animals were divided into three groups (6 animals in each group) where PVA sponges were soaked in either the vehicle solution (lactate Ringers' solution) in group #1 (control group), 100 µM dexamethasone in group #2 (treatment group), or 1 nM iloprost in group #3 (treatment group) prior to implantation. Two PVA sponges were implanted in the dorsal subcutaneous space of each animal. The incisions were closed using super glue. All animals were checked and weighed daily for the duration of the study. All rats were given a broad-spectrum antibiotic, Baytril (5 mg), each day post sponge implantation. A 100 µL daily booster dose, of the assigned treatments, lactate Ringers' solution to group #1 (control group), 100 µM dexamethasone to group #2 (treatment group), or 1 nM iloprost to group #3 (treatment group), was administered subcutaneously into each implantation site 24 hours after implantation until experiment completion (7 days post implantation). A week after implantation, animals were euthanized using CO_2 and the tissues surrounding the PVA sponge were excised for either histological/ immunohistochemical analysis or CCL2 quantification.

2.3.2. CCL2 quantification in the collected wound fluid using ELISA

After being explanted, sponges were squeezed into sterile protease inhibitors containing Eppendorf tubes to extract the wound fluid. Collected wound fluid was stored at -80 ºC until the day of analysis. CCL2 concentrations were quantified in the wound fluid collected after 7 days of implantation using a BD OptEIA™ rat MCP-1 ELISA set (BD Biosciences, San Jose, CA). The average collected volume obtained from each sponge was approximately 100 µL. The quantification procedure was followed according to the manufacturer's instructions. ELISA measurements were done in triplicates for each sample. The collected samples were diluted at a 1:500 ratio with the assay diluent provided with the ELISA kit. The concentration range of the ELISA kit was between 31.25 pg/mL and 2000 pg/mL. Quantified cytokine levels were normalized to the total protein levels in the wound fluid.

2.3.3. Immunohistochemical staining

Frozen tissues embedded in optimal cutting temperature solution were stored at -80°C and were cut at 10 µm thickness with a Leica CM3050 S cryostat (Leica Microsystems, Wetzlar, Germany) and mounted on microscope slides. Staining was performed as previously described in section 2.2.6 for the tissues around the microdialysis probes. After mounting, slides were fixed with methanol for 20 minutes at -20°C. Tissue sections were marked with a hydrophobic barrier pen, then incubated with a blocking buffer, composed of PBS + 2% (v/v) horse serum + 0.05% (v/v) Tween 20 + 0.1% (w/v) BSA, for 30 minutes in a humidity chamber. After that, 4 cycles of washes were applied for 5 minutes per wash. The primary antibodies that were used for staining were cluster of differentiation 68 (CD68) (Santa Cruz Biotechnology, Dallas, TX) and cluster of differentiation 163 (CD163) (Santa Cruz Biotechnology, Dallas, TX). Fluorophore conjugation to the antibodies was performed using APEX Antibody Labeling Kits (Life Technologies, Carlsbad, CA). CD68 was conjugated with Alexa Fluor 488 (Life Technologies, Carlsbad, CA), while CD163 was conjugated with Alexa Fluor 647 (Life Technologies, Carlsbad, CA). After the wash cycles, the tissue sections were incubated in the fluorophore- antibody conjugate solution at 4°C in the dark overnight. The antibodies- fluorophores conjugate solution had the following ratio (1:50 for CD163 and 1:125 for CD68). On the next day, the slides were washed three times for 15 minutes per wash in phosphate buffered saline with protection from light. The washing buffer residues were removed from the biological tissues using a KimWipe tissue. After that, the slides were counterstained with a nuclear stain (Hoechst 34580) and were incubated for 12 minutes at room temperature, protected from light with three wash cycles with phosphate buffered saline for 10 minutes per cycle. The washing buffer residues were removed from the tissues using KimWipes. Then, the tissue sections were covered with VECTASHIELD (Vector Laboratories, Burlingame, CA) and a cover slip was placed on top. A TCS SP5 II confocal microscope (Leica Microsystems, Wetzlar, Germany) was used to obtain images for the stained slides.

2.3.4. Histological Staining (H&E and Masson's Trichrome staining)

Tissue sections were prepared at 10 µm thickness using a Leica CM3050 S cryostat (Leica Microsystems, Wetzlar, Germany) and mounted on microscope slides. Tissues were first fixed with 10% neutral buffered formalin (BDH, VWR, West Chester, PA) overnight. Both H&E and Masson's Trichrome Staining were performed on the tissue sections following the standard protocol instructions. A Zeiss Axioskop II plus microscope (Carl Zeiss Inc., Thornwood, NY) with Cannon EOS Digital camera software was used to image the stained tissues.

2.3.5. Statistical analysis

Origin® 2018 software platform (OriginLab Corporation, Northampton, MA) was used for performing statistical analyses. To compare the levels of CCL2 collected from the wound fluid of the PVA sponges, CCL2 levels were first normalized to tissue protein concentrations. The normality of the obtained data and thus the possibility of using parametric statistics was determined using a Shapiro-Wilk test. The data was plotted as the mean value of the samples form 6 rats in each group, where error bars represented ±SD. Two-way ANOVA with repeated measurements and Bonferroni post-hoc test were performed to determine if there was a significant difference in CCL2 levels between the three groups. For comparing the $CD163^+$ $CD68^+$ cell percentages in the tissues around the PVA sponges, two-way ANOVA with repeated measurements and Bonferroni post-hoc test were performed to determine if there is a significant difference in the percentages between the tissues around the control and treatment sponges. Significance was defined as $p \leq 0.001$.

2.4. Comparison of Polyvinyl Alcohol (PVA) vs Collagen Sponges to Assess Macrophage Activation Patterns in Rats

2.4.1. Synthesis of collagen sponges

Collagen Isolation

The isolation process was adopted from a study published by Rajan *et al.* [10]. Collagen was extracted from the tails of male Sprague-Dawley rats that were included in previous studies. Prior to extraction, rat tails were soaked into 70% ethanol for 1-2 min followed by keeping it in phosphate buffered saline for couple of minutes. A small cut was made at the tip of the tails. Then, the tails were twisted to break cartilage. Skins were removed via lancet, and tendons were pulled with forceps to be removed. These steps were repeated until all tendons were removed. Obtained tendons were placed in a beaker containing 0.5 M acetic acid. Acetic acid/tendon mixture was magnetically stirred in an ice-bath for 4 hours and placed into a refrigerator (4°C) overnight.

Later, dissolved tendons were filtered through a sterile triangular bandage. Filtrates were poured into dialysis membranes (MWCO 6000-8000), and dialysis was performed against deionized water (pH < 3) for 3 days at room temperature. After dialysis, collagen solution was poured into centrifuge tubes followed by centrifugation at 10000 rpm for 20 min to remove residuals. Supernatants were collected and divided into petri dishes for the freeze-drying process. Prior to this process, collagen containing petri dishes were kept at - 80°C for 2 days followed by freeze-drying for 4 days. Lyophilized collagen was kept in a Ziploc bag at 4°C for short-term use (Figure 2.2).

Collagen Scaffold Development

Collagen solution (20 mg/mL) was prepared by dissolving lyophilized collagen in 0.5 M acetic acid. The dissolved collagen solution was divided into a 48-well plate as each well containing 500 µL collagen solution to produce collagen scaffolds that are close in dimensions to the PVA sponges used in chapter 4. The well plate was kept at - 80°C for a day followed by freeze-drying for 2 days. The developed collagen sponges were further cross-linked with glutaraldehyde (GA) solution. Collagen sponges were placed in a beaker containing 0.5 M GA solution and placed on a mini-shaker for 24 h. After the crosslinking treatment, the samples were kept in 0.1 M glycine for 24 h to remove excess glutaraldehyde. Later, the sponges were washed with DI water three times for further removal of excess chemicals. Then, the samples were frozen at -80°C for a day and freeze-dried for one day. Produced collagen scaffold were sterilized using ethylene oxide gas and stored until further use.

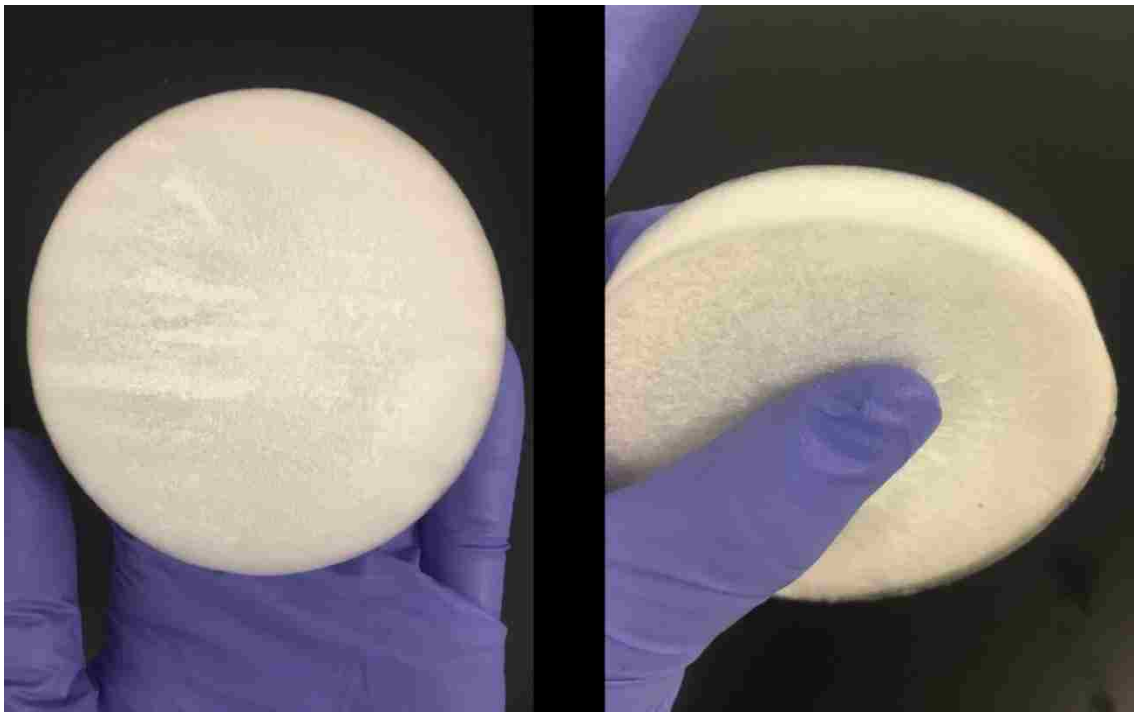

Figure 2.2. Produced collagen disc before glutaraldehyde crosslinking. Images were taken by the author.

2.4.2. Scaffold Characterization

The morphological analysis of the developed collagen sponges was performed via scanning electron microscopy (SEM). For this, the sponges were first coated with gold using a sputter coater. Later, the samples were mounted on a holder using a carbon tape and characterized with SEM.

2.4.3. Collagen sponge Implantation procedure.

Surgical procedures and protocols were approved by University of Arkansas Institutional Animal Care and Usage Committee (IACUC) and followed the NIH Guide for Care and Use of Laboratory Animals. Male Sprague-Dawley rats (Harlan Laboratories, Indianapolis, IN) in a weight range of 250 – 300 grams were used. Animals were acclimated and housed for 1 week before being selected for surgical operation in a temperature-controlled facility at 72°F with ad libitum access to food and water. Aseptic technique was used for all surgical procedures. All surgical instruments were autoclaved and cooled prior to use.

All collagen sponges were sterilized before implantation using ethylene oxide gas (Anderson Sterilizers, Inc., Haw River, NC). The same surgical procedures described in section 2.3.1 were followed. On the day of surgical procedures, animals were transported from the housing room to an appropriate procedure room in the animal care facility. Animals were induced with anesthetic using 5% isoflurane (Abbot Laboratories, North Chicago, IL) in 1 $L.min^{-1}$ oxygen by placing them in an induction chamber. Rats were maintained under anesthesia 3% isoflurane in 1 $L.min^{-1}$ oxygen using a nose cone. Body temperature was monitored and maintained during surgical operation at 37°C using a temperature-controlled heating pad. The dorsal side, surgical site, was shaved to have a final clipped area approximately 5 cm width by 7.5 cm long. The surgical site was scrubbed using chlorhexidine scrub moistened gauzes and 70% alcohol wipes. Two incisions were made (approximate ~1cm per incision) parallel to the spine through the skin to reach the subcutaneous space. One incision was positioned on the anterior end, slightly in front

of the shoulders blades, while the other was placed on the opposite posterior end. A small (1 cm) small subcutaneous pockets was created on the dorsal side where one collagen sponge was inserted to each pocket.

Animals were divided into three groups (6 animals in each group) where collagen sponges were soaked in either the vehicle solution (lactate Ringers' solution) in group #1 (control group), 100 µM dexamethasone in group #2 (treatment group), or 1 nM iloprost in group #3 (treatment group) prior to implantation. Two collagen sponges were implanted in the dorsal subcutaneous space of each animal. The incisions were closed using super glue. All animals were checked and weighed daily for the duration of the study. All rats were given a broad-spectrum antibiotic, Baytril (5 mg), each day post sponge implantation. A daily booster dose of the assigned treatment was administered subcutaneously into each implantation site 24 hours after implantation until experiment completion (7 days post implantation). A week after implantation, animals were euthanized using CO_2 and the tissues surrounding the collagen sponge were excised for either histological/ immunohistochemical analysis or CCL2 quantification.

2.4.4. CCL2 quantification in the collected wound fluid using ELISA

The accumulated wound fluid was extracted by squeezing the explanted sponges into sterile Eppendorf tubes containing protease inhibitors. Collected wound fluid was stored at -80ºC until the day of analysis. CCL2 concentrations were quantified in the wound fluid collected after 7 days of implantation using a BD OptEIA™ rat MCP-1 ELISA set (BD Biosciences, San Jose, CA). The average collected volume obtained from each sponge was approximately 100 µL. The quantification procedure was followed according to the manufacturer's instructions. ELISA measurements were done in triplicates for each sample. The collected samples were diluted at 1:500 ratio with the assay diluent provided with the ELISA kit. The concentration range of the ELISA kit was between 31.25 pg/mL and 2000 pg/mL. Quantified cytokine levels were normalized to the total protein levels in the wound fluid.

2.4.5. Immunohistochemical staining

Excised frozen tissues embedded in optimal cutting temperature solution were stored at -80°C and were cut at 10 µm thickness with a Leica CM3050 S cryostat (Leica Microsystems, Wetzlar, Germany) and mounted on microscope slides. Staining was performed as previously described for the tissues around the microdialysis probes. After mounting, slides were fixed with methanol for 20 minutes at -20°C. Tissue sections were marked with a hydrophobic barrier pen, then incubated with a blocking buffer, composed of PBS + 2% (v/v) horse serum + 0.05% (v/v) Tween 20 + 0.1% (w/v) BSA, for 30 minutes in a humidity chamber. After that, 4 cycles of washes were applied for 5 minutes per wash. The primary antibodies that were used for staining were cluster of differentiation 68 (CD68) (Santa Cruz Biotechnology, Dallas, TX) and cluster of differentiation 163 (CD163) (Santa Cruz Biotechnology, Dallas, TX). Fluorophore conjugation to the antibodies was performed using APEX Antibody Labeling Kits (Life Technologies, Carlsbad, CA). CD68 was conjugated with Alexa Fluor 488 (Life Technologies, Carlsbad, CA), while CD163 was conjugated with Alexa Fluor 647 (Life Technologies, Carlsbad, CA). After the wash cycles, the tissue sections were incubated in the fluorophore- antibody conjugate solution at 4°C in the dark overnight. The antibodies- fluorophores conjugate solution had the following ratio (1:50 for CD163 and 1:125 for CD68). On the next day, the slides were washed three times for 15 minutes per wash in phosphate buffered saline with protection from light. The washing buffer residues were removed from the biological tissues using a KimWipe tissue. After that, the slides were counterstained with a nuclear stain (Hoechst 34580) and were incubated for 12 minutes at room temperature, protected from light with three wash cycles with phosphate buffered saline for 10 minutes per cycle. The washing buffer residues were removed from the tissues using KimWipes. Then, the tissue sections were covered with VECTASHIELD (Vector Laboratories, Burlingame, CA) and a cover slip was placed on top. A TCS SP5 II confocal microscope (Leica Microsystems, Wetzlar, Germany) was used to obtain images for the stained slides.

2.4.6. Histological Staining (H&E and Masson's Trichrome staining)

Tissue sections were prepared at a 10 µm thickness using a Leica CM3050 S cryostat (Leica Microsystems, Wetzlar, Germany) and mounted on microscope slides. Tissues were first fixed with 10% neutral buffered formalin (BDH, VWR, West Chester, PA) overnight. Both H&E and Masson's Trichrome Staining were performed on the tissue sections following the standard protocol instructions. A Zeiss Axioskop II plus microscope (Carl Zeiss Inc., Thornwood, NY) with Cannon EOS Digital camera software was used to image the stained tissues.

2.4.7. Statistical analysis

Origin® 2018 software platform (OriginLab Corporation, Northampton, MA) was used for performing statistical analyses. To compare the levels of CCL2 collected from the wound fluid of the collagen sponges, CCL2 levels were first normalized to tissue protein concentrations. The normality of the obtained data and thus the possibility of using parametric statistics was determined using a Shapiro-Wilk test. The data was plotted as the mean value of the samples form 6 rats in each group, where error bars represented ±SD. Two-way ANOVA with repeated measurements and a Bonferroni post-hoc test were performed to determine if there was a significant difference in CCL2 levels between the three groups. For comparing the $CD163^+$ $CD68^+$ cell percentages in the tissues around the collagen sponges, two-way ANOVA with repeated measurements and a Bonferroni post-hoc test were performed to determine if there is a significant difference in the percentages between the tissues around the control and treatment sponges. Significance was defined as $p \leq 0.001$.

2.5. References

[1] A.A.D. Perez, Comparison of Different Modulators that Affect Macrophage Activation In Vitro, (2015).

[2] G.D. Keeler, J.M. Durdik, J.A. Stenken, Comparison of microdialysis sampling perfusion fluid components on the foreign body reaction in rat subcutaneous tissue, Eur. J. Pharm. Sci. 57 (2014) 60-67.

[3] G.D. Keeler, J.M. Durdik, J.A. Stenken, Effects of delayed delivery of dexamethasone-21-phosphate via subcutaneous microdialysis implants on macrophage activation in rats, Acta Biomater 23 (2015) 27-37.

[4] G.D. Keeler, J.M. Durdik, J.A. Stenken, Localized delivery of dexamethasone-21-phosphate via microdialysis implants in rat induces M(GC) macrophage polarization and alters CCL2 concentrations, Acta Biomater 12 (2015) 11-20.

[5] E.C.M. de Lange, Recovery and Calibration Techniques:Toward Quantitative Microdialysis, in: M. Müller (Ed.), Microdialysis in Drug Development, Springer, New York, 2013, pp. 13-33.

[6] D.K. Hansen, M.I. Davies, S.M. Lunte, C.E. Lunte, Pharmacokinetic and Metabolism Studies Using Microdialysis Sampling, Journal of Pharmaceutical Sciences 88(1) (1999) 14-27.

[7] L. Melgaard, K.J. Hersini, P. Gazerani, L.J. Petersen, Retrodialysis: a review of experimental and clinical applications of reverse microdialysis in the skin, Skin Pharmacol Physiol 26(3) (2013) 160-74.

[8] A. de la Pena, P. Liu, H. Derendorf, Microdialysis in peripheral tissues, Adv. Drug Delivery Rev. FIELD Full Journal Title:Advanced Drug Delivery Reviews 45(2-3) (2000) 189-216.

[9] C. Hocht, A.W. Opezzo Javier, A. Taira Carlos, Applicability of reverse microdialysis in pharmacological and toxicological studies, J Pharmacol Toxicol Methods FIELD Full Journal Title:Journal of pharmacological and toxicological methods 55(1) (2007) 3-15.

[10] N. Rajan, J. Habermehl, M.-F. Cote, C.J. Doillon, D. Mantovani, Preparation of ready-to-use, storable and reconstituted type I collagen from rat tail tendon for tissue engineering applications, Nat. Protoc. 1(6) (2006) 2753-2758.

Chapter 3

Iloprost affects macrophage activation and CCL2 concentrations in a microdialysis model in rats.

Co-authors: Tina M. Poseno, Alda Diaz Perez, Jeannine M. Durdik, and Julie A. Stenken

Reprinted from Pharmaceutical Research, 35, Kamel Alkhatib, Tina M. Poseno, Alda Diaz-Perez, Jeannine M. Durdik, and Julie A. Stenken, Iloprost affects macrophage activation and CCL2 concentrations in a microdialysis model in rats, Pages 1-10, Copyright (2018), with permission from Elsevier

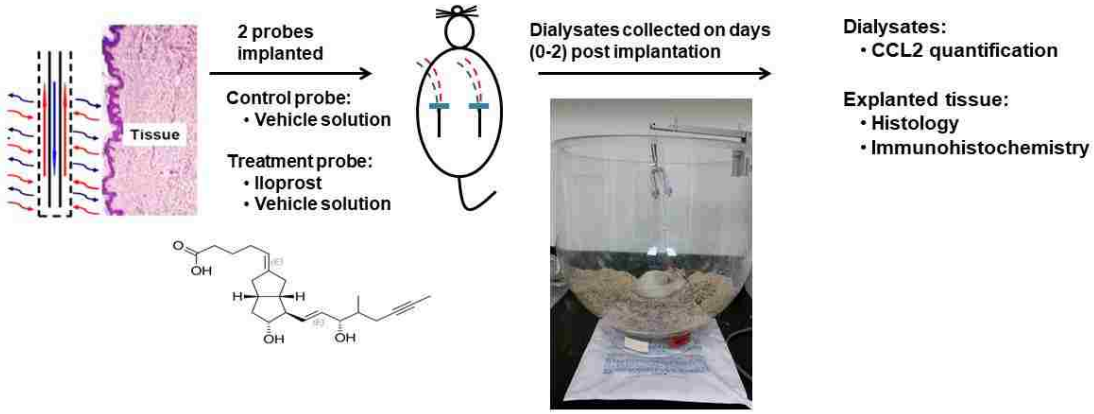

Figure 3.1. Experimental design overview of chapter 3.

3.1. Introduction

Macrophages are highly versatile immune cells that play a significant role in regulating various aspects of inflammation [1-3]. The response of macrophages to implanted materials is deemed critical to improved long-term outcomes of implanted biomedical devices [4-8].Macrophages with high expression of surface markers, CD68 and CD163, have been recognized as being anti-inflammatory, pro-wound healing, and pro-tissue remodeling cells which make them of high interest in the field of biomaterials [8, 9].

In this chapter, implanted microdialysis probes were used to locally deliver iloprost while simultaneously collecting CCL2 in dialysates. These initial studies aimed to investigate the role of locally-delivered iloprost, a synthetic prostacyclin analog, via microdialysis sampling in altering the macrophage activation state. Cytokine pharmacology is of significant biomedical interest since there are many studies showing relationships between pathophysiological processes and cytokine concentrations [10, 11]. Iloprost effectiveness towards reducing CCL2 concentrations and promoting a $CD163^{+}$ phenotype was assessed using cell culture techniques before use in our rat model. The microdialysis probe served as a foreign body implant and also allowed testing of the hypothesis that iloprost could serve as a macrophage modulator promoting an anti-inflammatory response at the implant site.

Microdialysis is a minimally-invasive diffusion-based sampling technique that has been widely used in neuroscience and pharmaceutics to collect bioactive molecules [12, 13]. Microdialysis probes are primarily used as sampling devices, but they can also be used to locally apply different drugs. A major advantage of microdialysis sampling is that it allows the delivery of biochemical agents, such as drugs and other molecules with a molecular weight smaller than the defined molecular weight cutoff (MWCO), to freely diffuse across the open pores of the semi-permeable membrane while performing simultaneous sampling collection of endogenous solutes from the tissue space [14].

The markers used to assess the effectiveness of iloprost and its pharmacodynamic response were the localized concentrations of CCL2 and the presence of $CD68^{+}CD163^{+}$ macrophages surrounding the microdialysis implant in excised tissue.

3.2. Results

3.2.1. Cell culture

Dosing NR8383 cells with iloprost (10 and 100 nM) in combination with LPS caused a significant reduction in measured concentrations of CCL2 from the culture media at 24 hours post stimulation (Figure 3.2a). The level of expression for the surface markers CD163 and CD206, which are indicative of anti-inflammatory macrophages, was increased in the presence of iloprost (Figure 3.2b).

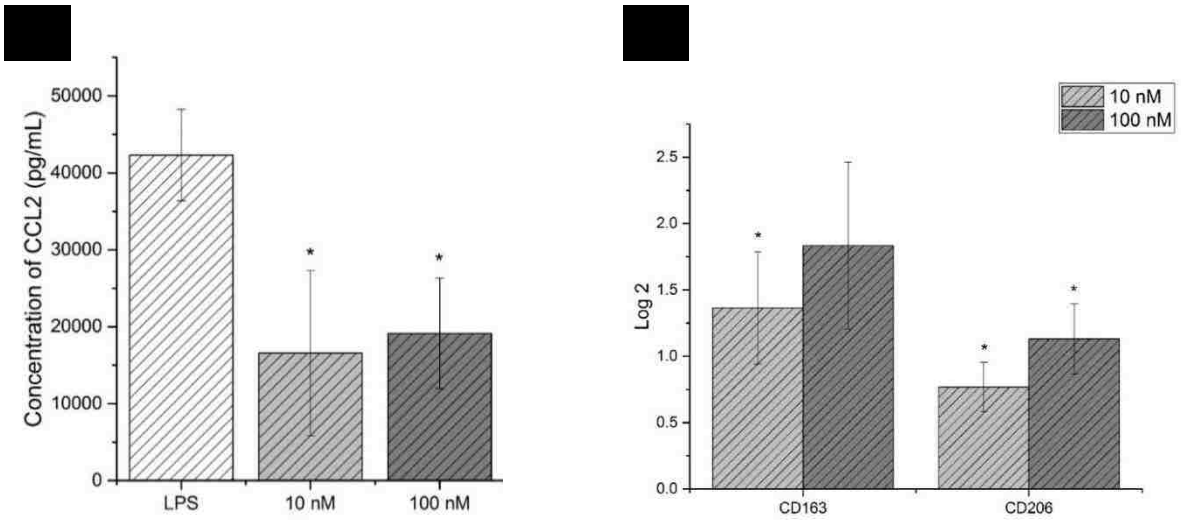

Figure 3.2. (a) CCL2 concentrations from NR8383 macrophage cultures 24 hr after LPS (50 ng/mL) or LPS + iloprost. **(b)**. CD163 and CD206 gene expression with LPS and iloprost relative to LPS stimulation. * denotes $p \leq 0.05$.

3.2.2. Iloprost dose optimization

One of the challenges encountered during this study was to determine the optimal dose of iloprost. Iloprost has not been used as a macrophage modulator in any foreign-body reaction study. Since iloprost has anticoagulant properties, it was necessary to determine if different doses would affect the localized healing of the implanted microdialysis probe. Our initial studies used 100 pg/mL of iloprost in the perfusion fluid. However, when using this dose, it was observed that wounds created during the microdialysis probe implantation would not properly heal. Frequently, bleeding was observed around the implanted probe. In several cases, the probe would fail before the end of the study. For this reason, the infusion dose in the perfusion fluid was reduced to 1 pg/mL during the study. This reduction of iloprost dosage to 1 pg/mL resulted in greatly minimizing the observed anticoagulation effect and significantly improved probe longevity (Figure 3.3).

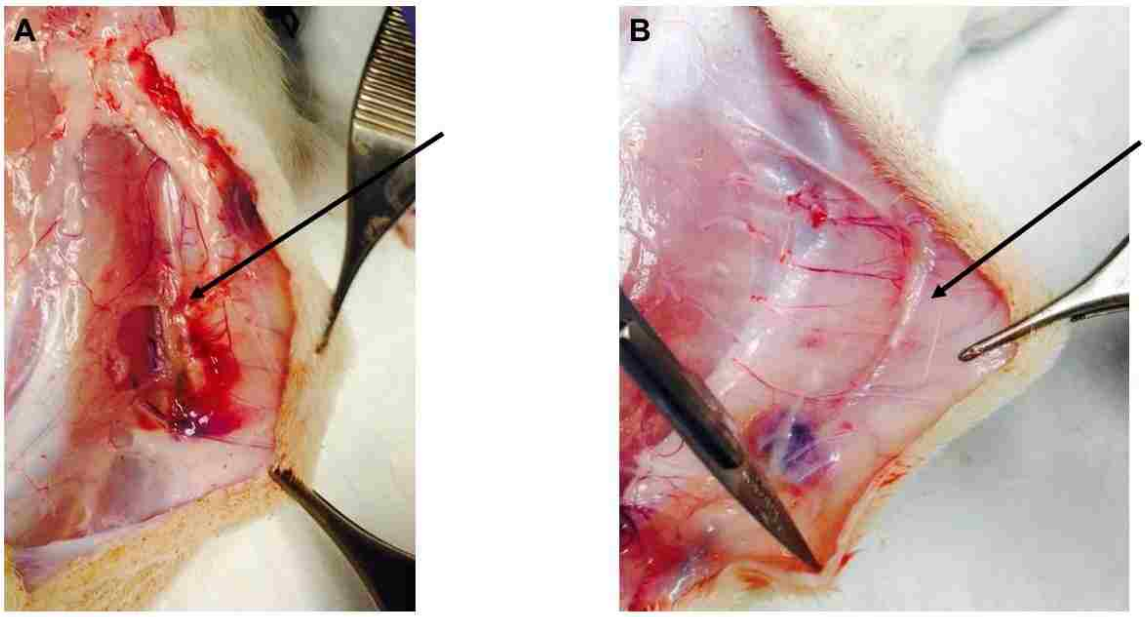

Figure 3.3. (A) Image showing observed bleeding around implanted microdialysis probe delivering 100 pg/mL of iloprost. (B) Image showing implanted microdialysis probe delivering 1 pg/mL. Arrows point at the site of microdialysis probe implantation. Images were taken by the author

3.2.3. Iloprost release characterization

Approximately, 90% absolute recovery was achieved during the necessary sample preparation steps with the dialysates for iloprost. The limit of detection (LOD) and limit of quantification (LOQ) were determined to be at 0.9 and 3 µg/mL, respectively.

The estimation of the percent recovery was calculated based on the loss of iloprost from the perfusate, assuming that the percent recovery equals the percent loss during retrodialysis [15]. The loss of iloprost was 17% indicating that an approximate delivery *in vivo* was 0.188 pg/mL (17% EE / 0.9 absolute recovery for sample preparation) at the 1.0 µL/min perfusion rate through the implanted microdialysis probe.

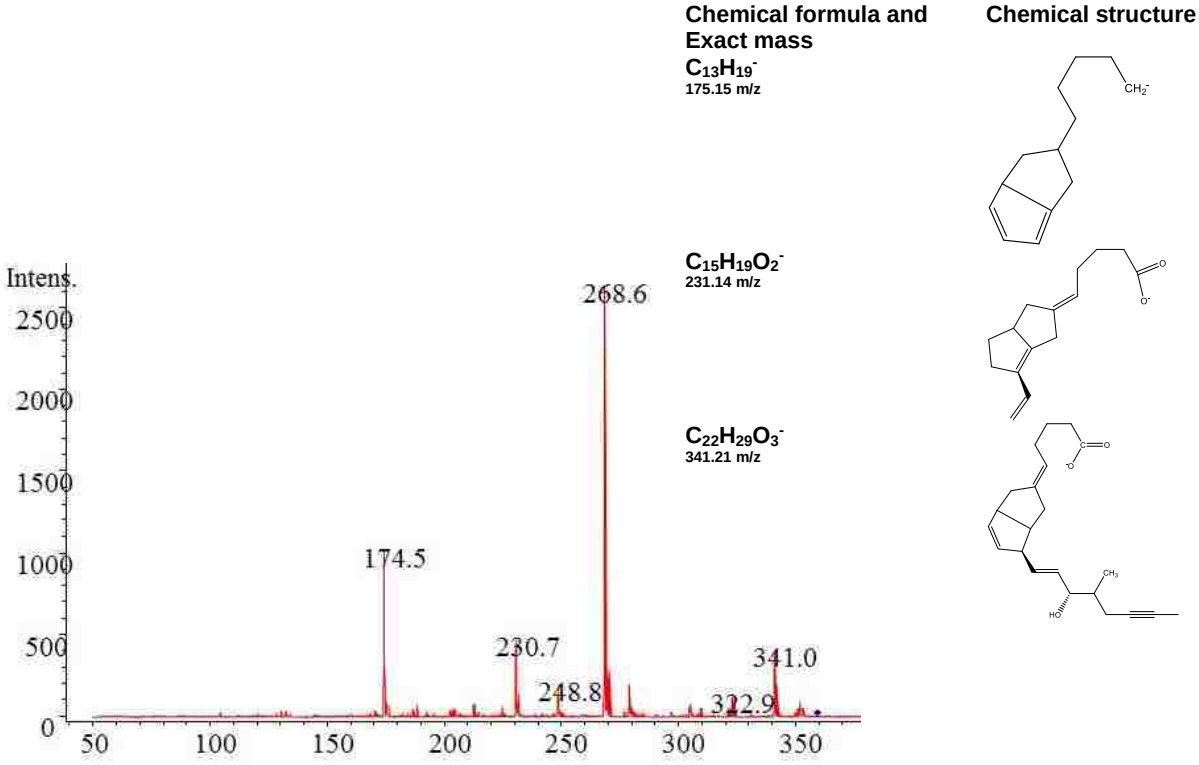

Figure 3.4. Mass spectrum representing fragmentation of iloprost using HPLC-ESI-MS

3.2.4. CCL2 quantification in the dialysates:

On the day of implantation, CCL2 concentrations were between 200 pg/mL and 12,000 pg/mL in control animals vs. 250 pg/mL to 6000 pg/mL in animals with iloprost treatment. No significant difference was observed in the CCL2 concentrations between in the control and the treatment dialysates collected during the flush and hours 1 through 3. By hour 4, CCL2 concentrations between controls and iloprost treatment dialysates were significantly different (Figure 3.5a).

One-day post implantation (Figure 3.5b), CCL2 concentrations were between 4000 – 7500 pg/mL in the dialysates collected from the control probe. For the iloprost treatment, CCL2 concentrations decreased from 4000 pg/mL during the initial flush to 2500 pg/mL by the end of the four-hour collection period. CCL2 concentrations were found to be significantly different between the control and the treatment probes during this 4^{th} collection hour.

Two days post implantation (Figure 3.5c), the CCL2 concentrations collected remained steady and like those from one-day post implantation in the range of 5000-6500 pg/mL for both the control and treatment probes. Additionally, the treatment dialysates exhibit similar concentration decreases as those observed on one-day post implantation with CCL2 concentrations decreasing from 5000 to 1800 pg/mL. The CCL2 concentrations between the control vs. the treatment dialysates were significantly different for the 2-, 3- and 4-hour collection points.

a **Implantation Day** **b** **Day 1 Post Implantation**

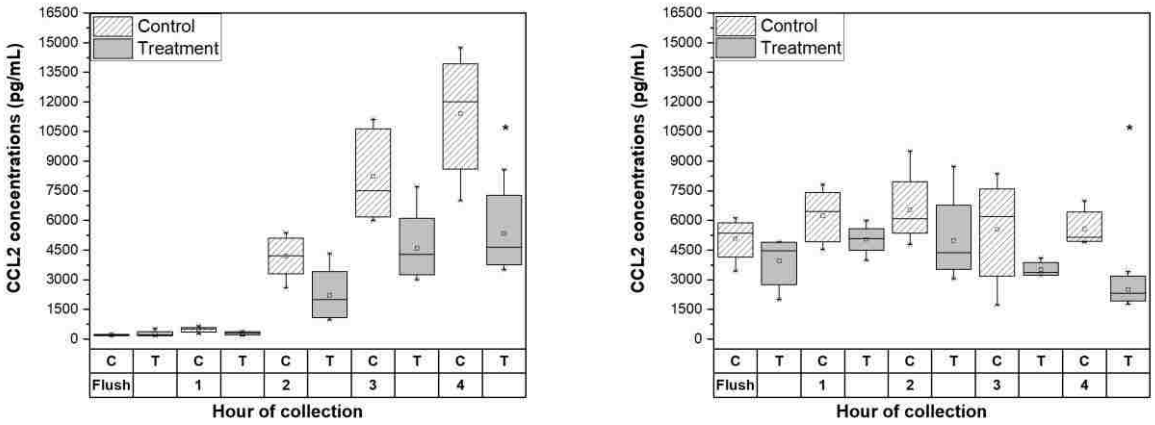

c **Day 2 Post Implantation**

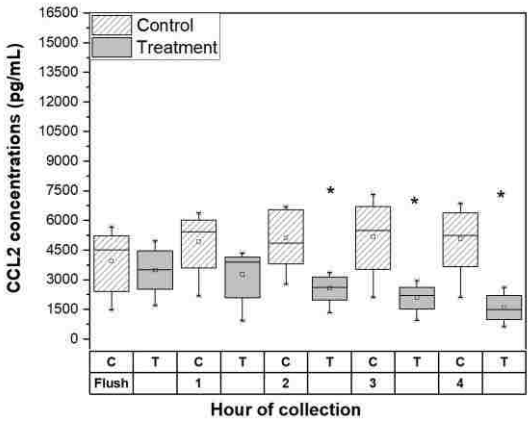

Figure 3.5. Box-and-whiskers plots of CCL2 concentrations in the dialysates collected from both (1 pg/mL) iloprost treatment probes (T) and control (C) on the same day of implantation **(a)**, 24-h post implantation **(b)** and 48 h post implantation **(c)**. The box represents the 25–75 percentiles. The line through the box represents the median, whiskers represent the fence and ▫ represents the mean. *p ≤ 0.05, n=5 where n represents the number of animals.

3.2.5. Histological analysis:

Both H&E and Masson's trichrome staining were performed on the tissue sections surrounding the control and treatment probes to investigate and compare both cellular and collagen distribution in tissues around the explanted probes. Less cellular density was observed around the iloprost-treated probes as compared to the control probes (Figures 3.6 and 3.7). A higher cellular density was observed with the control implants. At higher magnification, collagen density was less in the tissues immediately surrounding the iloprost-treated probe compared to the tissues immediately surrounding the control probes (Figure 3.7).

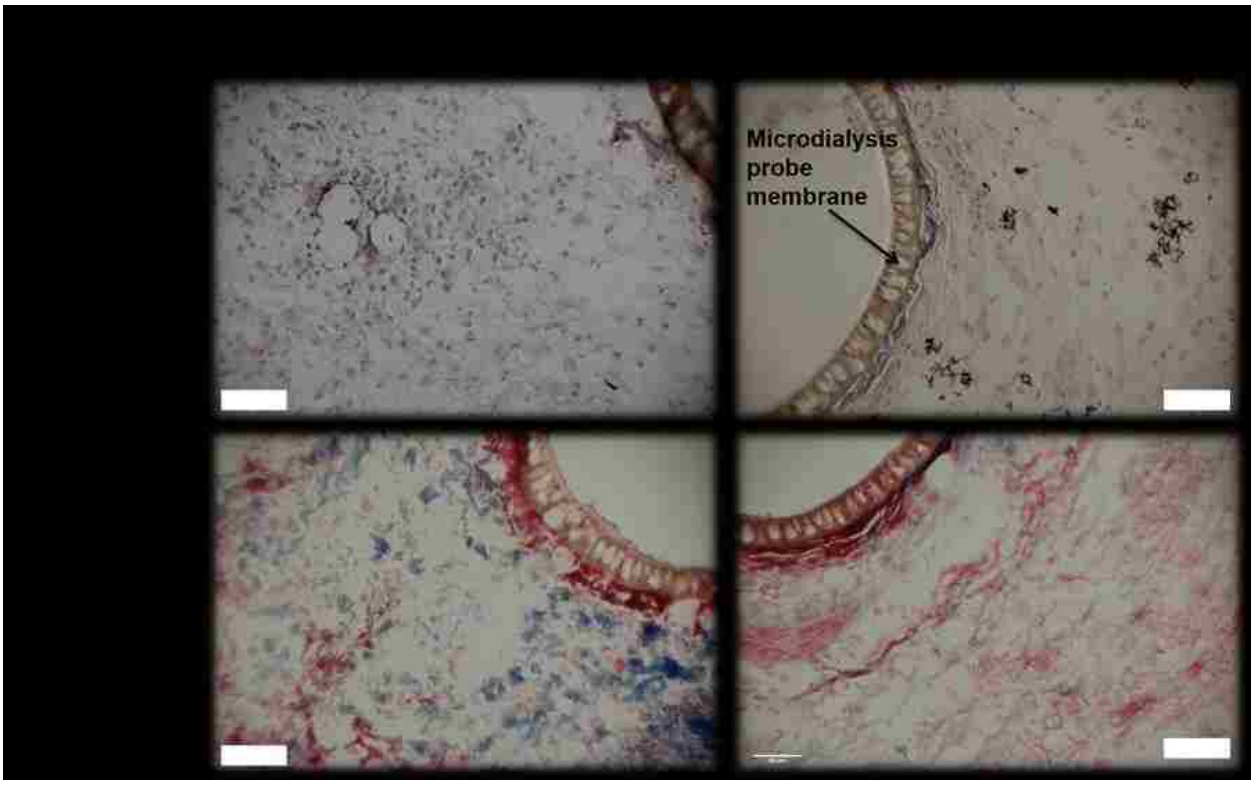

Figure 3.6. H&E and Masson's Trichrome staining for tissues around the explanted microdialysis probe. Scale bars represent 50 μm.

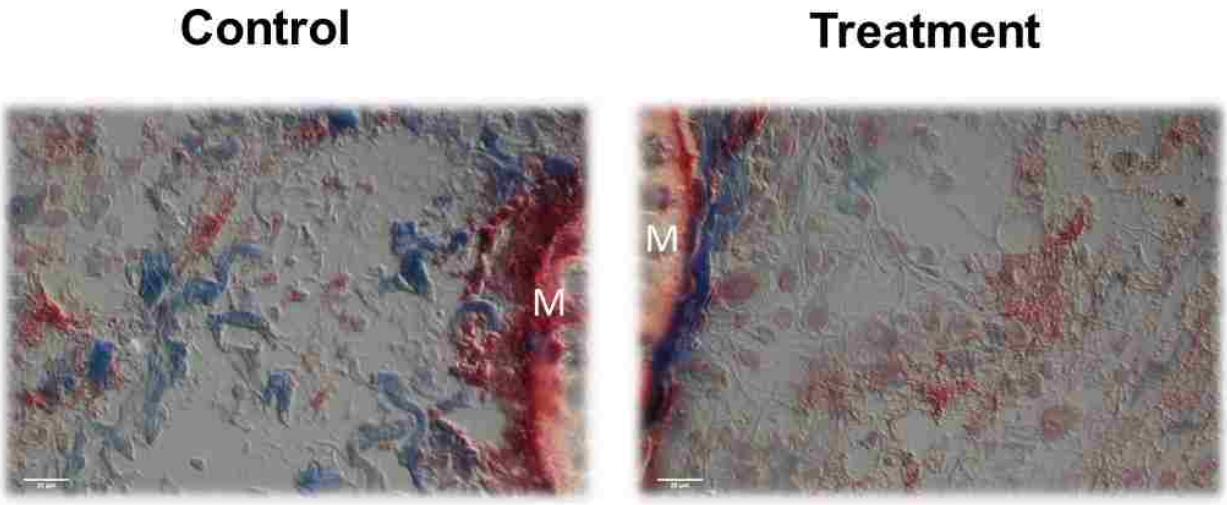

Figure 3.7. Masson's Trichrome staining for tissues around the explanted microdialysis probe. Scale bars represent 20 µm. **(M)** indicates a microdialysis probe membrane.

3.2.6. Immunohistochemistry analysis

Immunohistochemical staining was performed to determine the presence and the population of $CD163^{+}CD68^{+}$ macrophages among macrophages ($CD68^{+}$ cells) in tissues surrounding the implant. At lower magnification (Figure 3.8), a greater population of ($CD163^{+}CD68^{+}$) cells in the tissue around the treatment probe compared to the control probe was observed to be denser in the range of 100-500 µm around the probe. At higher magnification, fewer $CD163^{+}$ cells were observed in the tissue immediately surrounding the iloprost-treated probe compared to the cells further away. However, this population was greater than the $CD163^{+}$ cell population in the tissue immediately surrounding the control probe. The percentage of $CD163^{+}CD68^{+}$ among $CD68^{+}$ cells was calculated manually and compared in both treatment and control probes at the higher magnification (40X) to determine the population of these cells immediately around the probe (Figure 3.9).

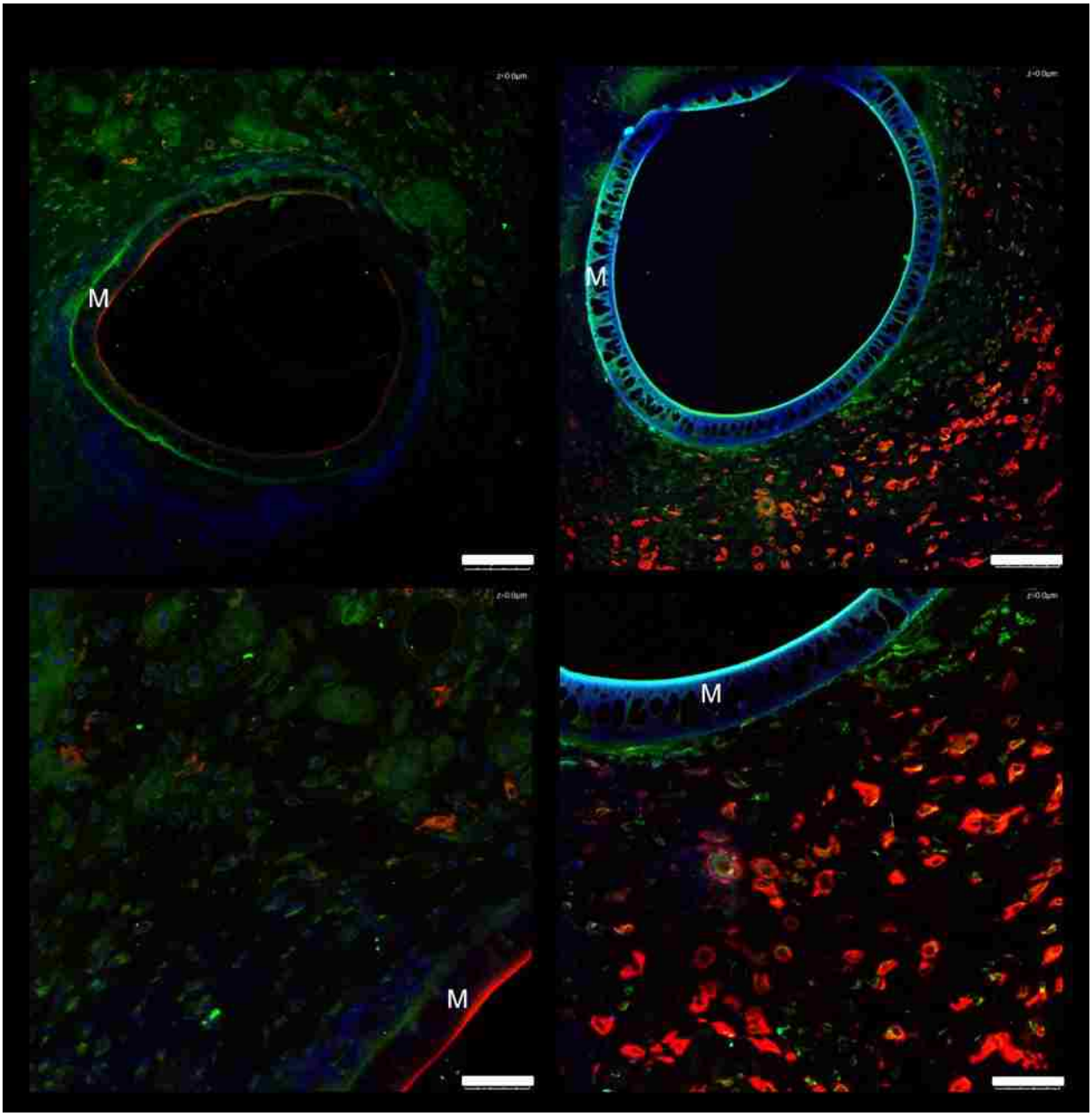

Figure 3.8. Immunohistochemical staining for CD68 (green), CD163 (red), and nuclei (blue) in the tissue surrounding microdialysis probe. Overlapped colors represent $CD68^{+}CD163^{+}$ macrophages. Indicates a microdialysis probe membrane. Scale bars represent 100 µm in top images and 50 µm in the bottom images.

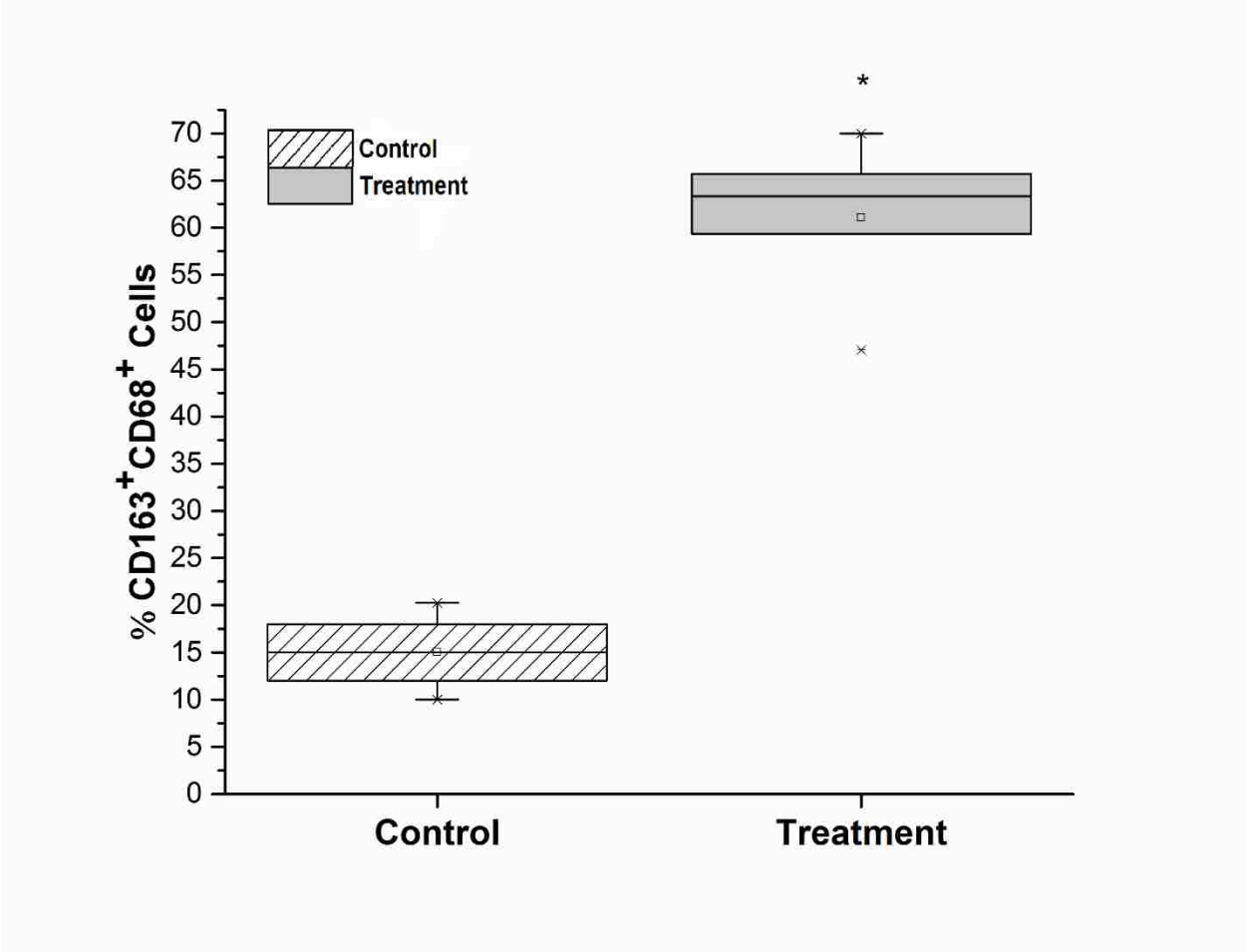

Figure 3.9. Box charts represent the percentage of $CD68^{+}CD163^{+}$ cells among CD68+ cells in the tissues immediately surrounding both control and treatment probes. The box represents the 25-75 percentiles. The line through the box represents the median, whiskers represent the fence and ▫ represents the mean. *p ≤0.01, n = 5 where n represent the number of measurements.

3.3. Discussion

A significant effort in the field of implanted biomedical devices and regenerative medicine has focused on modulating macrophages to their alternatively activated state [16]. There have been more recent molecular approaches to elucidating different effects of macrophage activation [3, 17] as well as directing macrophage activation to a desired endpoint [18]. Modulating the foreign body reaction to implanted biomedical devices to provide an appropriate microenvironment that leads to improved tissue integration and implant outcomes has been of historical interest for both the pharmaceutical and the biomaterial research community [3].

Depending on the stimulus, the macrophage population can be shifted to a desirable phenotype. Our recent studies have demonstrated that *in vivo* localized delivery of dexamethasone to the biomaterial implantation site could shift the macrophages to a $CD163^+$ state [19, 20]. However, there have been concerns regarding using steroids with respect to dampening too much of the initial inflammatory response [21]. For this reason, a prostaglandin approach was applied.

The microdialysis sampling probe serves as both the implanted biomaterial as well as the means to both deliver modulators and collect cytokines. Since the loss of iloprost was approximately 15% from the microdialysis probe, this means that 1×10^{-19} g per minute of iloprost was being released into the tissue from the microdialysis probe. It is not possible to perform an *in viv*o calibration as the concentrations being delivered are too low to detect. Iloprost has been reported to be highly potent in different studies so the low concentrations necessary here for altering macrophage phenotype and response are reasonable. In macrophage culture iloprost concentrations as low as 10 nM (3.6 ng/mL) caused a suppression of the inflammatory response to LPS. *In vivo*, the use of iloprost caused a reduction in CCL2 collected concentrations and increased the presence of $CD163^+$ cells in the tissue surrounding the implant.

After microdialysis probe insertion, the concentrations of CCL2 steadily rose with concentrations greatly increasing 2 hours post implantation. At the hour 2 collection point, the CCL2 concentrations with iloprost treatment appear to be depressed and reach a significant reduction relative to controls by 4 hours post implantation. Within one-day post implantation, CCL2 levels were lower than the previous day around 6,000 pg/mL for controls. As iloprost was locally delivered, the CCL2 concentrations gradually decreased and were significantly different at hour 4. At two days post implantation, the CCL2 levels were lower than the previous day with controls averaging roughly 4,500 pg/mL. After 2 days, iloprost infusion to the tissue appeared to affect CCL2 concentrations faster than the previous day around 2 hours after initiation of the iloprost infusion.

The time delay in observing an effect with decreased CCL2 concentrations with iloprost is consistent with our observations for another anti-inflammatory drug, dexamethasone.[20] Immediately after probe implantation, the expected cascade of cellular infiltration would be platelets (from breaching blood vessels) to neutrophils and ultimately macrophages. Platelets are known to release chemokines such as CCL2. By one-day post implantation, there are likely several types of cells focused on resolving the inflammation from the implant. This may contribute to the longer time needed to see an effect in CCL2 concentrations from iloprost delivery. By two days, the wound induced by the implant is starting to reorganize the tissue and macrophages would be the expected resident cells at this point in the continuum. This may be the reason CCL2 concentrations are observed to decline after initiation of the iloprost treatment.

The data also illustrates that CCL2 levels rebound in the treatment group after removal of the iloprost. A limitation of using 100 kDa MWCO membranes with microdialysis probes is their propensity to be affected by either air bubbles or other unwanted experimental artifacts. While many other microdialysis studies, particularly in the brain, have been reported for long-term continuous collection, this is not practicable with these probes. Thus, iloprost treatment was not

continuous. CCL2 concentrations quantified in the flush fluid were similar for both treatment and control. While this flush fluid represents an approximate representation of the localized cytokine levels surrounding the probe outside of the collection period, both probes are treated equally with respect to perfusion fluid flow rates. Since the flow rate starts at 3 µL/min to flush potential air out of the lines and to maintain a steady flow, the CCL2 concentrations are higher than collections from the 1 to 4-hour time points. This is because microdialysis extraction efficiency (EE) is flow rate dependent and EE is lower at higher flow rates. It is common for microdialysis probes to be flushed before use at higher flow rates, but often these solutions are thrown away and not quantified. For cytokine analysis, we chose to keep these samples and analyze them as their values may provide useful information. Since all the dialysates are run on a single ELISA plate for quantitation, this does not provide an increase in workload.

Microdialysis sampling will remove endogenous mediators from the local implantation site. In these studies, alterations in the CCL2 concentrations that would be caused by continuous perfusion were not observed. If this occurred, the concentrations of CCL2 collected would be expected to decline during sampling. A steady-state of CCL2 concentrations appears to be maintained for control probes at the one and two-day time points. This may be occurring because the relative amount of CCL2 being removed is approximately 10% or lower. Our typical in vitro recovery for CCL2 across these membranes is roughly 10%. However, *in vivo* CCL2 can bind tissue glycosaminoglycans allowing for a potential dynamic equilibrium with the removal of the material. Nevertheless, while it is likely and expected the microdialysis probe removes different signaling compounds from the tissue space, iloprost delivery affected the localized response to the implanted dialysis probes.

Histological analyses showed the tissues surrounding the treatment probe to be more fragile with less cellular infiltration and less collagen distribution compared to tissues around the control probes. This is observed in Figures 3.4 and 3.5 where iloprost caused less tissue

integration with the host tissue. This also has been observed in our studies with the immediate infusion of dexamethasone [20]. This observed effect is likely due to the effect of iloprost reducing TGF-β1- induced procollagen mRNA expression and has prevented collagen formation and increased collagen turnover [22]. The immunohistochemical analysis showed that local delivery of iloprost affected macrophage phenotype by shifting them to $CD163^+$ macrophages, which are known to be tissue remodeling and major promoters for the wound healing process. At higher magnification, $CD163^+$ macrophages were observed in the tissues immediately surrounding the treatment probe (< 50μm). This is also interesting since iloprost was not continuously delivered to the implantation site suggesting that macrophage modulation does not need continuous exposure to a modulator to change phenotype.

The microdialysis technique has limitations in this type of research. The main issue is the diffusion restrictions affecting the collection of larger molecular weight solutes [23]. Collecting cytokines *in vivo* is a challenge and many cytokines that are known to be part of macrophage signaling particularly with respect to the inflammatory (IL-1β, IL-6, and TNF-α) and anti-inflammatory response (IL-10) are difficult to collect due to their size and/or their low localized concentrations within the probe-implanted space. CCL2 has a much lower molecular weight than these other cytokines and is more abundant in concentration. The use of much higher molecular weight cutoff membranes (1 MDa) combined with special pumps (push/pull) may allow collection of these larger cytokine proteins.

3.4. Conclusion

Iloprost has been used in this work to successfully modulate macrophage phenotypes *in vivo*. The localized delivery of iloprost led to a decrease in concentration of the pro-inflammatory chemokine (CCL2), less cellular density and less collagen formation surrounding probes suggesting the potential use of iloprost in modulating the foreign body response to an implanted biomaterial. There is a need to investigate other potential macrophage modulators besides steroids since the

use of corticosteroids to suppress the inflammatory response may ultimately fail to prevent unwanted secondary fibrosis due to the loss of the beneficial effects caused by blocking endogenous prostaglandin induction [21]. This work constitutes a first building block toward conducting future studies to determine the utility of iloprost and other potential modulators during distinct stages of the foreign body response. Other experimental variables such as delay in infusion time (waiting a few days post implantation), and how long a macrophage phenotypic response is maintained are questions that can be answered with further research.

3.5. References

[1] F. Porcheray, S. Viaud, A.C. Rimaniol, C. Leone, B. Samah, N. Dereuddre-Bosquet, D. Dormont, G. Gras, Macrophage activation switching: An asset for the resolution of inflammation, Clin. Exp. Immunol. 142(3) (2005) 481-489.

[2] J. Kzhyshkowska, A. Gudima, V. Riabov, C. Dollinger, P. Lavalle, N.E. Vrana, Macrophage responses to implants: prospects for personalized medicine, J. Leukocyte Biol. 98(6) (2015) 953-962.

[3] R. Sridharan, A.R. Cameron, D.J. Kelly, C.J. Kearney, F.J. O'Brien, Biomaterial based modulation of macrophage polarization: a review and suggested design principles, Mater. Today (Oxford, U. K.) 18(6) (2015) 313-325.

[4] J.M. Anderson, K.M. Miller, Biomaterial biocompatibility and the macrophage, Biomaterials 5(1) (1984) 5-10.

[5] A. Remes, D.F. Williams, Immune response in biocompatibility, Biomaterials 13(11) (1992) 731-43.

[6] W.-J. Hu, J.W. Eaton, L. Tang, Molecular basis of biomaterial-mediated foreign body reactions, Blood 98(4) (2001) 1231-1238.

[7] P.M. Kou, J.E. Babensee, Macrophage and dendritic cell phenotypic diversity in the context of biomaterials, J. Biomed. Mater. Res., Part A 96A(1) (2011) 239-260.

[8] D.M. Mosser, J.P. Edwards, Exploring the full spectrum of macrophage activation, Nat. Rev. Immunol. 8(12) (2008) 958-969.

[9] A. Mantovani, S.K. Biswas, M.R. Galdiero, A. Sica, M. Locati, Macrophage plasticity and polarization in tissue repair and remodelling, The Journal of pathology 229(2) (2013) 176-185.

[10] D.H. Adams, A.R. Lloyd, Chemokines: leucocyte recruitment and activation cytokines, Lancet 349(9050) (1997) 490-5.

[11] Z. Zidek, P. Anzenbacher, E. Kmonickova, Current status and challenges of cytokine pharmacology, Br. J. Pharmacol. 157(3) (2009) 342-361.

[12] X. Ao, J.A. Stenken, Microdialysis sampling of cytokines, Methods 38(4) (2006) 331-341.

[13] B.H.C. Westerink, T.I.F.H. Cremers, Handbook of microdialysis: methods, applications and perspectives, Academic Press2007.

[14] X. Mou, M.R. Lennartz, D.J. Loegering, J.A. Stenken, Modulation of the foreign body reaction for implants in the subcutaneous space: microdialysis probes as localized drug delivery/sampling devices, J Diabetes Sci Technol 5(3) (2011) 619-31.

[15] E.C.M. de Lange, Recovery and Calibration Techniques:Toward Quantitative Microdialysis, in: M. Müller (Ed.), Microdialysis in Drug Development, Springer, New York, 2013, pp. 13-33.

[16] K.L. Spiller, R.R. Anfang, K.J. Spiller, J. Ng, K.R. Nakazawa, J.W. Daulton, G. Vunjak-Novakovic, The role of macrophage phenotype in vascularization of tissue engineering scaffolds, Biomaterials 35(15) (2014) 4477-4488.

[17] L.B. Moore, A.J. Sawyer, A. Charokopos, E.A. Skokos, T.R. Kyriakides, Loss of monocyte chemoattractant protein-1 alters macrophage polarization and reduces NFκB activation in the foreign body response, Acta Biomater. 11 (2015) 37-47.

[18] R.M. Boehler, R. Kuo, S. Shin, A.G. Goodman, M.A. Pilecki, J.N. Leonard, L.D. Shea, Lentivirus delivery of IL-10 to promote and sustain macrophage polarization towards an anti-inflammatory phenotype, Biotechnol. Bioeng. 111(6) (2014) 1210-1221.

[19] G.D. Keeler, J.M. Durdik, J.A. Stenken, Effects of delayed delivery of dexamethasone-21-phosphate via subcutaneous microdialysis implants on macrophage activation in rats, Acta Biomater 23 (2015) 27-37.

[20] G.D. Keeler, J.M. Durdik, J.A. Stenken, Localized delivery of dexamethasone-21-phosphate via microdialysis implants in rat induces M(GC) macrophage polarization and alters CCL2 concentrations, Acta Biomater 12 (2015) 11-20.

[21] R. Stratton, X. Shiwen, Role of prostaglandins in fibroblast activation and fibrosis, J Cell Commun Signal 4(2) (2010) 75-7.

[22] J. Gomez-Arroyo, A.A. Syed, L. Farkas, D. Kraskauskas, N.F. Voelkel, M. Sakagami, P.R. Byron, T.B. Van, A. Abbate, S. Mizuno, H.J. Bogaard, Iloprost reverses established fibrosis in experimental right ventricular failure, Eur Respir J 45(2) (2015) 449-62.

[23] S.B. Jadhav, V. Khaowroongrueng, H. Derendorf, Microdialysis of Large Molecules, J. Pharm. Sci. 105(11) (2016) 3233-3242.

Chapter 4

Optimizing the Use of Sponge Implants as a Model to Study Macrophage Activation

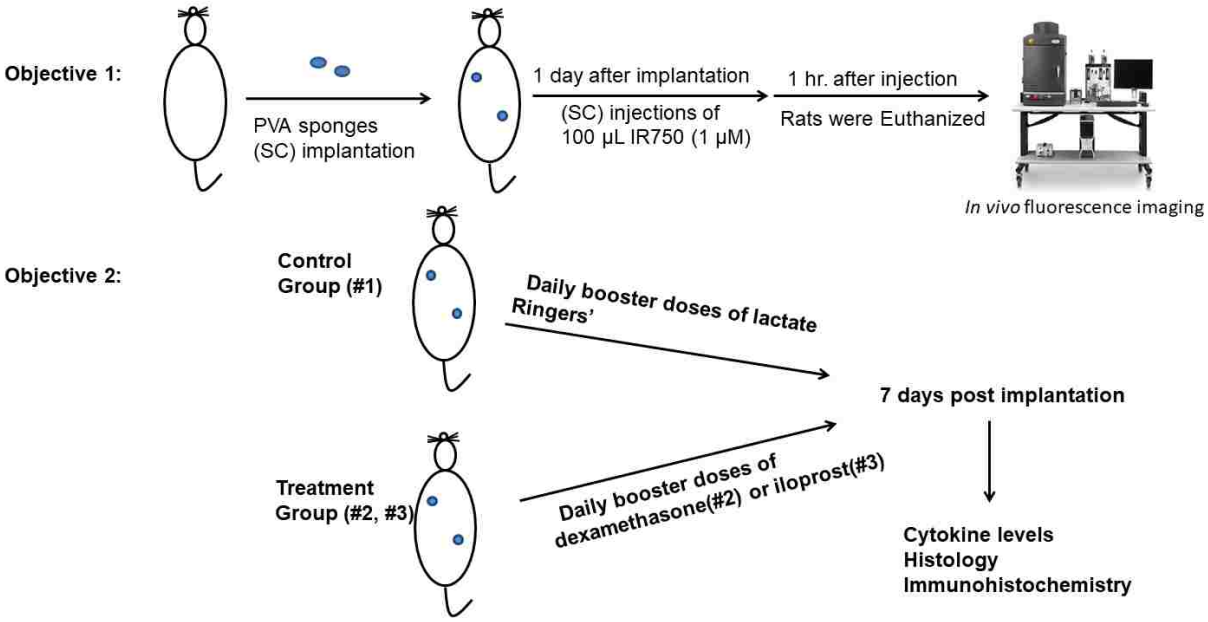

Figure 4.1. Experimental design overview of chapter 4.

4.1. Introduction

Macrophage activation concepts have been utilized in the field of biomaterials to promote wound healing and enhance the biomaterials/tissue integration. Shifting the macrophages to their pro wound healing $CD163^{+}CD68^{+}$ state has been desirable to prolong the implants life and decrease the encapsulation around the implanted devices [1-4]. Among the materials incorporated in the biomaterials structure to be later used in wound healing and tissue repair studies is polyvinyl alcohol (PVA) [5-8].

This study ultimately aims to optimize the use of PVA sponge implants and modulators delivery to shift the macrophage activation state to their pro wound healing state, $CD163^{+}CD68^{+}$ to provide better biomaterial/tissue integration outcomes at a longer time period. This study also aimed to testing the ability of iloprost as a macrophage modulator at a longer time, 7 days post sponge implantation, than what was tested for in chapter 3, 2 days post implantation. Using sponge implants in macrophage activation studies will serve the interest of evaluating the macrophage response at longer time periods. This study included optimizing the direct dosing system using IR-750 fluorophore to determine flow paths of the injection surrounding the PVA sponge implant and to isolate the variable for the subcutaneous injections administration to the sponge implantation site. This was followed with using both dexamethasone as the gold standard to assess the use of PVA sponges as a model to study macrophage activation and optimizing the use of iloprost as another modulator at 7 days post implantation time point.

Using a PVA sponge as a model in wound healing studies is advantageous because of the ability to collect the wound fluid and various cytokines and chemokines at the implantation site which can be later quantified to provide an indication about the progression of the inflammatory status at the targeted time point. Collecting wound fluid from implanted PVA sponges allows for both qualitative and quantitative analyses that can evaluate the macrophage activation and cytokine profile around the implant. Moreover, the PVA sponge can serve as a drug

delivery vehicle, directly releasing the drug at the implantation site which is advantageous in biomaterial-host interaction studies. Thus, assessment of different drugs or biomolecules to modulate the microenvironment around the implanted biomaterial can be rapidly performed along with estimates of effective dosages that would be needed to achieve a desired biological outcome.

4.2. Results

4.2.1. Optimize the direct dosing protocol using IR750

To ensure the injected modulator drugs at the implant site were reaching the implantation site and eliminate the variability in the subcutaneous booster dosing system, subcutaneous injections of fluorescent material, 100 µL IR750 (1 µM), were administered to one site of sponge implantation in each animal one day post implantation. Those injections helped determine the flow paths of the injection surrounding the implant which was observed using an IVIS Lumina XR system (Figure 4.2). These injections matched the volume that was useed in for the booster dose injections.

To compare the distribution profiles of the fluorophore subcutaneous images, another set of 100 µL IR750 (1 µM) subcutaneous IR750 injections were administered to the other sponges in each animal. Interpretation of the obtained images suggested using the implanted sponges to deliver the same treatment in each animal to prevent any possible intervention between different treatments at the site of implantation.

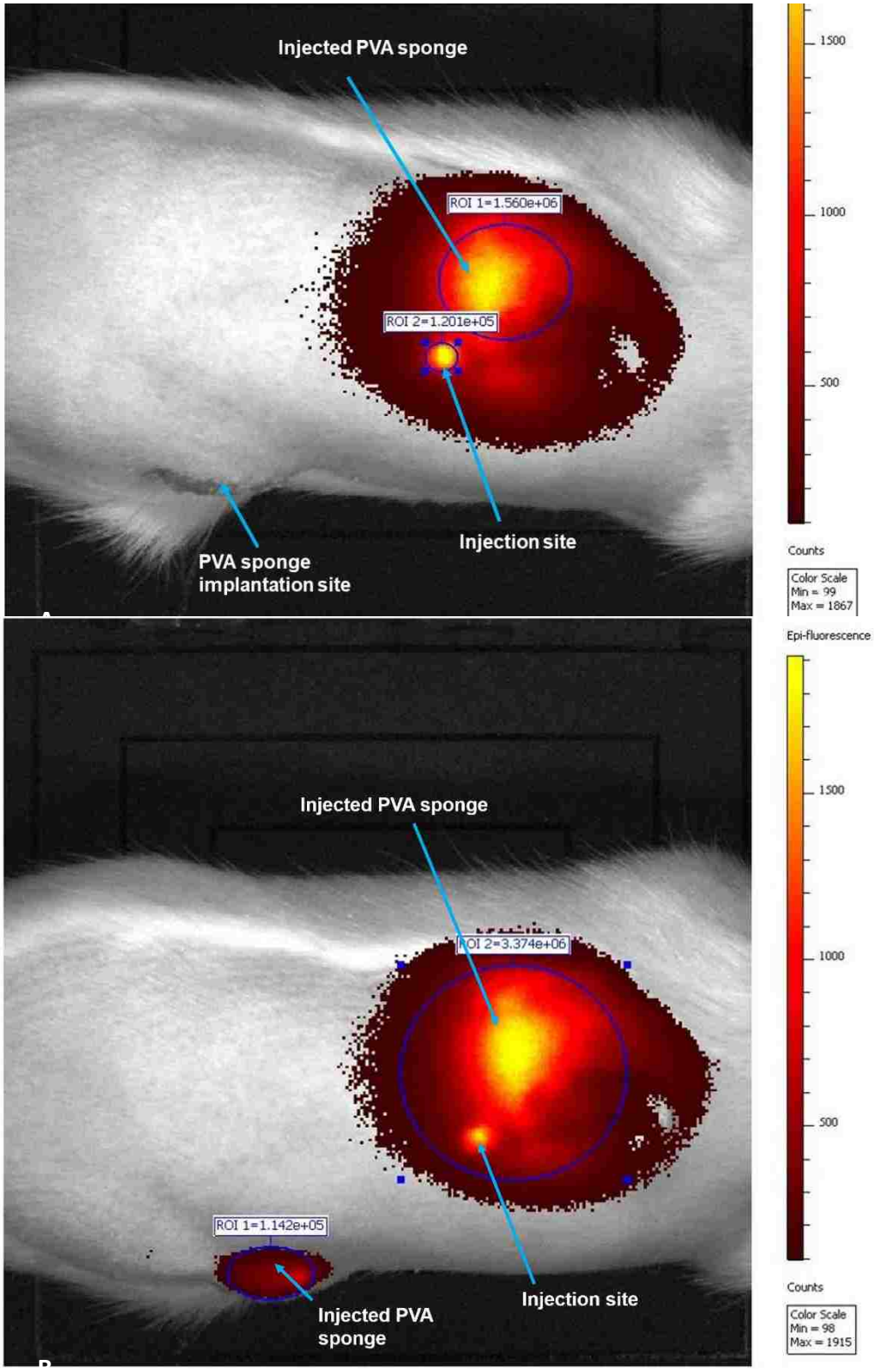

Figure 4.2. Flow path of SC injections surrounding the PVA sponge implants. **(A)** Fluorescence image obtained after one hour of 100 µL SC IR750 (1 µM) injection at the PVA sponge implantation site. **(B)** Fluorescence image obtained immediately after a 100 µL SC IR750 (1 µM) injection at the PVA sponge.

4.2.2. CCL2 quantification in the wound fluid collected from PVA sponges

The average volume of the collected wound fluid from each sponge was 100 µL. Wound fluid was extracted from the control, dexamethasone-treated, and iloprost-treated sponges on day 7. CCL2 levels were determined using ELISA and were normalized to total protein concentrations found in the sample. Data has been plotted at the mean value of samples from 6 rats. Error bars represent the ±SD.

The levels of CCL2 in the wound fluid collected from the dexamethasone treated sponges and those collected from the iloprost treated sponges were found to be significantly less than the wound fluid levels of CCL2 from the control sponges ($p \leq 0.001$). No significant difference was found between the wound fluid levels of CCL2 from dexamethasone-treated sponges vs. iloprost-treated sponges (Figure 4.3).

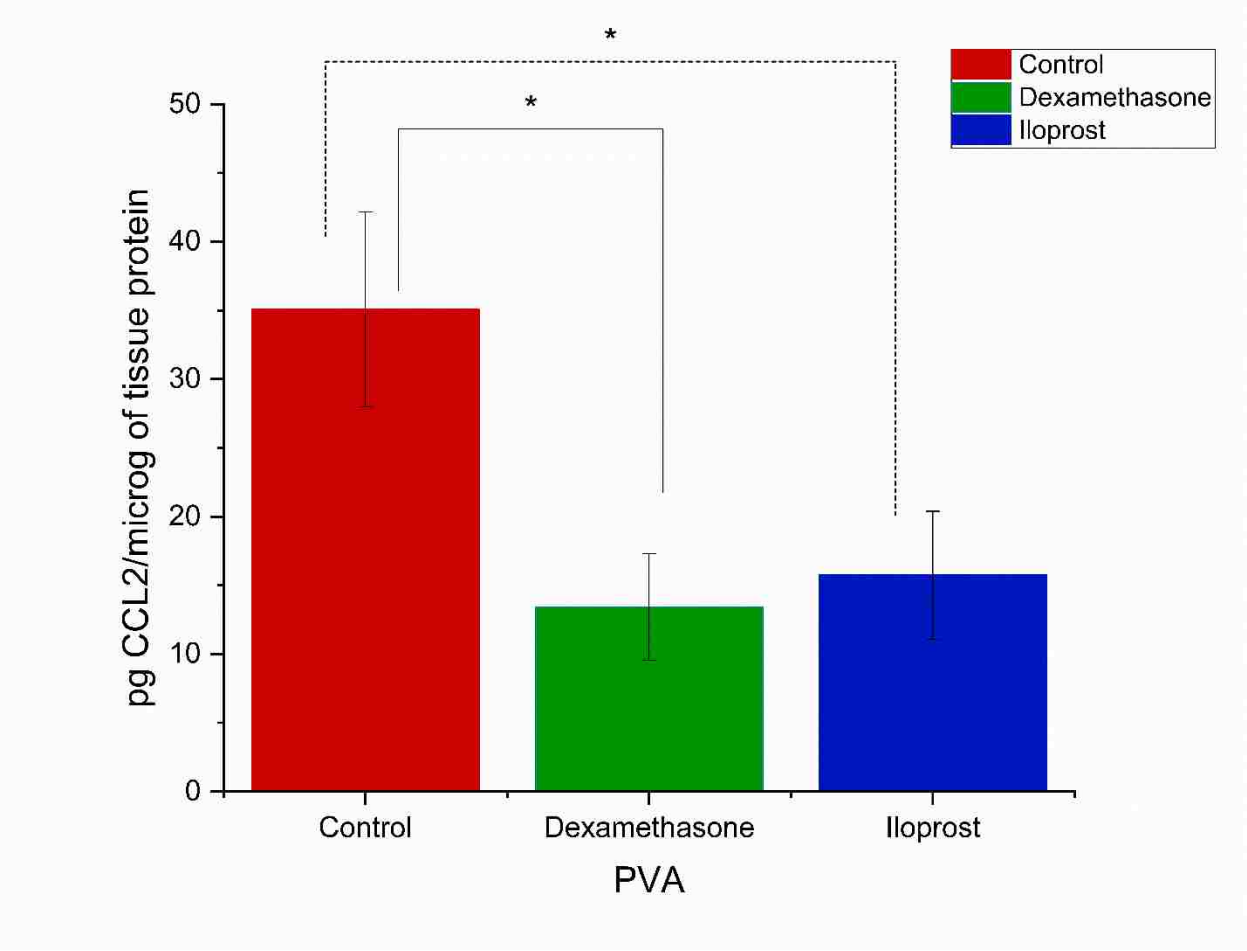

Figure 4.3. Bar graphs showing the concentration of CCL2 collected from the wound fluid around the control, dexamethasone-treated, and iloprost-treated sponges respectively after 7 days of implantation. Concentrations are given as the mean from six animals. Error bars represent the ± SD. Significance is denoted by *p ≤0.001, n=6 where n represent the number of animals.

4.2.3. Histological analyses

H&E and Masson's trichrome staining were performed on the tissue sections around the control, dexamethasone-treated sponges, and iloprost-treated sponges to evaluate the cellular density and the collagen distribution at the tissue/sponge interface.

Fewer cells were observed in the tissues surrounding both iloprost treated sponges and dexamethasone treated sponges compared to the tissues around the control sponges ($p \leq 0.001$). Cellular density in the tissues around the iloprost treated sponges was found to be similar to that around the dexamethasone treated sponges (Figures 4.4 and 4.5). At a higher magnification, less collagen density was observed in the tissues surrounding both iloprost treated sponges and dexamethasone treated sponges compared to the tissues around the control sponges (Figure 4.6).

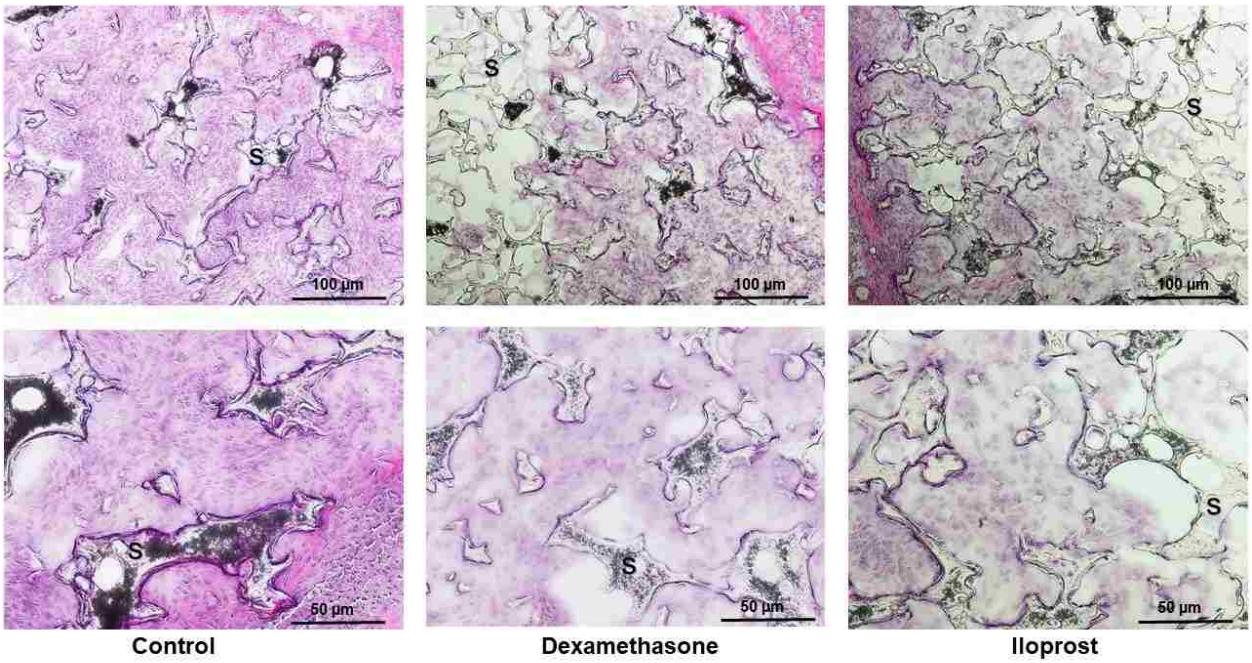

Figure 4.4. H&E staining for tissues around the explanted PVA sponges. Top scale bars represent 100 µm. Bottom scale bars represent 50 µm. (S) indicates a sponge.

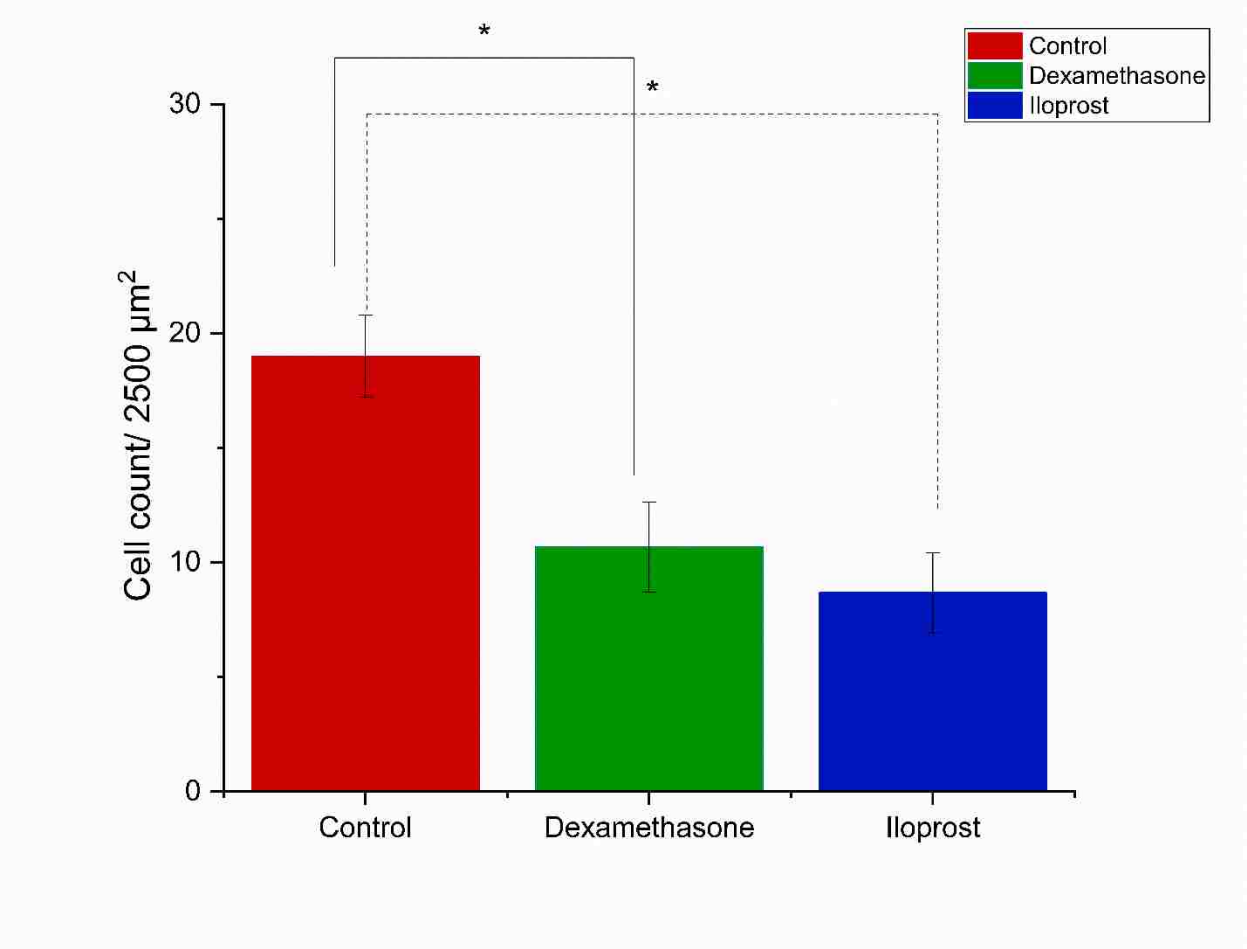

Figure 4.5. Bar graphs showing the cell count/2500 µm^2 of the tissues surrounding the control, dexamethasone-treated, and iloprost-treated sponges respectively after 7 days of implantation. The cell counts are presented as the mean from six animals. Error bars represent the ± SD. Significance is denoted by *p ≤0.001, n=6 where n represent the number of animals.

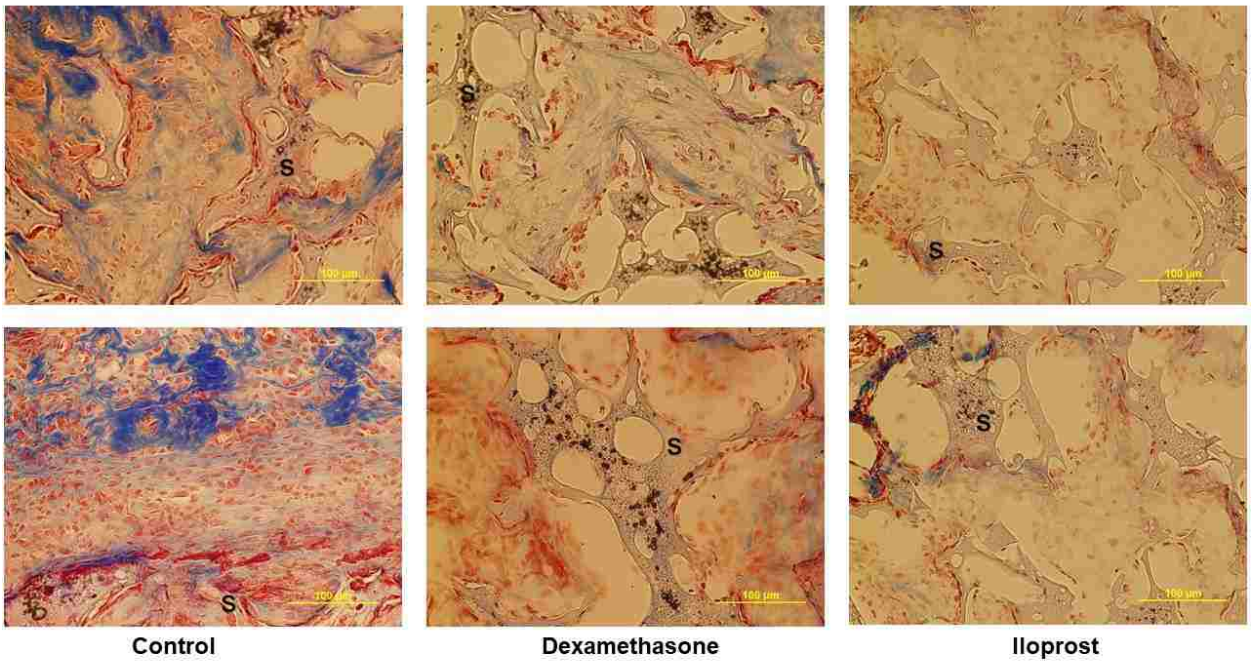

Figure 4.6. Masson's Trichrome staining for tissues around the explanted PVA sponges. Scale bars represent 100 µm. (S) indicates a sponge.

4.2.4. Immunohistochemistry Analysis

Immunohistochemical staining was performed to determine the presence and the subset population of $CD163^{+}CD68^{+}$ macrophages among macrophages ($CD68^{+}$ cells) in tissues surrounding the control and treatment PVA sponges. More $CD163^{+}CD68^{+}$ cells were observed in the tissues around the iloprost-treated sponges and dexamethasone treated sponges compared to the tissues around the control sponges ($p \leq 0.001$). The presence of the $CD163^{+}CD68^{+}$ cells was noticeable in the tissues at a range of (0 – 250 µm) surrounding the dexamethasone treated sponges and iloprost-treated sponges compared to almost no $CD163^{+}CD68^{+}$ cells around the control sponges at the same range. The percentage of $CD163^{+}CD68^{+}$ among $CD68^{+}$ cells was calculated manually in both treatment and control probes at the higher magnification (20X) to evaluate the population of these cells around the implanted sponges (Figure 4.8).

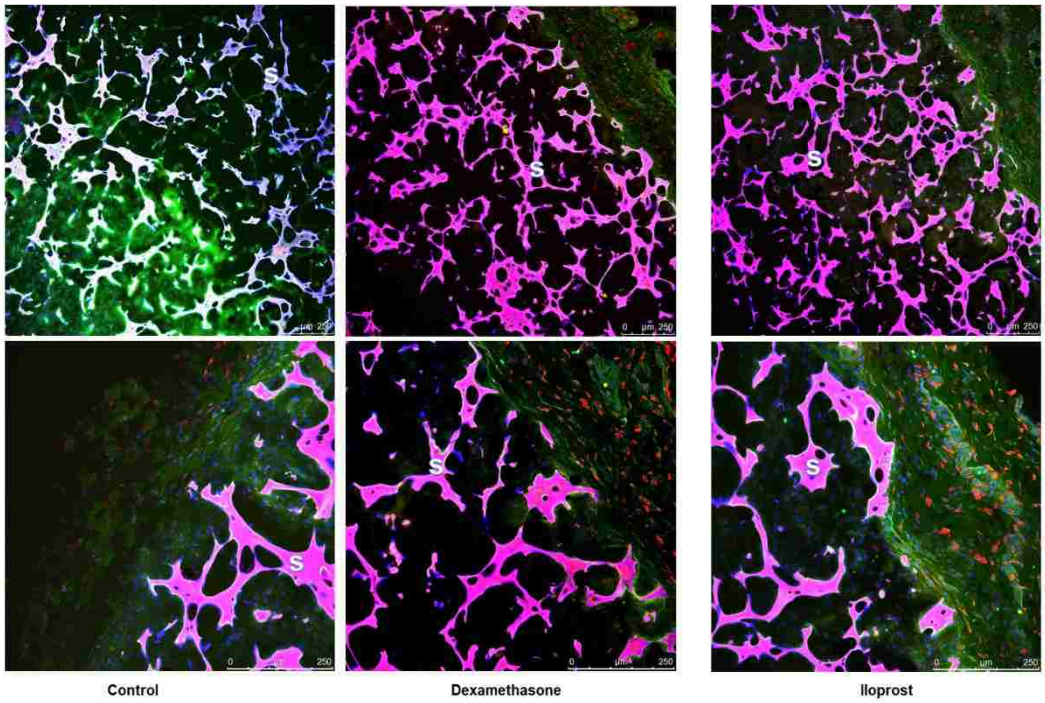

Figure 4.7. Immunohistochemical staining for CD68 (green), CD163 (red), and nuclei (blue) in the tissue around the explanted PVA sponges. Overlapped colors represent $CD68^{+}CD163^{+}$ macrophages. Scale bars represent 250 µm. The sponge material is shown in pink. (S) Indicates a sponge.

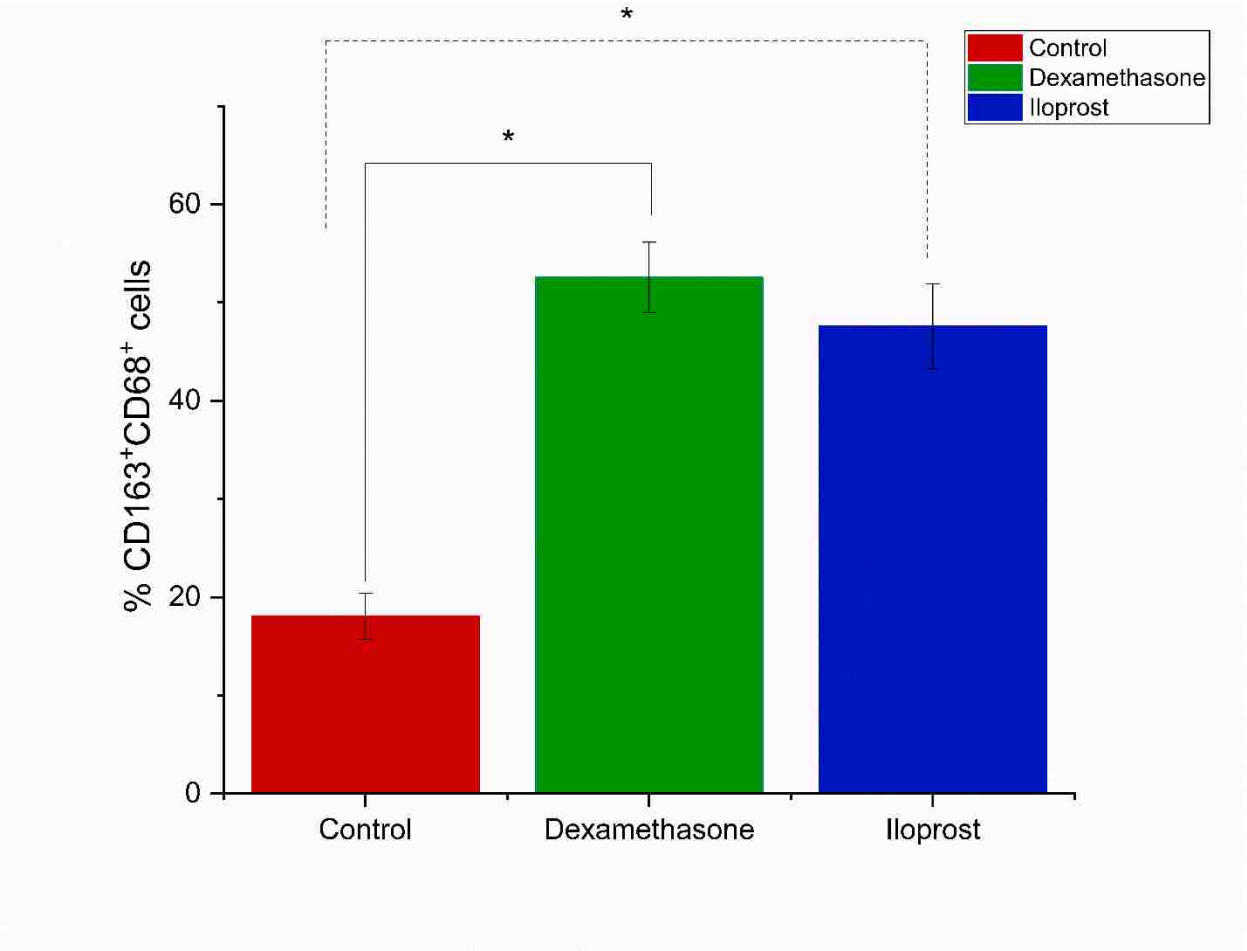

Figure 4.8. Bar graphs showing the percentage of $CD163^{+}CD68^{+}$cells among $CD68^{+}$ cells in the tissues around the control, dexamethasone-treated, and iloprost-treated sponges respectively after 7 days of implantation. The percentages are given as the mean from six animals. Error bars represent the ± SD. Significance is denoted by *p ≤0.001, n=6 where n represent the number of animals.

4.3. Discussion

Historically, there has been significant interest in the role macrophages serve with respect to modulating the undesirable fibrotic outcome to implanted materials [9-12]. Macrophages functional behavior is mainly affected by their surrounding environmental cues where they become activated existing in a continuum of highly inflammatory to highly pro-wound healing phenotypes that are of importance to prevent the unwanted outcomes to biomedical implants [13-15].

Dexamethasone is a synthetic glucocorticoid with prevailing anti-inflammatory and immunosuppressive properties and has been considered the “gold” standard” in the biomaterials field [16-22]. Dexamethasone has shown ability to shift macrophages to their $CD163^{+}CD68^{+}$ phenotype, formerly called M2c activation state, which is considered critical to wound healing [23, 24]. These studies have shown that tissue surrounding dexamethasone eluting materials are characterized as having reduced cellular density. Noteworthy, this finding has also been consistent when studying the macrophage activation after the PVA sponge implantation. Iloprost has also been studied in our lab for its ability to shift macrophages to their $CD163^{+}CD68^{+}$ phenotype in both cell culture and *in-vivo* at 3 days post implantation time point [25, 26]. This study introduced the importance of studying the effect of this modulator drug at a longer time point.

The use of PVA sponge implants in our study not only served the interest of evaluating the macrophage response at longer time periods but also constituted a delivery vehicle of different drug modulators to evaluate the macrophage activation phenotype shifts in response to these modulators. PVA, a synthetic polymer, has been widely used in the past 30 years in several medical devices due its chemical resistance and its low protein adsorption properties [27-29].

CCL2 is a chemokine known to recruit monocytes to the implantation site in response to acute tissue injuries [30]. The levels of the pro-inflammatory chemokine CCL2 were significantly

decreased in the wound fluid collected from the dexamethasone-treated sponges and the iloprost-treated sponges compared to the control sponges. This decrease in CCL2 levels confirms that both modulators exert expected anti-inflammatory properties after being administered to the implantation site.

Fewer cells and less collagen distribution have been noted during the histological analyses in the tissues surrounding dexamethasone-treated sponges and the iloprost-treated sponges compared to the tissues surrounding the control sponges (Figures 4.3 and 4.4). These finding have also been noted in the tissues treated with iloprost at 3 days post implantation time point and the previously performed dexamethasone studies [23-25]. The iloprost effect on collagen comes from the fact that iloprost is considered an exogenous agonist to anti-fibrotic receptors that augment the downstream biological responses to suppress fibrosis and is mainly used to reverse right ventricle fibrosis by re-orchestrating the collagen balance [31].

Treating the implanted PVA sponges with dexamethasone or iloprost resulted in shifting the macrophages to the $CD163^{+}CD68^{+}$ phenotype which is a crucial turning point toward improved integration. This confirmed the ability to use iloprost as a macrophage modulator at a longer time period, and allowed to study the cellular distribution around the implant. The manual quantification of the $CD163^{+}CD68^{+}$ phenotype among $CD68^{+}$ suggested no significant difference in the ability of iloprost and dexamethasone to shift the macrophages to their desired $CD163^{+}CD68^{+}$ phenotype. However, it is also important to note that this quantification represents only the cells shown in the obtained immunohistochemistry images and this suggestion cannot be definitive since not the whole tissue was spanned to quantify the percentage of the $CD163^{+}CD68^{+}$ cells.

4.4. Conclusion

The implanted PVA sponges provided a useful tool to study the macrophage activation profile at 7 days post implantation in addition to deliver drug modulators to the surrounding tissues in the aim of shifting the macrophages to their $CD163^{+}CD68^{+}$ phenotype. CCL2 in the wound fluid collected from the dexamethasone treated sponges and those collected from the iloprost treated sponges were found to be significantly less than the wound fluid levels of CCL2 from the control sponges, with no significant difference found between the wound fluid levels of CCL2 from dexamethasone-treated sponges vs. iloprost-treated sponges. Less cellular infiltration and less collagen formation was observed in the tissues surrounding both iloprost treated sponges and dexamethasone treated sponges compared to the tissues around the control sponges. Greater presence of $CD163^{+}CD68^{+}$ cells was observed in the tissues surrounding both iloprost-treated sponges and dexamethasone-treated sponges compared to the tissues around the control sponges which confirms iloprost as a potent modulator of macrophage phenotype.

References

[1] J.H. Graversen, M. Madsen, S.K. Moestrup, CD163: a signal receptor scavenging haptoglobin-hemoglobin complexes from plasma, Int J Biochem Cell Biol 34(4) (2002) 309-14.

[2] J.H. Thomsen, A. Etzerodt, P. Svendsen, S.K. Moestrup, The haptoglobin-CD163-heme oxygenase-1 pathway for hemoglobin scavenging, Oxid Med Cell Longev 2013 (2013) 523652.

[3] B.N. Brown, R. Londono, S. Tottey, L. Zhang, K.A. Kukla, M.T. Wolf, K.A. Daly, J.E. Reing, S.F. Badylak, Macrophage phenotype as a predictor of constructive remodeling following the implantation of biologically derived surgical mesh materials, Acta Biomater 8(3) (2012) 978-987.

[4] P.F. Slivka, C.L. Dearth, T.J. Keane, F.W. Meng, C.J. Medberry, R.T. Riggio, J.E. Reing, S.F. Badylak, Fractionation of an ECM hydrogel into structural and soluble components reveals distinctive roles in regulating macrophage behavior, Biomater. Sci. 2(10) (2014) 1521-1534.

[5] M. Kastellorizios, F. Papadimitrakopoulos, D.J. Burgess, Multiple tissue response modifiers to promote angiogenesis and prevent the foreign body reaction around subcutaneous implants, J Control Release 214 (2015) 103-11.

[6] V. Maquet, D. Martin, B. Malgrange, R. Franzen, J. Schoenen, G. Moonen, R. Jerome, Peripheral nerve regeneration using bioresorbable macroporous polylactide scaffolds, J. Biomed. Mater. Res. 52(4) (2000) 639-651.

[7] T. Noguchi, T. Yamamuro, M. Oka, P. Kumar, Y. Kotoura, S. Hyon, Y. Ikada, Poly(vinyl alcohol) hydrogel as an artificial articular cartilage: evaluation of biocompatibility, J Appl Biomater 2(2) (1991) 101-7.

[8] N. Charernsriwilaiwat, T. Rojanarata, T. Ngawhirunpat, P. Opanasopit, Electrospun chitosan/polyvinyl alcohol nanofibre mats for wound healing, Int Wound J 11(2) (2014) 215-22.

[9] J.M. Anderson, K.M. Miller, Biomaterial biocompatibility and the macrophage, Biomaterials (Guildford, Engl.) 5(1) (1984) 5-10.

[10] A. Remes, D.F. Williams, Immune response in biocompatibility, Biomaterials 13(11) (1992) 731-43.

[11] W.J. Hu, J.W. Eaton, T.P. Ugarova, L. Tang, Molecular basis of biomaterial-mediated foreign body reactions, Blood 98(4) (2001) 1231-8.

[12] P.M. Kou, J.E. Babensee, Macrophage and dendritic cell phenotypic diversity in the context of biomaterials, J. Biomed. Mater. Res., Part A 96A(1) (2011) 239-260.

[13] R.D. Stout, C. Jiang, B. Matta, I. Tietzel, S.K. Watkins, J. Suttles, Macrophages sequentially change their functional phenotype in response to changes in microenvironmental influences, J Immunol 175(1) (2005) 342-9.

[14] B.N. Brown, R. Londono, S. Tottey, L. Zhang, K.A. Kukla, M.T. Wolf, K.A. Daly, J.E. Reing, S.F. Badylak, Macrophage phenotype as a predictor of constructive remodeling following the implantation of biologically derived surgical mesh materials, Acta Biomater 8(3) (2012) 978-87.

[15] F. Porcheray, S. Viaud, A.C. Rimaniol, C. Leone, B. Samah, N. Dereuddre-Bosquet, D. Dormont, G. Gras, Macrophage activation switching: An asset for the resolution of inflammation, Clin. Exp. Immunol. 142(3) (2005) 481-489.

[16] Y. Moussy, L. Hersh, P. Dungel, Distribution of [3H]Dexamethasone in Rat Subcutaneous Tissue after Delivery from Osmotic Pumps, Biotechnol. Prog. FIELD Full Journal Title:Biotechnology Progress 22(3) (2006) 819-824.

[17] J.M. Morais, F. Papadimitrakopoulos, D.J. Burgess, Biomaterials/tissue interactions: possible solutions to overcome foreign body response, AAPS J. 12(2) (2010) 188-196.

[18] U. Klueh, M. Kaur, D.C. Montrose, D.L. Kreutzer, Inflammation and glucose sensors: use of dexamethasone to extend glucose sensor function and life span in vivo, J Diabetes Sci Technol 1(4) (2007) 496-504.

[19] L.W. Norton, J. Park, J.E. Babensee, Biomaterial adjuvant effect is attenuated by anti-inflammatory drug delivery or material selection, J. Controlled Release 146(3) (2010) 341-348.

[20] N.M. Vacanti, H. Cheng, P.S. Hill, J.D.T. Guerreiro, T.T. Dang, M. Ma, S. Watson, N.S. Hwang, R. Langer, D.G. Anderson, Localized delivery of dexamethasone from electrospun fibers reduces the foreign body response, Biomacromolecules 13(10) (2012) 3031-3038.

[21] M. Rubert, Y.-F. Li, J. Dehli, M.B. Taskin, F. Besenbacher, M. Chen, Dexamethasone encapsulated coaxial electrospun PCL/PEO hollow microfibers for inflammation regulation, RSC Adv. 4(93) (2014) 51537-51543.

[22] S.G. Vallejo-Heligon, B. Klitzman, W.M. Reichert, Characterization of porous, dexamethasone-releasing polyurethane coatings for glucose sensors, Acta Biomater. 10(11) (2014) 4629-4638.

[23] G.D. Keeler, J.M. Durdik, J.A. Stenken, Localized delivery of dexamethasone-21-phosphate via microdialysis implants in rat induces M(GC) macrophage polarization and alters CCL2 concentrations, Acta Biomater 12 (2015) 11-20.

[24] G.D. Keeler, J.M. Durdik, J.A. Stenken, Effects of delayed delivery of dexamethasone-21-phosphate via subcutaneous microdialysis implants on macrophage activation in rats, Acta Biomater 23 (2015) 27-37.

[25] K. Alkhatib, T.M. Poseno, A. Diaz Perez, J.M. Durdik, J.A. Stenken, Iloprost Affects Macrophage Activation and CCL2 Concentrations in a Microdialysis Model in Rats, Pharm. Res. 35(1) (2018) 1-10.

[26] A.A.D. Perez, Comparison of Different Modulators that Affect Macrophage Activation In Vitro, (2015).

[27] M.I. Baker, S.P. Walsh, Z. Schwartz, B.D. Boyan, A review of polyvinyl alcohol and its uses in cartilage and orthopedic applications, J. Biomed. Mater. Res., Part B 100B(5) (2012) 1451-1457.

[28] M.-H. Alves, B.E.B. Jensen, A.A.A. Smith, A.N. Zelikin, Poly(Vinyl Alcohol) Physical Hydrogels: New Vista on a Long Serving Biomaterial, Macromol. Biosci. 11(10) (2011) 1293-1313.

[29] J.A. Buckwalter, H.J. Mankin, Articular cartilage: degeneration and osteoarthritis, repair, regeneration, and transplantation, Instr Course Lect 47 (1998) 487-504.

[30] E.J. Leonard, T. Yoshimura, Human monocyte chemoattractant protein-1 (MCP-1), Immunol Today 11(3) (1990) 97-101.

[31] J. Gomez-Arroyo, M. Sakagami, A.A. Syed, L. Farkas, B. Van Tassell, D. Kraskauskas, S. Mizuno, A. Abbate, H.J. Bogaard, P.R. Byron, N.F. Voelkel, Iloprost reverses established fibrosis in experimental right ventricular failure, The European respiratory journal 45(2) (2015) 449-462.

Chapter 5

Comparison of Polyvinyl Alcohol (PVA) vs Collagen Sponges to Assess Macrophage Activation Patterns in Rats

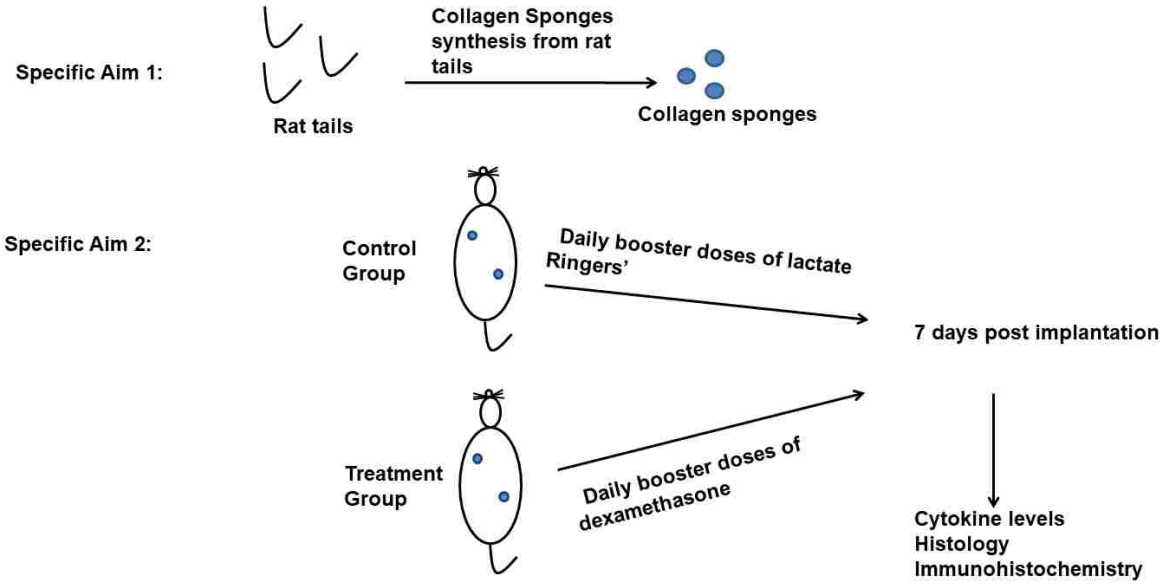

Figure 5.1. Experimental design overview of chapter 5.

5.1. Introduction

Implanted biomaterials are widely used to improve the quality of life for many different patient subgroups. Macrophages are the primary cells that direct immune functions and influence the severity of the FBR [1-3]. Biomaterials scientists have been interested in locally modulating macrophages at the site of the biomaterial to the alternatively activated, pro-wound healing state to improve the integration of many biomaterials with their host, thus saving costs and greatly improving quality of life [4-8].

After confirming the ability of iloprost to modulate the macrophages phenotype, a material-based study was designed to assess macrophage activation caused by implanted polyvinyl alcohol sponges vs. collagen sponges in the subcutaneous space of male Sprague Dawley rats. This project aimed to comparing the findings from the polyvinyl alcohol studies performed in chapter 4 to modulating macrophage activation phenotype after the implantation collagen biodegradable sponges in the subcutaneous space of male Sprague Dawley rats. The first aim of this project focuses on creating synthetic collagen scaffolds (sponges) in house using natural collagen from the rat tail. The collagen scaffolds prepared were assessed for pore size and pore size distribution using scanning electron microscopy (SEM).

The second aim included implanting collagen sponges and evaluating the foreign body response to these implants. This also includes the delivery of the previously tested modulators, dexamethasone and iloprost, for their ability to shift macrophages to their pro-wound healing state. The use of these modulators enable screening and comparing the effect of the chemistry of biomaterial on macrophage activation.

Collagen is a natural raw material that has been incorporated in the structure of implanted biomaterials to serve various applications [9, 10]. As researchers are getting more interested in including modulators into these matrices, it is of biomedical significance to determine how different modulators affect this material as well as the PVA sponge.

5.2. Results

5.2.1. Collagen Sponges Characterization

The morphology of collagen sponges was analyzed with the SEM. The sponges revealed homogenous porosity with interconnected pore networks. The pore size at the sponge surface was measured in a range between 100 and 200 μm, while the pore size at the inner core of the sponges was 30-40 μm (Figure 5.2). Developing sponges with high porosity is important, because the surface area increases with the porosity; and as a result, higher amounts of drug can be adsorbed on the surface of the sponges [11, 12].

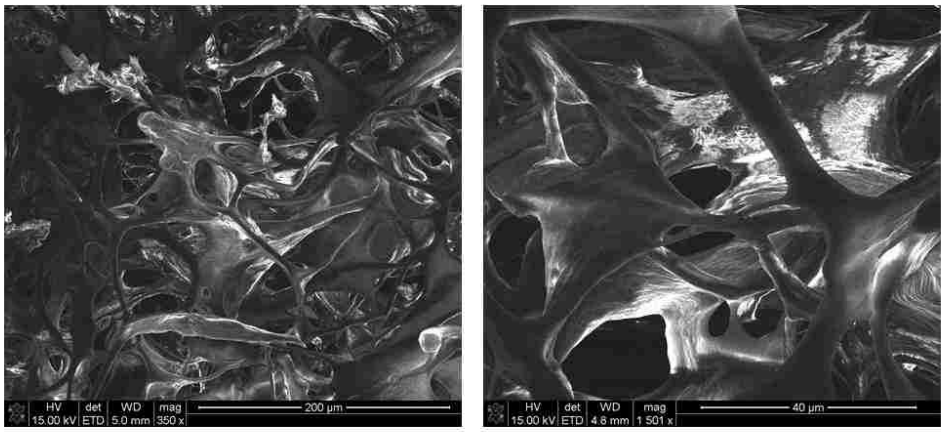

Figure 5.2. Scanning electron microscope (SEM) images representing the morphology of collagen sponges at their surface and the inner core.

5.2.2. CCL2 Quantification in the wound fluid collected from the collagen sponges

The average volume of the collected wound fluid from each sponge was 100 µL. Wound fluid was extracted from the control, dexamethasone-treated, and iloprost-treated sponges on day 7. CCL2 levels were determined using ELISA and were normalized to total protein concentrations found in the sample. Data has been plotted at the mean value of samples from 6 rats. Error bars represent the ±SD.

The levels of CCL2 in the wound fluid collected from the dexamethasone-treated sponges and those collected from the iloprost-treated sponges were found to be significantly less than the wound fluid levels of CCL2 from the control sponges in both the PVA and the collagen sponges. No significant difference was found between the wound fluid levels of CCL2 from dexamethasone-treated PVA sponges vs. iloprost-treated PVA sponges. Similarly, the wound fluid levels of CCL2 from the dexamethasone-treated collagen sponges and the iloprost-treated collagen sponges were also found to be similar. Interestingly, the levels of CCL2 in the wound fluid collected from the collagen control sponges were significantly less those collected from the PVA sponges (Figure 5.3).

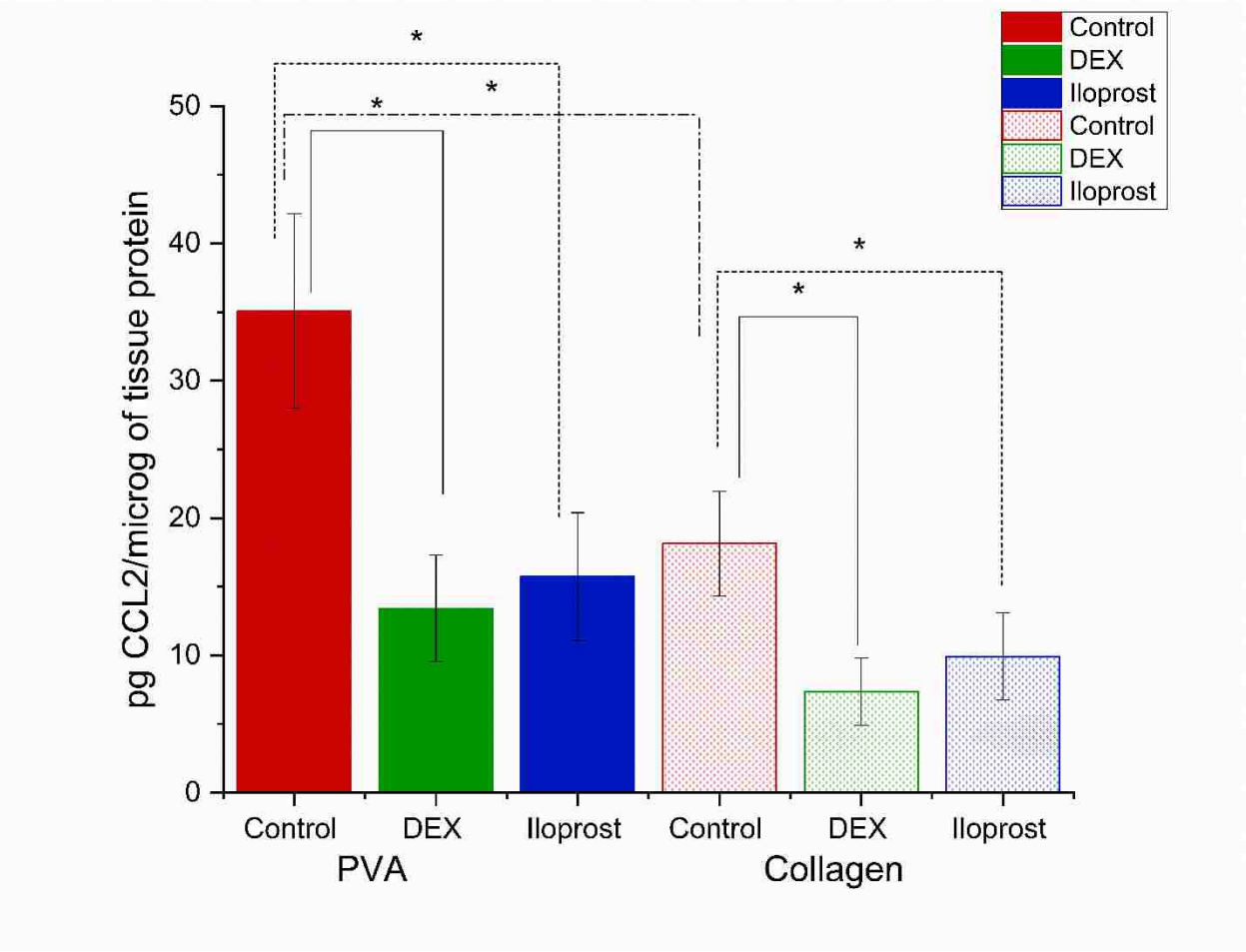

Figure 5.3. Bar graphs showing the concentration of CCL2 collected from the wound fluid around the control, dexamethasone-treated, and iloprost treated sponges respectively after 7 days of implantation. Concentrations are given as the mean from six animals. Error bars represent ± SD. Significance is denoted by *p ≤0.001, n=6 where n represent the number of animals.

5.2.3. Histological analyses

H&E and Masson's trichrome staining were performed on the tissue sections around the control, dexamethasone-treated sponges, and iloprost-treated sponges for both PVA and collagen sponges to evaluate the cellular density and the collagen distribution at the tissue/sponge interface.

Fewer cells were found around the dexamethasone-treated collagen sponges and the iloprost-treated collagen sponges compared to those around the control collagen sponges ($p \leq 0.001$) (Figures 5.4 and 5.6). On the other hand, fewer cells were observed in the tissues surrounding both iloprost-treated PVA sponges and dexamethasone-treated PVA sponges compared to the tissues around the control sponges. Cell count around the iloprost-treated PVA sponges was found to be similar to that around the dexamethasone-treated PVA sponges ($p \leq 0.001$) (Figure 5.5 and 5.6).

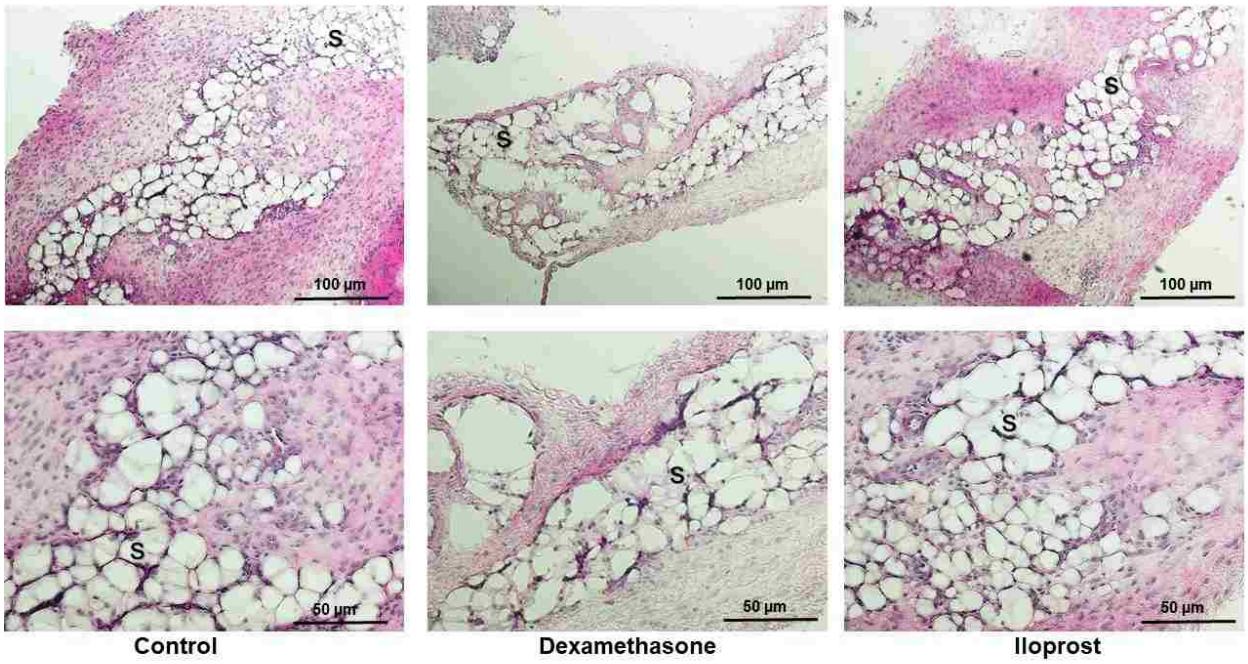

Figure 5.4. H&E staining for tissues around the explanted Collagen sponges. Nuclei: blue; eosinophilic structures: red; basophilic structures; purple. Top scale bars represent 100 µm. Bottom scale bars represent 50 µm. (S) indicates a sponge.

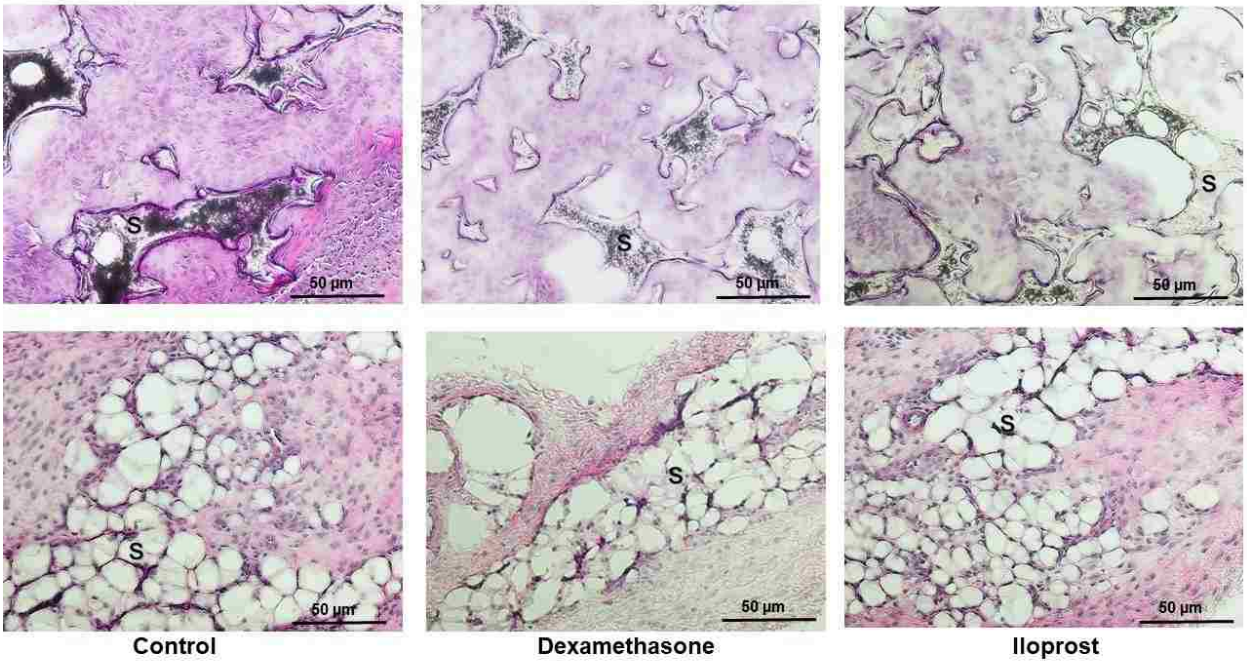

Figure 5.5. H&E staining for tissues around the explanted sponges. Nuclei: blue; eosinophilic structures: red; basophilic structures; purple. **Top images**: PVA sponges. **Bottom images**: Collagen sponges. Scale bar represent 50 µm. (S) Indicates a sponge.

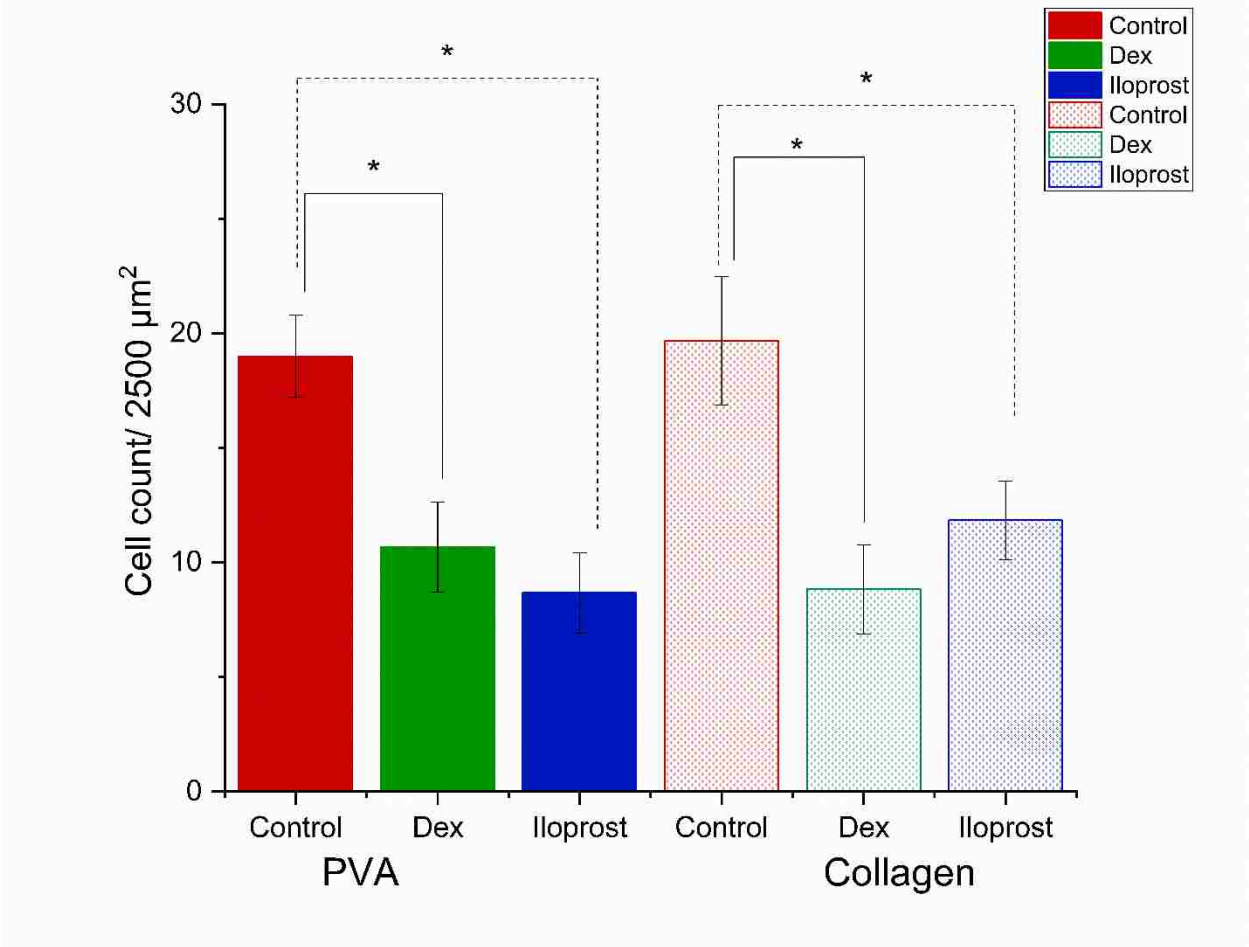

Figure 5.6. Bar graphs showing the cell count/2500 µm^2 of the tissues surrounding the control, dexamethasone-treated, and iloprost-treated sponges respectively after 7 days of implantation. The cell counts are presented as the mean from six animals. Error bars represent the ± SD. Significance is denoted by *p ≤0.001, n=6 where n represent the number of animals.

Collagen distribution was observed to be less in the tissues surrounding the dexamethasone-treated collagen sponges and the iloprost-treated collagen sponges when compared to the tissue around the control collagen sponges (Figures 5.7 and 5.8). Likewise, less collagen distribution was observed in the tissues surrounding the dexamethasone-treated PVA sponges and the iloprost-treated PVA sponges compared to the tissue around the control PVA sponges (Figure 5.7)

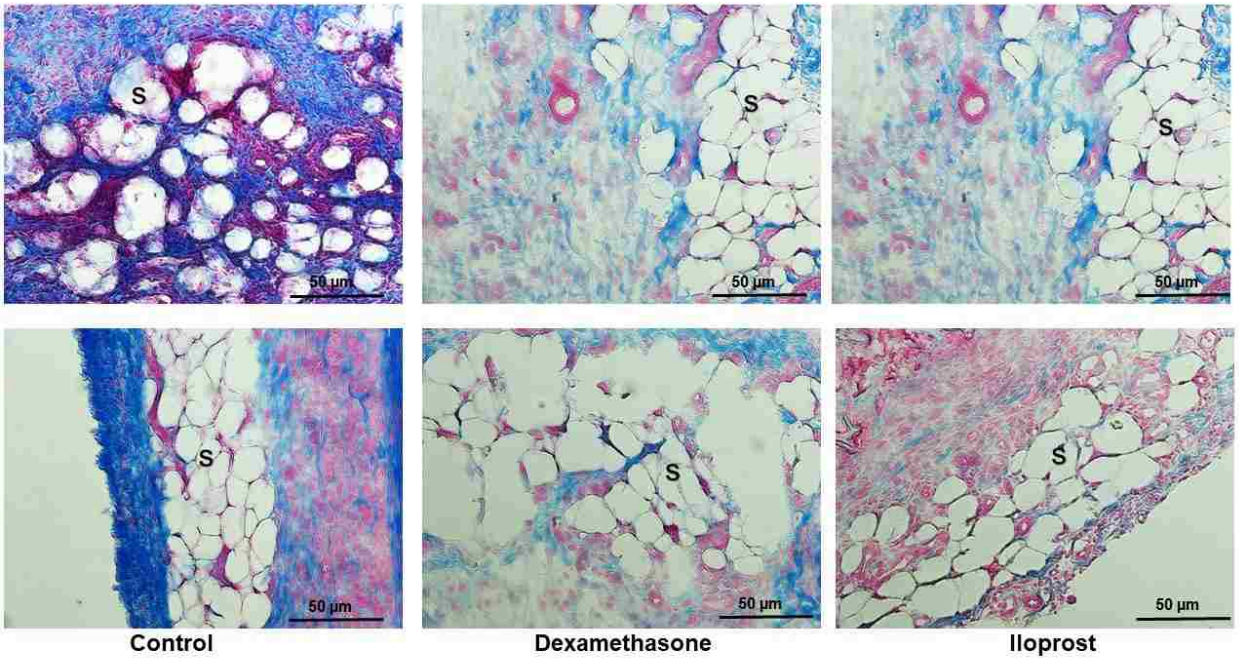

Figure 5.7. Masson's Trichrome staining for tissues around the explanted Collagen sponges. Cytoplasm: light red; collagen: blue. Scale bars represent 50 µm. (S) indicates a sponge.

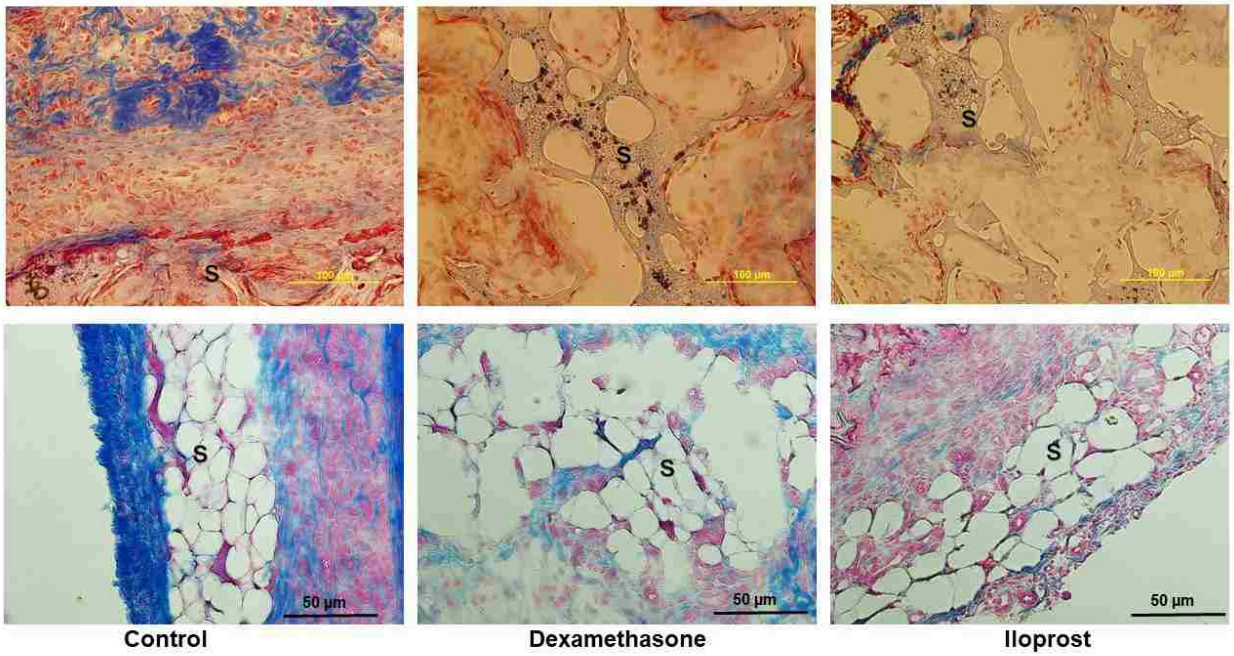

Figure 5.8. Masson's Trichrome staining for tissues around the explanted sponges. **Top images:** PVA sponges where scale bars represent 100 µm. Cytoplasm: light red; collagen: blue. **Bottom images:** Collagen sponges where scale bar represent 50 µm. (S) Indicates a sponge.

5.2.4. Immunohistochemistry Analysis

Immunohistochemical staining was performed to determine the presence of $CD163^+CD68^+$ macrophages among macrophages ($CD68^+$ cells) in tissues surrounding the control and treatment PVA and collagen sponges. The percentage of $CD163^+CD68^+$ among $CD68^+$ cells was calculated manually in both treatment and control sponges at the higher magnification (20X) to evaluate the population of these cells around the implanted sponges (Figure 5.9). The percentage of $CD163^+CD68^+$ cells among $CD68^+$ cells was higher in the tissues around the iloprost treated sponges and dexamethasone treated sponges compared to the tissues around the control sponges when calculated for the PVA and collagen sponges ($p \leq 0.001$) (Figure 5.10).

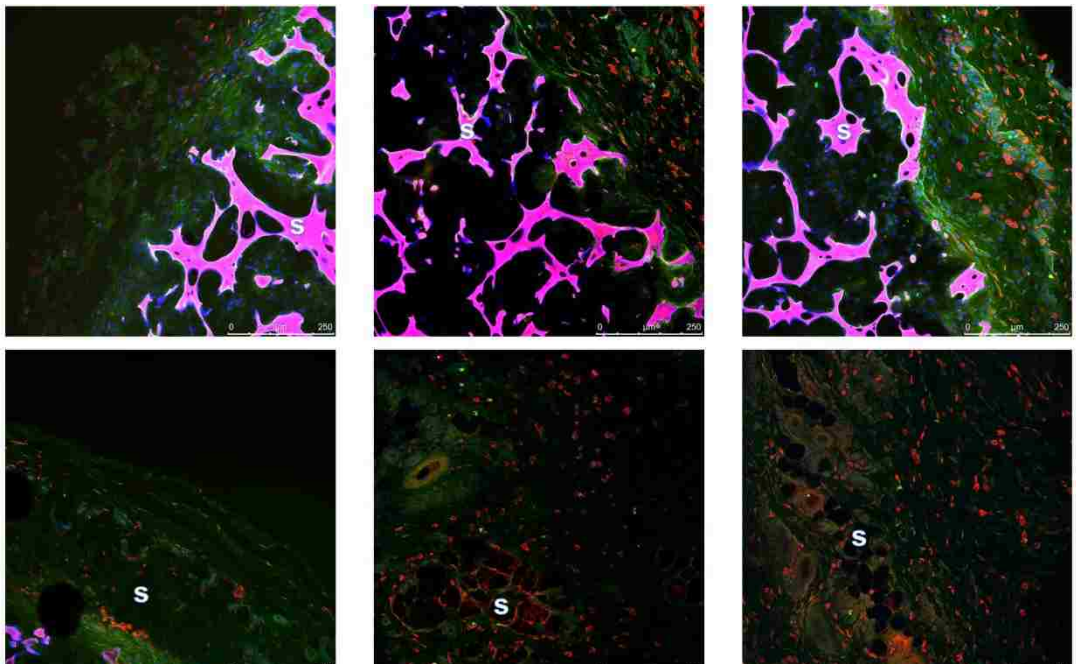

Figure 5.9. Immunohistochemical staining for CD68 (green), CD163 (red), and nuclei (blue) in the tissue around the explanted PVA sponges. Overlapped colors represent $CD163^+CD68^+$ macrophages. **Top images:** PVA sponges; where the sponge material is shown in pink. **Bottom images:** Collagen sponges. Scale bars represent 250 µm. (S) Indicates a sponge.

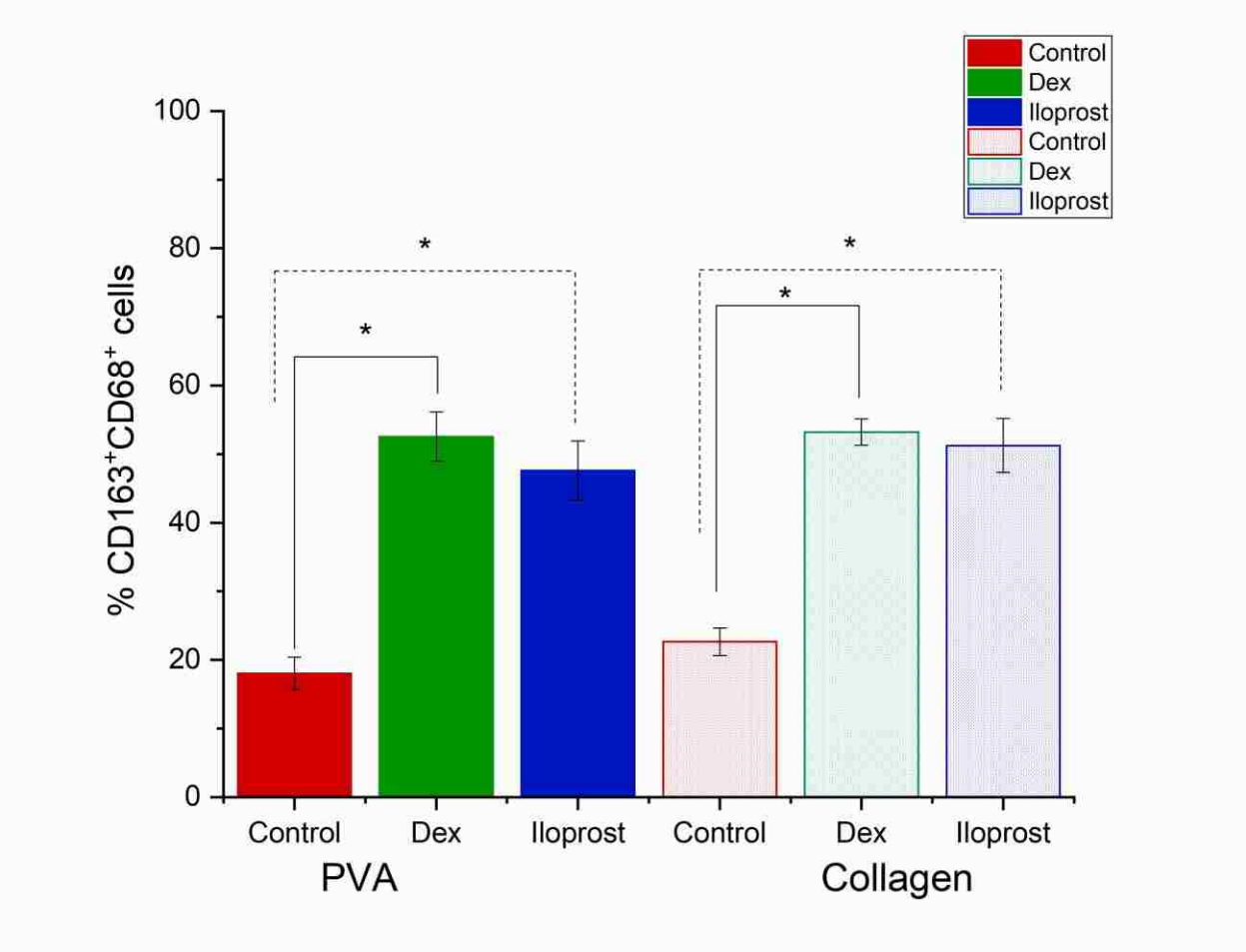

Figure 5.10. Bar graphs showing the percentage of $CD163^{+}CD68^{+}$cells among $CD68^{+}$ cells in the tissues around the control, dexamethasone-treated, and iloprost-treated PVA sponges and collagen sponges respectively after 7 days of implantation. The percentages are given as the mean from six animals. Error bars represent the ± SD. Significance is denoted by *p ≤0.001 n=6 where n represent the number of animals.

5.3. Discussion

This project aims to present a model to study and compare macrophage activation in response to polyvinyl alcohol (PVA) non-biodegradable sponges and collagen biodegradable sponges after being implanted subcutaneously in male Sprague Dawley rats. These two materials represent a model for a degradable vs. non-degradable material. There are many types of materials, so it is certainly important to note we are not claiming that this model system covers all possible materials/tissue possibilities. While there is a growing interest in using collagen matrices in biomedical implants and as degradable drug-delivery scaffolds, it is necessary to study how the collagen matrices affect the macrophage activation patterns. It is also important to determine how different modulators affect the biodegradable materials of collagen sponges and compare that effect to the non-biodegradable material of PVA sponges.

The physiochemical properties of the biomaterial surface play a major role in the composition of the early provisional matrix [20]. The relationship between the chemistry of the biomaterial and its influence on the foreign body response have been of major interest in terms of protein adsorption and complement activation [21, 22]. It has also been shown that the capsule formation during the inflammatory response after biomaterials implantation is dependent on the shape of the implant [23-25]. Cell bioactivity has been shown to be affected by the physical properties of implanted biomaterials including their structural composition, mechanical properties, and microarchitecture [13-16]. Scaffold architecture is of critical importance in the field of tissue engineering where scaffolds requires interconnected structure with high porosity to allow the cellular infiltration, ensure adequate diffusion of the nutrients into the infiltrating cells as well as adequate diffusion of waste products out of the scaffolds [17]. One study showed that using polytetrafluoroethylene materials of different pore sizes resulted in differential expression of pro-inflammatory cytokines *in vitro* and decreased fibrous capsule thickness *in vivo* [18].

Collagen scaffolds have been used as a delivery vehicle of anti-inflammatory agents, such as the anti-inflammatory cytokine IL-10 [19, 20] . Thus, studying the macrophage activation profiles after the implantation of collagen scaffolds while delivering anti-inflammatory drugs/modulators has a promising potential to present biomaterials with the capacity to promote regeneration as well as modulating the inflammatory response at the implantation site. The administration of iloprost and dexamethasone lead to a decrease in the levels of the pro-inflammatory chemokine CCL2 when they were used in two different sponge models; the PVA and collagen. Noteworthy, the levels of CCL2 were statistically less in the wound fluid collected from the control collagen sponges when compared to the control PVA sponges.

Fewer cells were observed around the dexamethasone-treated collagen sponges and the iloprost-treated collagen sponges when compared to those around the control collagen sponges. Cells are known to mainly interact with scaffolds via ligands on the material surface. In the case of natural origin materials, such as collagen, the surface of these materials has Arg-Gly-Asp (RGD) integrin binding sequences ligands which allows for efficient binding between the cells and scaffold [21, 22]. However, the scaffolds made from synthetic materials don't possess these ligands on their material surface. Less cellular density was observed in the tissues surrounding both iloprost-treated PVA sponges and dexamethasone-treated PVA sponges compared to the tissues around the control sponges, which has been consistent with our previous studies on both modulators [23-25]. Cellular density in the tissues around the iloprost-treated PVA sponges was found to be similar to that around the dexamethasone-treated PVA sponges.

Both modulators, dexamethasone and iloprost, shifted the macrophages to their $CD163^{+}CD68^{+}$ pro-wound healing, anti-inflammatory state and the population of these cells was significantly higher than those around the control sponges despite differences in the scaffold materials. Both modulators shifted the macrophages to their pro-wound healing state within the

collagen sponge pores in the iloprost-treated sponges and the dexamethasone-treated sponges, which is critical to improve the integration of tissue/biomaterial interface.

5.4. Conclusion

The administration of iloprost and dexamethasone lead to a decrease in the levels of CCL2, less collagen formation, and an increase in the population of $CD163^{+}CD68^{+}$ in both sponge models compared to their corresponding control sponges. Although the levels of CCL2 in the wound fluid collected from the collagen control sponges were significantly less those collected from the PVA sponges, both materials initiated an inflammatory response cascade that was similar in terms of collagen distribution and $CD163^{+}CD68^{+}$ macrophages around the implant. Successfully synthesizing collagen scaffolds allows the use of a scaffold that is of natural origin and isolated from the same rat strain. Given the significance of using collagen scaffolds for many types of biomedical implants, this gives us an important starting point for many future studies that includes the use of collagen scaffolds as delivery vehicle in addition of being a tool to study wound healing and tissue regeneration.

5.5. References

[1] W. Kenneth Ward, A review of the foreign-body response to subcutaneously-implanted devices: the role of macrophages and cytokines in biofouling and fibrosis, Journal of diabetes science and technology 2(5) (2008) 768-777.

[2] D.J. Holt, D.W. Grainger, Host response to biomaterials, CRC Press, 2012, pp. 91-118.

[3] Z. Sheikh, P.J. Brooks, O. Barzilay, N. Fine, M. Glogauer, Macrophages, Foreign Body Giant Cells and Their Response to Implantable Biomaterials, Materials (Basel) 8(9) (2015) 5671-5701.

[4] B.N. Brown, B.D. Ratner, S.B. Goodman, S. Amar, S.F. Badylak, Macrophage polarization: An opportunity for improved outcomes in biomaterials and regenerative medicine, Biomaterials 33(15) (2012) 3792-3802.

[5] N. Wang, H. Liang, K. Zen, Molecular mechanisms that influence the macrophage m1-m2 polarization balance, Front Immunol 5 (2014) 614.

[6] A. Das, M. Sinha, S. Datta, M. Abas, S. Chaffee, C.K. Sen, S. Roy, Monocyte and Macrophage Plasticity in Tissue Repair and Regeneration, Am. J. Pathol. 185(10) (2015) 2596-2606.

[7] K.L. Spiller, T.J. Koh, Macrophage-based therapeutic strategies in regenerative medicine, Adv. Drug Delivery Rev. (2017) Ahead of Print.

[8] J.M. Morais, F. Papadimitrakopoulos, D.J. Burgess, Biomaterials/tissue interactions: possible solutions to overcome foreign body response, Aaps j 12(2) (2010) 188-96.

[9] J. Glowacki, S. Mizuno, Collagen scaffolds for tissue engineering, Biopolymers 89(5) (2008) 338-344.

[10] F.J. O'Brien, Biomaterials & scaffolds for tissue engineering, Mater. Today (Oxford, U. K.) 14(3) (2011) 88-95.

[11] S.J. Hollister, Porous scaffold design for tissue engineering, Nat. Mater. 4(7) (2005) 518-524.

[12] D. Yoo, New paradigms in hierarchical porous scaffold design for tissue engineering, Mater. Sci. Eng., C 33(3) (2013) 1759-1772.

[13] M.G. Haugh, C.M. Murphy, R.C. McKiernan, C. Altenbuchner, F.J. O'Brien, Crosslinking and mechanical properties significantly influence cell attachment, proliferation, and migration within collagen glycosaminoglycan scaffolds, Tissue Eng Part A 17(9-10) (2011) 1201-8.

[14] I.V. Yannas, D.S. Tzeranis, B.A. Harley, P.T. So, Biologically active collagen-based scaffolds: advances in processing and characterization, Philos Trans A Math Phys Eng Sci 368(1917) (2010) 2123-39.

[15] R.A. Hortensius, B.A.C. Harley, The use of bioinspired alterations in the glycosaminoglycan content of collagen–GAG scaffolds to regulate cell activity, Biomaterials 34(31) (2013) 7645-7652.

[16] J.C. Lee, C.T. Pereira, X. Ren, W. Huang, D. Bischoff, D.W. Weisgerber, D.T. Yamaguchi, B.A. Harley, T.A. Miller, Optimizing Collagen Scaffolds for Bone Engineering: Effects of Cross-linking and Mineral Content on Structural Contraction and Osteogenesis, J Craniofac Surg 26(6) (2015) 1992-6.

[17] H.C. Ko, B.K. Milthorpe, C.D. McFarland, Engineering thick tissues--the vascularisation problem, Eur Cell Mater 14 (2007) 1-18; discussion 18-9.

[18] P.C. Bota, A.M. Collie, P. Puolakkainen, R.B. Vernon, E.H. Sage, B.D. Ratner, P.S. Stayton, Biomaterial topography alters healing in vivo and monocyte/macrophage activation in vitro, J Biomed Mater Res A 95(2) (2010) 649-57.

[19] C. Holladay, K. Power, M. Sefton, T. O'Brien, W.M. Gallagher, A. Pandit, Functionalized Scaffold-mediated Interleukin 10 Gene Delivery Significantly Improves Survival Rates of Stem Cells In Vivo, Molecular Therapy 19(5) (2011) 969-978.

[20] C.A. Holladay, A.M. Duffy, X. Chen, M.V. Sefton, T.D. O'Brien, A.S. Pandit, Recovery of cardiac function mediated by MSC and interleukin-10 plasmid functionalised scaffold, Biomaterials 33(5) (2012) 1303-1314.

[21] F.J. O'Brien, B.A. Harley, I.V. Yannas, L.J. Gibson, The effect of pore size on cell adhesion in collagen-GAG scaffolds, Biomaterials 26(4) (2005) 433-41.

[22] C.M. Murphy, M.G. Haugh, F.J. O'Brien, The effect of mean pore size on cell attachment, proliferation and migration in collagen-glycosaminoglycan scaffolds for bone tissue engineering, Biomaterials 31(3) (2010) 461-6.

[23] G.D. Keeler, J.M. Durdik, J.A. Stenken, Localized delivery of dexamethasone-21-phosphate via microdialysis implants in rat induces M(GC) macrophage polarization and alters CCL2 concentrations, Acta Biomater 12 (2015) 11-20.

[24] G.D. Keeler, J.M. Durdik, J.A. Stenken, Effects of delayed delivery of dexamethasone-21-phosphate via subcutaneous microdialysis implants on macrophage activation in rats, Acta Biomaterialia 23 (2015) 27-37.

[25] K. Alkhatib, T.M. Poseno, A. Diaz Perez, J.M. Durdik, J.A. Stenken, Iloprost Affects Macrophage Activation and CCL2 Concentrations in a Microdialysis Model in Rats, Pharm. Res. 35(1) (2018) 1-10.

Chapter 6

Summary and Future Directions

The presented studies in this dissertation focused on determining the effect of locally delivered bioactive modulators on macrophage activation at the implantation site of different biomaterials in rats. This project has initially tested different modulator candidates, such as iloprost, for their ability to direct macrophages to their pro-wound healing phenotype after the implantation of a microdialysis probe in the subcutaneous space of male Sprague Dawley rats. This was followed by studying macrophage activation after the implantation of PVA sponges to improve tissue integration and thus long-term/successful outcomes for biomedical implants. The last part of this project focused on assessing macrophage activation after implanting polyvinyl alcohol non-biodegradable vs. collagen biodegradable sponges in the subcutaneous space of male Sprague Dawley rats.

Modulating the macrophage response to implants is of significant interest as a means to promote improved biomaterial/tissue integration. Macrophages play a key role in regulating the foreign body response. The initial studies aimed to investigate the role of locally-delivered iloprost, a synthetic prostacyclin analog, via microdialysis sampling in altering the macrophage activation state. The microdialysis sampling probe served as both the implanted biomaterial as well as the means to both deliver iloprost and collect the pro-inflammatory chemokine, CCL2. The macrophage phenotype surrounding the dialysis probes was assessed by the presence of $CD163^{+}CD68^{+}$ cells in the tissue surrounding the implant and by measuring CCL2 concentrations collected in the dialysates. This localized delivery of iloprost via the implanted microdialysis probes resulted in a decrease of the pro-inflammatory chemokine CCL2 and an increase the population of $CD163^{+}CD68^{+}$ macrophages at two days post implantation. $CD163^{+}CD68^{+}$ macrophages are characterized as being anti-inflammatory, pro-wound healing and pro-tissue remodeling cells. These initial studies showed that iloprost can shift macrophage activation states in vivo to the pro-wound healing phenotype and demonstrated the need for more experiments to

determine the effect of locally delivered iloprost during distinct stages of the foreign body response.

To study the effect of iloprost on macrophage activation at longer time periods after the implantation of non-biodegradable implants, PVA sponges were chosen as a model to assist achieving this aim. This study ultimately aimed to determine the appropriate time sequences necessary to achieve optimal modulation of macrophages that affect the tissue integration and thus long-term/successful outcomes for biomedical implants. This study included optimizing the direct dosing system using IR-750 fluorophore to determine flow paths of the injection surrounding the PVA sponge implant. This was followed by comparing dexamethasone (a commonly used steroid) with iloprost to assess this model. Optimizing the use of iloprost as a modulator at 7 days post implantation time point was necessary. The implanted PVA sponges provided a useful tool to study the macrophage activation profile at 7 days post implantation by also delivering drug modulators to the surrounding tissues in the aim of shifting the macrophages to their pro-wound healing phenotype. CCL2 in the wound fluid collected from the dexamethasone treated sponges and those collected from the iloprost treated sponges were found to be significantly less than the wound fluid levels of CCL2 from the control sponges with no significant difference found between the wound fluid levels of CCL2 from dexamethasone-treated sponges vs. iloprost-treated sponges. Less cellular infiltration and less collagen formation were observed in the tissues surrounding both iloprost-treated sponges and dexamethasone-treated sponges compared to the tissues around the control sponges. Greater presence of $CD163^{+}CD68^{+}$ cells was observed in the tissues surrounding both iloprost treated sponges and dexamethasone treated sponges compared to the tissues around the control sponges, which confirms iloprost as a potent modulator of macrophage phenotype

Completing the previous studies confirmed the ability of iloprost to modulate the macrophage phenotype. A material-based study was designed to assess macrophage activation caused by

implanted polyvinyl alcohol non-biodegradable vs. collagen biodegradable sponges in the subcutaneous space of male Sprague Dawley rats. This project started by synthesizing and characterizing natural origin collagen scaffolds isolated from the same rat strain, followed by implanting collagen sponges that delivered the previously tested drug modulators, dexamethasone and iloprost, for their ability to shift macrophages to their pro-wound healing state. The administration of iloprost and dexamethasone lead to a decrease in the levels of pro-inflammatory CCL2, less collagen formation, and an increase in the population of $CD163^{+}CD68^{+}$ in both sponge models compared to their correspondent control sponges. Although, the levels of CCL2 in the wound fluid collected from the collagen control sponges were significantly less than those collected from the PVA sponges, both materials initiated an inflammatory response cascade that was similar in terms of collagen distribution and $CD163^{+}CD68^{+}$ macrophages around the implant.

Multiple studies have shown the importance of macrophage activation in wound healing and tissue repair. Understanding the macrophage response to different chemical cues in the surrounding microenvironment has been crucial to improve the implanted biomaterials integration. However, there is still a need to explore the effect of drug modulators on different cell lines to ensure that no counteractions could potentially lead to unintended side effects that hinder biomaterial/tissue integration.

Since collagen scaffolds have been widely used for different applications in the biomedical field, this study provides an important starting point for many future studies that includes the use of collagen scaffolds as delivery vehicles in addition of being a tool to study wound healing and tissue regeneration. Also, these scaffolds will provide a tool to serve the objective of determining integration outcomes for sponge implants at 14 and 28 days post implantations time points during the foreign body response given that our past studies have only determined acute outcomes at 3- and 7-days post implantation. These sponges can also serve the need to provide more

information on macrophage behavioral changes once the delivery of modulator is terminated or interrupted. It is important to determine how different timing of macrophage modulator application during the initial phase of the FBR (first 7 days) affects longer-term outcomes at 14 and 28-days post implantation. Performing these studies will demonstrate how long the effect of these modulators will last after being delivered and will determine if continuous dosing system is necessary to maintain the desired outcome. Noteworthy, controlling the degradation rate of collagen scaffolds is an important factor in long term tissue/biomaterial interaction studies. This can be achieved by controlling the crosslinking degree of the collagen. Another aspect that requires further investigation is the pore size of scaffolds and their role in wound healing with the presence of macrophage modulators. Pore size has been denoted as a critical property for modulating macrophages to their pro-wound healing state. controlling the scaffolds pore size can be utilized to control the integration speed of the implant with the surrounding tissues [1].

This research provides an opportunity for further investigation to improve the longevity and integration of biomaterials into the host tissue. Given the complexity of the extracellular environment, a comprehensive analysis approach is a necessity to determine interactions between biomaterials and their surrounding microenvironment. Optimization of robust microdialysis probes allows the localized delivery of macrophage modulators while simultaneously sampling during further time points during foreign body response, such as +14 days after implantation, as fibrosis begins to peak at this time point. Performing these studies can provide real time cytokine profiles, gene expression levels, and histochemical and histological data which can be combined to further understand the molecular interaction between biomaterials and host tissues. Additionally, the sponge experiments are useful for the extraction of different cells to perform phenotypic analysis using flow cytometry and gene expression assays.

Another important future aspect that is recently gaining major interest in the field of biomaterials is adjusting the balance between classically activated macrophages and alternatively

activated macrophages. Lately, some studies have hypothesized that allowing the biomaterials to first promote the classically activated phenotype of macrophages before shifting them to their alternatively activated phenotype would enhance the ultimate healing. This can be done by controlling the dosing system of the administered modulators and compare the outcomes between delayed macrophage modulation vs. immediate (after implantation) macrophage modulation.

While these studies show a great promise to use iloprost as modulator for macrophage activation to their $CD163^{+}CD68^{+}$ pro-wound healing state *in vivo* resulting in improved wound healing, they are still limited on a handful of markers, and it may be appropriate to include a markers panel that provides a more conclusive characterization of the macrophage response associated with iloprost administration. Such panels can be provided by studying the gene expression profiles by isolating the macrophages from the *in vivo* environment and correlate these profiles to the available *in vitro* profile provided by different macrophage phenotypes [2]. Using flow cytometric and cell sorting analyses constitute a powerful tool to identify activated macrophage phenotypes throughout the use of a multiple cell surface markers panel [3, 4]. Moreover, differentiating the angiogenesis assays has been also described as a method to recognize the different behaviors between macrophage phenotypes [5]. $CD163^{+}CD68^{+}$ macrophages are known to promote angiogenesis and tissue repair, while M1 macrophages are mainly anti-angiogenic [6, 7]. Optimizing the use of the microdialysis techniques further allows collecting cytokines to provide a real time protein secretion profile around the implants. However, the main challenge is the diffusion restrictions affecting the collection of larger molecular weight solutes due to the fact that many cytokines that play a role in macrophage signaling such as IL-1β, IL-6, and TNF-α and IL-10 are difficult to collect due to their size and/or their low localized concentrations within the probe-implanted space [8, 9].The use of large pore microdialysis probes with molecular weight cutoff membranes (1 MDa) combined with special pumps (push/pull) may allow collection of these larger cytokine proteins [8, 10].

References

[1] E.M. Sussman, L.R. Madden, B.D. Ratner, Pore size of implanted biomaterials modulates macrophage polarity, Trans. Annu. Meet. Soc. Biomater. 32(Annual Meeting of the Society for Biomaterials: Giving Life to a World of Materials, 2010, Volume 1) (2010) 247.

[2] J. Xue, S.V. Schmidt, J. Sander, A. Draffehn, W. Krebs, I. Quester, D. De Nardo, T.D. Gohel, M. Emde, L. Schmidleithner, H. Ganesan, A. Nino-Castro, M.R. Mallmann, L. Labzin, H. Theis, M. Kraut, M. Beyer, E. Latz, T.C. Freeman, T. Ulas, J.L. Schultze, Transcriptome-based network analysis reveals a spectrum model of human macrophage activation, Immunity 40(2) (2014) 274-88.

[3] A.V. Misharin, L. Morales-Nebreda, G.M. Mutlu, G.R. Budinger, H. Perlman, Flow cytometric analysis of macrophages and dendritic cell subsets in the mouse lung, Am J Respir Cell Mol Biol 49(4) (2013) 503-10.

[4] F. Porcheray, S. Viaud, A.C. Rimaniol, C. Leone, B. Samah, N. Dereuddre-Bosquet, D. Dormont, G. Gras, Macrophage activation switching: An asset for the resolution of inflammation, Clin. Exp. Immunol. 142(3) (2005) 481-489.

[5] F.H. Barnett, M. Rosenfeld, M. Wood, W.B. Kiosses, Y. Usui, V. Marchetti, E. Aguilar, M. Friedlander, Macrophages form functional vascular mimicry channels in vivo, Sci. Rep. 6 (2016) 36659.

[6] N. Jetten, S. Verbruggen, M.J. Gijbels, M.J. Post, M.P. De Winther, M.M. Donners, Anti-inflammatory M2, but not pro-inflammatory M1 macrophages promote angiogenesis in vivo, Angiogenesis 17(1) (2014) 109-18.

[7] K.L. Spiller, R.R. Anfang, K.J. Spiller, J. Ng, K.R. Nakazawa, J.W. Daulton, G. Vunjak-Novakovic, The role of macrophage phenotype in vascularization of tissue engineering scaffolds, Biomaterials 35(15) (2014) 4477-88.

[8] S.B. Jadhav, V. Khaowroongrueng, H. Derendorf, Microdialysis of Large Molecules, J. Pharm. Sci. 105(11) (2016) 3233-3242.

[9] X. Ao, J.A. Stenken, Microdialysis sampling of cytokines, Methods (San Diego, CA, U. S.) 38(4) (2006) 331-341.

[10] S.B. Jadhav, V. Khaowroongrueng, M. Fueth, M.B. Otteneder, W. Richter, H. Derendorf, Tissue Distribution of a Therapeutic Monoclonal Antibody Determined by Large Pore Microdialysis, J. Pharm. Sci. 106(9) (2017) 2853-2859.

Appendix A

Research Compliance Protocol Letters

UNIVERSITY OF ARKANSAS

Office of Research Compliance

MEMORANDUM

TO: Julie Stenken

FROM: Craig N. Coon, Chairman
Institutional Animal Care and Use Committee

DATE: May 2, 2014

SUBJECT: IACUC APPROVAL
Expiration date: May 11, 2017

The Institutional Animal Care and Use Committee (IACUC) has APPROVED protocol 14041: "Inducing and Monitoring Macrophage Polarization at an Implant Site in a Rat Subcutaneous Model" for the period of May 12, 2014 thru May 11, 2017

In granting its approval, the IACUC has approved only the protocol provided. Should there be any further changes to the protocol during the research, please notify the IACUC in writing (via the Modification form) prior to initiating the changes. If the study period is expected to extend beyond May 11, 2017you must submit a new protocol. By policy the IACUC cannot approve a study for more than 3 years at a time.

The IACUC appreciates your cooperation in complying with University and Federal guidelines for involving animal subjects.

CNC/aem

cc: Animal Welfare Veterinarian

Administration Building 210 • 1 University of Arkansas • Fayetteville, AR 72701-1201 • 479-575-4572
Fax: 479-575-3846 • http://vpred.uark.edu/199

UNIVERSITY OF ARKANSAS

Office of Research Compliance

To:	Julie Stenken
Fr:	Craig Coon
Date:	May 22nd, 2017
Subject:	IACUC Approval
Expiration Date:	May 22nd, 2019

The Institutional Animal Care and Use Committee (IACUC) has APPROVED your protocol # **17078:** *Optimizing Sponge Implants for Studies of Macrophage Polarization in Rat Subcutaneous Tissue*

In granting its approval, the IACUC has approved only the information provided. Should there be any further changes to the protocol during the research, please notify the IACUC in writing (via the Modification form) prior to initiating the changes. If the study period is expected to extend beyond May 22nd, 2019 you can submit a modification to extend project up to 3 years, or submit a new protocol. By policy the IACUC cannot approve a study for more than 3 years at a time.

The following individuals are approved to work on this study: Please submit personnel additions to this protocol via the modification form prior to their start of work.

The IACUC appreciates your cooperation in complying with University and Federal guidelines involving animal subjects.

CNC/tmp

17078